



Universität für Bodenkultur Wien
University of Natural Resources and Life Science, Vienna

Department for Agrobiotechnologie, IFA – Tulln
Institute for Environmental Biotechnologie

DNA: a promising new flame-retardant compound for PET and Nylon fabrics

Master Thesis

submitted by
Klemens Kremser, BSc.
Vienna 2018

Supervisor
Univ. Prof. DI Dr. Georg Gübitz
Mag. Dr. Doris Ribitsch
Felice Quartinello, MSc.

Acknowledgements

I want to thank all people that supported me during my studies and always offered me a helping hand. Special thanks go to my parents, which supported me financially and with their knowledge. Without them, it would have been not possible to finish my educational career in reasonable time. I also want to thank my girlfriend who was always very understanding and patient.

I especially want to thank my supervisor Univ. Prof. DI Dr. Georg Gübitz as well as Mag. Dr. Doris Ribitsch who gave me the possibility to work at the Institute for Environmental Biotechnology.

Furthermore, I want to thank Dr. Alessandro Pellis from the Department of Chemistry, University of York, for his help with the TGA-measurements.

Special thanks go to Felice Quartinello who guided me through the lab and had always a helping hand. I learned a lot from him and during my time here he became a real friend to me. At the end, I want to thank all people in the whole BET working group for their support during my time there.

Abstract

Synthetic polymers, like Poly(ethylene terephthalate) and Nylon have very favourable properties like strength and stability and as well elasticity. These properties make them interesting for a brought range of applications like in packaging and textile industry. Therefore, the call for smart textiles (engineered fabric for specific application), is becoming bigger.

In this context flame-retardant textiles are gaining a crucial role for working cloths and furniture. Such materials serve to protect the public from accidentally occurring fires by reducing heat, producing non-combustible gases or simply cover the combustible material by char-formation. Commercial available flame retardants often consist of brominated and chlorinated compounds which can accumulate in the aquatic environment and in the human body, causing major health risks. Deoxyribose Nucleic Acid (DNA) was investigated in this study to be a green and eco-friendly alternative by providing flame retardant properties due to its structure and availability.

In order to increase the surface reactivity of PET and Nylon, enzymatic hydrolysis was performed with two different enzymes. Released hydrolysates were measured *via* HPLC, showing *Humicola insolens* cutinase (HiC) to be the most promising functionalization agent (1 mM of BHET and 0.07 mM of caprolactam after 72h, respectively). Immobilization of DNA was done using three different techniques (EDC/NHS, Dopamine and Tyrosine) for crosslinking. Tyrosine/DNA coating showed outstanding flame-retardant properties with a very low burning rate and total burning time (35 s, 150 mm and 4.3 mm*s⁻¹ for the blank and 3.5 s, 17.5 mm and 5 mm*s⁻¹ for Nylon/Tyrosine/DNA) which was also confirmed by FT-IR, ESEM and TGA measurements.

Kurzfassung

Polyethylenterephthalat und Nylon sind synthetische Kunststoffe mit vielen nützliche Eigenschaften wie Stabilität, Widerstandsfähigkeit aber auch Elastizität. Diese Eigenschaften machen sie zu einigen der weltweit am meisten produzierten Polymeren. Sie finden unter anderem Verwendung in unterschiedlichen Verpackungsmaterialien und Textilien.

Die Nachfrage nach so genannten „smarten“ Textilien, welche chemisch, physikalisch oder biologisch verändert wurden, um neue und verbesserte Eigenschaften zu besitzen, wächst weltweit. Schwer entflammbare Stoffe gehören zu diesen Materialien und sollen die vor Bränden und Hitzeeinwirkung schützen, indem sie die entstehende Hitze reduzieren, nicht-brennbare Gase produzieren oder das brennbare Material überdecken. Im letzten Fall sind die Materialien zwar brennbar, erzeugen aber eine Kohle-Schicht, die das darunterliegende Material schützt. Viele schwer entflammbare Materialien enthalten Brom und Chlor, was sie zu potentiell umweltgefährlichen Substanzen macht. Diese sind bioakkumulativ und können von Fischen und Menschen im Fett- und Muskelgewebe abgelagert werden. Als umweltfreundliche Alternative wird in dieser Arbeit Desoxyribonukleinsäure (DNA) genutzt, da sie aufgrund ihrer Struktur alle Eigenschaften eines schwer entflammaren Stoffes besitzt und daher eine nachhaltige Alternative zu chlor- und bromhaltigen Stoffen darstellt.

Um DNA auf der Oberfläche von Polymeren zu immobilisieren, wurden in einem ersten Schritt die beiden Stoffe mit zwei hydrolytischen Enzymen behandelt, wodurch die Oberflächen-Reaktivität verbessert wurde. Die besten Ergebnisse konnten mit einer Cutinase von *Humicola insolens* erzielt werden. Die Effizienz der Oberflächenbehandlung wurde chromatographisch über die Konzentration der Monomere der abgebauten Kunststoffe gemessen. Nach 72 h wurde 1 mM BHET und 0.07 mM Caprolactam freigesetzt. Im zweiten Schritt wurde die DNA mithilfe von drei verschiedenen Methoden (EDC/NHS, Dopamin und Tyrosin) immobilisiert. Dabei zeigte sich, dass Tyrosin Immobilisierung zu einer deutlichen Reduktion der Abbrandrate und der totalen Abbrand-Zeit (35 s, 150 mm und 4.3 mm*s⁻¹ für Nylon blank und 3.5 s, 17.5 mm und 5 mm*s⁻¹ für Nylon/Tyrosin/DANN) bei beiden Polymeren führt. Dies wurde auch durch weitere Messung wie FT-IR, ESEM und TGA bestätigt.

Table of content

1. Introduction	6
1.1. Smart textiles	6
1.1.1. Poly(ethylene terephthalate) (PET)	7
1.1.2. Polyamide 6 (Nylon 6)	8
1.2. Flame retardants	9
1.2.1. Mode of combustion and developing of a fire	10
1.2.2. General mechanism of flame retardants	12
1.2.3. Chemical structure and properties of FRC	13
1.2.3.1. Inorganic flame retardants	13
1.2.3.2. Halogenated flame retardants	14
1.2.3.3. Phosphorus-based flame retardants	14
1.2.4. Environmental impact of commercial flame retardants	15
1.2.5. Novel and green flame retardants	16
1.2.5.1. Proteins	17
1.2.5.2. DNA as flame retardant	18
1.3. Surface functionalization of PET and Nylon	19
1.3.1. Alkaline treatment	19
1.3.2. Plasma treatment	20
1.3.3. Enzymatic treatment	20
1.3.3.1. Cutinase	20
1.3.3.2. Dihydropyrimidase (DHPase)	22
1.4. Enzymatic functionalization of PET and Nylon	24
1.5. DNA immobilisation	26
1.5.1. 1-Ethyl-3-(3-dimethylaminopropyl)carbodiimide/ N-Hydroxysuccinimide (EDC/NHS)	27
1.5.2. Dopamine	28
1.5.3. Tyrosine	29
2. Material and Methods	30
2.1. List of Chemicals	30
2.1.1. Enzyme Characterization	30
2.1.2. Washing steps	30
2.1.3. Sample Characterization	30
2.1.4. DNA Immobilisation	30
2.2. Methods	31
2.2.1. Protein concentration	31
2.2.2. Esterase activity assay	31
2.2.3. DHPase activity assay	32

2.2.4.	SDS-PAGE	32
2.2.5.	Enzyme recycling – Ultrafiltration.....	33
2.2.6.	Washing of PET and Nylon samples.....	33
2.2.7.	Enzymatic hydrolysis of PET and Nylon.....	34
2.2.8.	Detection of surface reactive groups – Colorimetric method	34
2.2.9.	High Performance Liquid Chromatography (HPLC)	36
2.2.10.	DNA – Agarose Gel Electrophoresis.....	37
2.2.11.	Nanodrop.....	37
2.2.12.	DNA – Immobilisation	38
2.2.12.1.	EDC/NHS	38
2.2.12.2.	Dopamine/Tyrosine.....	38
2.2.13.	Fourier-transformed Infrared Spectroscopy (FT-IR)	39
2.2.14.	Environmental Scanning Electron Microscopy (ESEM).....	40
2.2.15.	Flame-retardant Characterizations.....	40
2.2.15.1.	Flammability test.....	40
2.2.15.2.	Thermogravimetric Analysis (TGA)	41
3.	Results and Discussion	42
3.1.	Enzyme Characterization.....	42
3.2.	Enzymatic Hydrolysis.....	44
3.3.	DNA – Immobilisation	50
3.4.	Flame retardant characterization	63
4.	Conclusion	67
5.	Appendix	70
5.1.	FT-IR Spectra	70
5.2.	ESEM	78
6.	References	83

List of Figures

	Page
Fig. 1 Synthesis of PET	7
Fig. 2 Synthesis of Nylon 6	8
Fig. 3 Structure of PET and Nylon	9
Fig. 4 Annual financial damage due to fire in Austria	10
Fig. 5 Fire triangle	11
Fig. 6 Fire developing curve	12
Fig. 7 Flame-retardants in our daily life	13
Fig. 8 Inorganic flame-retardants	14
Fig. 9 Halogenated flame-retardants	14
Fig. 10 Nitrogen-based flame-retardants	15
Fig. 11 Release of brominated flame-retardants	16
Fig. 12 Proteins as flame-retardant compounds	18
Fig. 13 DNA as flame-retardant compound	19
Fig. 14 Hydrolysis reaction mechanism	20
Fig. 15 Catalytic triad of HiC	21
Fig. 16 Structure of HiC	22
Fig. 17 Degradation pathway of pyrimidines	23
Fig. 18 Structure of DHPase	24
Fig. 19 Enzymatic hydrolysis of PET and Nylon	26
Fig. 20 EDC/NHS crosslinking system	27
Fig. 21 Dopamine as linking molecule	28
Fig. 22 Synthesis pathway of neurotransmitter	29
Fig. 23 Tyrosine as linking molecule	29
Fig. 24 Esterase activity assay	32
Fig. 25 Vivaflow ultrafiltration	33
Fig. 26 Washing procedure of PET and Nylon	34
Fig. 27 Acid and basic dye	35
Fig. 28 Colorlite Spectrophotometer	36
Fig. 29 Coating procedure	39
Fig. 30 ESEM and EDS principle	40
Fig. 31 Flammability test procedure	41
Fig. 32 TGA	42
Fig. 33 SDS-PAGE of HiC and DHPase	43
Fig. 34 Bradford and activity assay	44
Fig. 35 HPLC results after 72h	45

Fig. 36	HPLC results for big stripes	46
Fig. 37	Colour change after staining	46
Fig. 38	FT-IR spectra of PET before and after hydrolysis	48
Fig. 39	FT-IR spectra of Nylon before and after hydrolysis	49
Fig. 40	ESEM image of PET and Nylon after hydrolysis	50
Fig. 41	Agarose gel electrophoresis of salmon DNA	51
Fig. 42	FT-IR spectra of salmon DNA	51
Fig. 43	FT-IR spectra of PET with EDC/NHS/DNA crosslinking	52
Fig. 44	FT-IR spectra of Nylon with EDC/NHS/DNA crosslinking	53
Fig. 45	FT-IR spectra of PET/Dopamine	54
Fig. 46	FT-IR spectra of PET/Dopamine/DNA	54
Fig. 47	FT-IR spectra of Nylon/Dopamine	55
Fig. 48	FT-IR spectra of Nylon/Dopamine/DNA	56
Fig. 49	ESEM image of PET and Nylon after Dopamine/DNA coating	57
Fig. 50	FT-IR spectra of PET/Tyrosine	58
Fig. 51	FT-IR spectra of PET/Tyrosine/DNA	58
Fig. 52	FT-IR spectra of Nylon/Tyrosine	59
Fig. 53	FT-IR spectra of Nylon/Tyrosine/DNA	60
Fig. 54	ESEM image of PET and Nylon after Tyrosine/DNA coating	61
Fig. 55	EDS spectra of PET and Nylon after Tyrosine/DNA coating	62
Fig. 56	Results flammability test PET	65
Fig. 57	Results flammability test Nylon	66
Fig. 58	ESEM image of burned PET and Nylon samples after Tyrosine/DNA coating	67
Fig. 59	TGA curve of PET and Nylon	68

List of Tables

		Page
Tab. 1	HPLC Gradients	37
Tab. 2	Results colorimetric measurements	47
Tab. 3	Results flammability test (all treatments)	64
Tab. 4	Results flammability test PET/Tyrosine/DNA	65
Tab. 5	Results flammability test Nylon/Tyrosine/DNA	65

List of Equations

		Page
Equ. 1	Inhibition reaction of halogenated flame-retardants	14
Equ. 2	Inhibition reaction of phosphorus-based flame retardants	15
Equ. 3	Calculation of colour difference	35

Abbreviations

PET	Poly(ethylene Terephthalate)
HPLC	High Performance Liquid Chromatography
HiC	Humicola insolens Cutinase
BHET	Bis-hydroxy Ethylene Terephthalate
DNA	Deoxyribonucleic Acid
EDC	1-Ethyl-3-(3-dimethylaminopropyl) carbodiimide
NHS	N-Hydroxysuccinimide
FT-IR	Fourier Transformed Infrared Spectroscopy
ESEM	Environmental Scanning Electron Microscopy
EDS	Energy-dispersive X-ray spectroscopy
TGA	Thermogravimetric Analysis
FRC	Flame Retardant Compound
BFR	Brominated Flame Retardant
CFR	Chlorinated Flame Retardant
PBDE	Polybrominated Diphenyl Ethers
WPC	Whey Protein Concentrate
WPI	Whey Protein Isolate
WPH	Whey Protein Hydrolysate
HFBI	Hydrophobin Class I
HFB II	Hydrophobin Class II
NaOH	Sodium Hydroxide
kDa	Kilodalton
DHPase	Dihydropyrimidase
PLA	Poly Lactic Acid
Ta	Terephthalic Acid
MHET	Mono-hydroxy Ethylene Terephthalate
CL	Caprolactam
6-ACA	6 Aminocaproic Acid
DMSO	Dimethyl Sulfoxide
SDS	Sodium Dodecyl Sulphate
BSA	Bovine Serum Albumin
M	molar

mM	millimolar
μM	micromolar
kg	kilogram
g	gram
mg	milligram
L	litre
mL	millilitre
μL	microliter
mm	millimetre
nm	nanometre
h	hours
min	minutes
s	seconds
PAGE	Polyacrylamide Gel Electrophoresis
rpm	rounds per minute
HRR	Heat Release Rate
TTI	Time to Ignition
THR	Total Heat Release
pkHRR	Peak of the Heat Release Rate
TSR	Total Smoke Release
FIGRA	Fire Growth Rate
bp	base pairs
TBT	Total Burning Time
DHU	Dihydrouracil

1. Introduction

The amount of synthetic polymers, like PET and Nylon, in furniture and clothing is rising every year. The burning of these polymers during house fires or working accidents releases high amounts of toxic substances and provides major risks for consumers as well for fire fighters. Flame retardant substances can help to reduce the risk of accidentally burning events and increase the time during the developing phase of a fire.

The aim of this work was to find a new and eco-friendly way to make PET and Nylon fabric flame retardant by coating with Deoxyribonucleic acid (DNA). As polymer pre-treatment, two types of enzymes within the class of esterases, namely cutinase and dihydropyrimidase, were used. These enzymes were used for the hydrolysis of the polymers, to create more surface reactive groups, to which the DNA can be covalently bound. Therefore, three different ways of immobilisation techniques were used including EDC/NHS, dopamine and tyrosine. Within the different immobilisation techniques, tyrosine in combination with DNA seems to be the most promising, which resulted it in a decreasing burning length (17.5 mm) and self-extinguishing of the flame compared to the blank, which completely burned.

1.1. Smart textiles

Nowadays, still about 40 % (~25.4 Mio tons) of the fibres used worldwide in textile production, are cotton fibres¹. Synthetic fibres, like polyethylene terephthalate (PET) and Nylon, have nowadays overruled the natural ones, with an annual production of about 55.2 M tons worldwide². Despite their favourable properties, the production of such is based on petrochemicals which leads to problems during disposal and recycling.

In Europe, textile industry is one of the biggest industries, with about 1.7 million employees and a turnover of about 170 billion euros per year. Despite the classical clothing and fashion market, there is a call for smart and high-performance materials. Such kind of high-performance fibres can have their origin in different bulk materials like polymers, carbon, glass, basalt and metals which can be processed to valuable and functional fibres and textiles by different kinds of finishes and additives. The processing of these bulk fibres and textiles can be performed chemically, mechanically or even biologically. In this sense, the enzymatic treatment

of polymers presents an eco-friendly alternative compared to the rather aggressive and environmentally harmful chemical ways of finishing. The functionalization of these kinds of materials leads to an increase in the fibre and textile value and their applications have a growing market in medicine, protection equipment, sportswear and many others.

1.1.1. Poly(ethylene terephthalate) (PET)

PET is synthetic aliphatic polyester which can be produced in two ways. The first way is the production out of Dimethyl terephthalate (DMT), which is melted in a reactor at about 150 – 160 °C, followed by transesterification reaction in another reactor at about 200 °C in the first step. In a second step, polycondensation of the transesterification product is done in a reactor which is heated up to 280 °C. The second way of PET production is the direct esterification of terephthalic acid with ethylene glycol in a reaction at high pressure (2-5 bar) and temperatures of about 200 °C³.

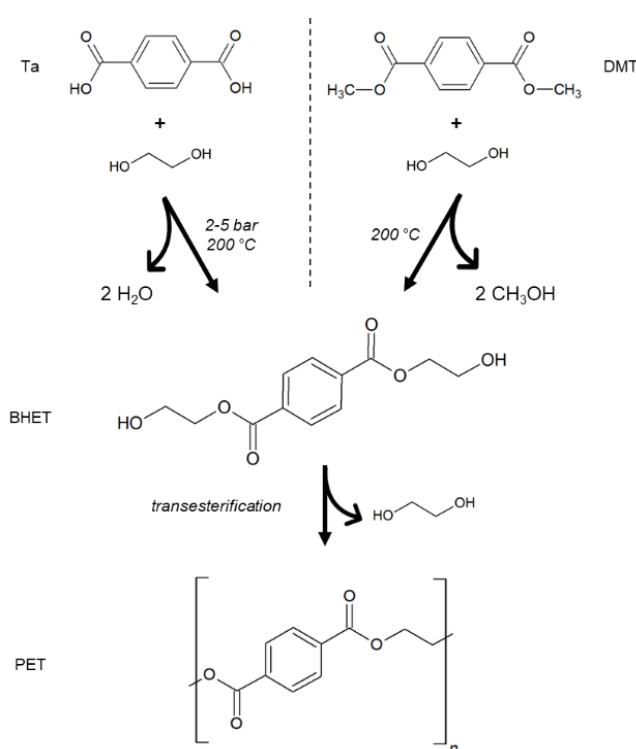


Figure 1: Synthesis of PET out of Ta (left) or DMT (right)

Due to its excellent fibre properties and low hydrophilicity, like other synthetic fibres, PET finds bright applications. Its strength and stiffness, as well as the high resistance against chemicals makes PET one of the most produced synthetic fibres around the globe. Depending on the production and the use, PET is produced as

amorphous or semi-crystalline material. Due to its thermal stability, semi-crystalline PET is used for the housing of electrical devices and 3D printable thermoplastics. Amorphous PET on the other hand is transparent and is used in packaging materials like plastic bottles and food packaging. Despite the advantages of PET, its hydrophobicity and difficulty to release oil stains, causes problems with comfort properties and within finishing processes⁴.

1.1.2. Polyamide 6 (Nylon 6)

Nylon 6 is produced by a polymerization reaction which is initiated with the ring opening of caprolactam (CL) by the addition of water. In this reaction aminocaproic acid is produced to a certain extent. When a certain concentration of aminocaproic acid has been produced, further CL units are linked to the already growing chain to produce a polymer with 2 or more repeats. The last step is a condensation reaction, where two chains which have both, amine and carboxylic groups, react to form an amide linkage. The whole reaction is performed at a temperature between 240 °C and 270 °C.

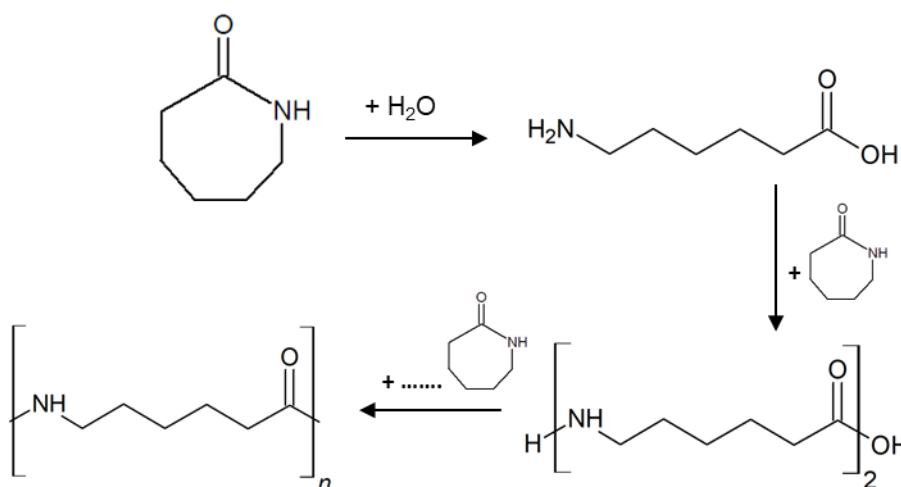


Figure 2: Synthesis of Nylon 6 via caprolactam

The applications of nylon 6 are quite similar to the ones of PET but nylon fibres play a more important role in the textile industry. Due to its properties like high strength, elasticity, abrasion resistance, dyability and shape holding, Nylon is used in clothing and home furnishing. It is most often produced as fibre and finds applications in socks, sporting goods, carpets and in upholstering of furniture⁴. The versatile use of Nylon is one reason why nylon fabric became important for our study. In case of a

house fire, furniture like the flooring or carpets and other synthetic materials will provide a major source of combustible material.

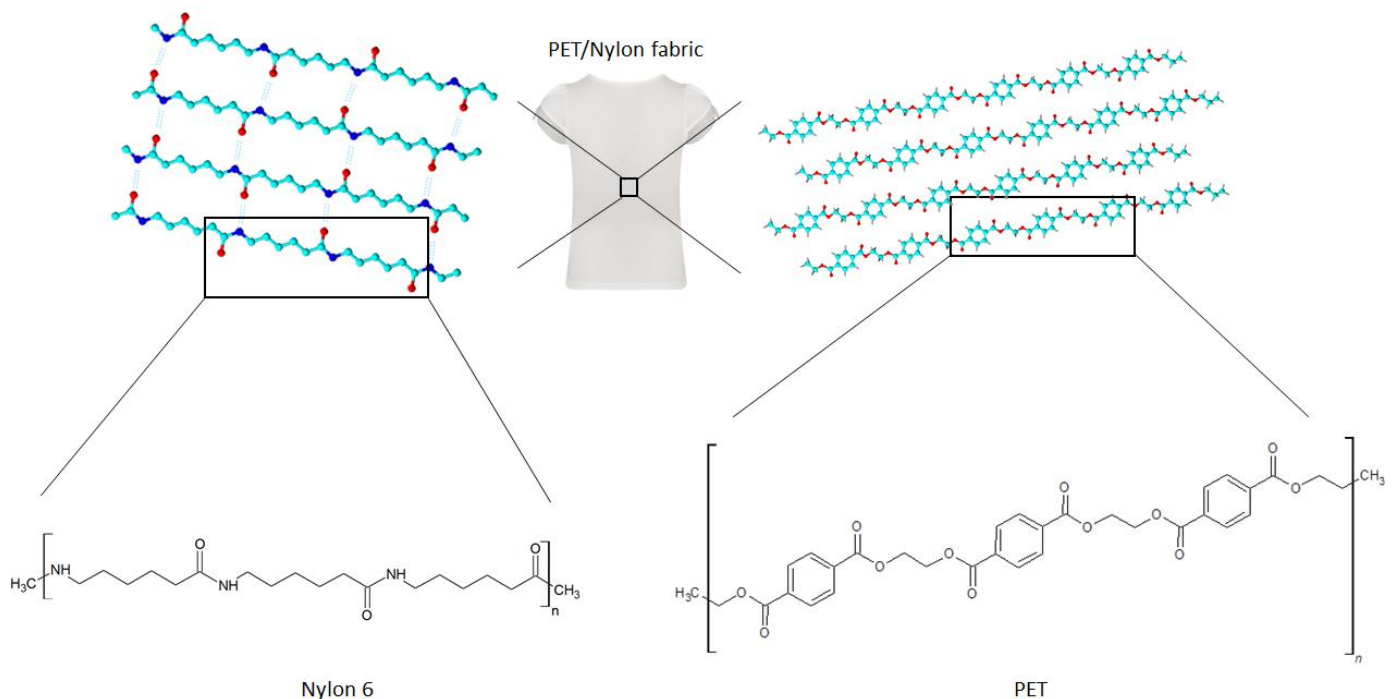


Figure 3: Structure of Nylon 6 (left) and PET (right) from the fabric to the single polymer chains

1.2. Flame retardants

In Europe, every year 2.0 – 2.5 million fires are reported resulting in about 25.000 fire deaths and about 500.000 fire injuries every year. Most of the incidents, about 80 %, occur in private homes where easy ignitable materials, like synthetic polymers, contribute to a fast fire spreading⁵. Within the European statistic, the fire brigade in Austria fights about 25 000 fires every year, which means that in average every 20 minutes, a fire occurs. About half of these events lead to major damages with high financial losses, huge damages of properties and in the worst case, the loss of lives. The total financial loss every year due to fires in industry, business, private and agricultural sites is about 260 Mio €⁶.

The application of flame retardants has the possibility to reduce the annual costs resulting from the fires. They can be applied for example in working clothes to reduce the risk of burning injuries for the employees which work at high temperature and open fire. In the private and business sectors, flame retardants have major applications in furniture, flooring and insulations of private houses and in hotels and office complexes. Here they should serve to protect the public from accidental fires by increasing the resistance to ignition.

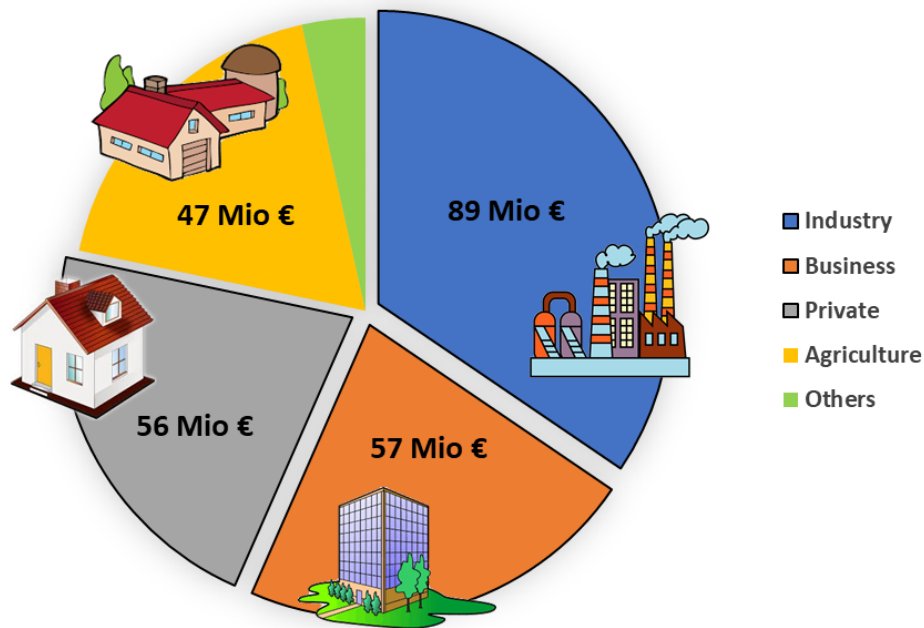


Figure 4: Annual financial costs caused by fire in the different fields of Industry, Business, Private and Agriculture in Austria

1.2.1. Mode of combustion and developing of a fire

The mode of combustion can be explained by the “fire triangle” (Figure 5). A fire occurs when all the three elements, combustible material (or fuel), heat and oxygen are present in the right ratio. For such reason for extinguishing a fire, it is necessary to remove at least one of the three elements. To give an example, water is the most often used element to extinguish a fire by the mode of cooling and removing therefore the heat. As described later, also flame-retardant compound (FRC) can be a potential material for fire extinguishing by acting as a flame-retardant compound and removing one of the three elements within the fire triangle.

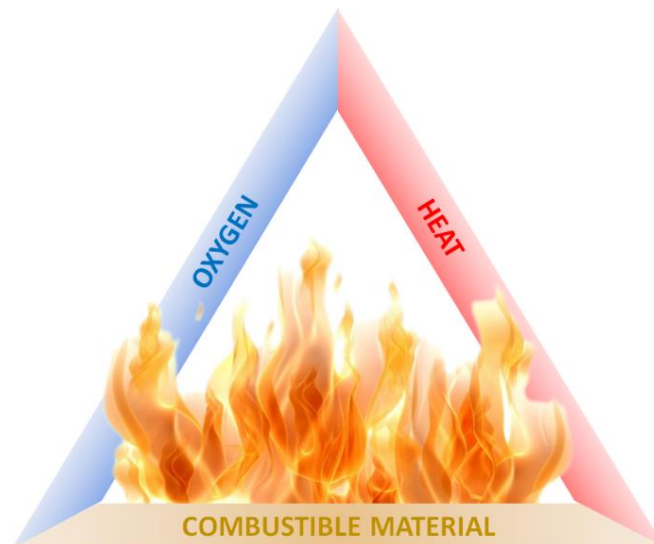


Figure 5: Fire triangle, showing the three elements necessary to start a fire

In general, the developing of a fire or the so called “fire developing curve” (Figure 6), can be separated into five phases. In the first phase, the ignition, the right conditions as described in the mode of combustion, have to be present to get a fire started. For example, the ignition and the start of a house fire could be represented by cigarette dropped on a bed or sofa by a sleeping person. The cigarette provides the heat source and together with the furniture textile as combustible material and the oxygen in the room a fire can start. In the second phase, the “developing of the fire”, the fire starts to become bigger due to the increasing heat and the so called “pyrolysis” which is the thermal decomposition of organic and inorganic materials leading the production of smaller molecules which increase the fire, since they are easier to burn easier. The third step, defined as “flash over”, is the most dangerous where flammable gases are released by all materials due to pyrolysis ignite spontaneously at the same time. After this phase, normally the whole room is on fire. This leads to a fully developed fire, which is the fourth phase in the fire developing curve. At such moment all of the combustible material will burn until one of the three elements for the combustion is removed. The “cooling down” is the last phase of a burning event, where one of the elements heat, combustible material or oxygen has been removed and the fire is no longer burning.

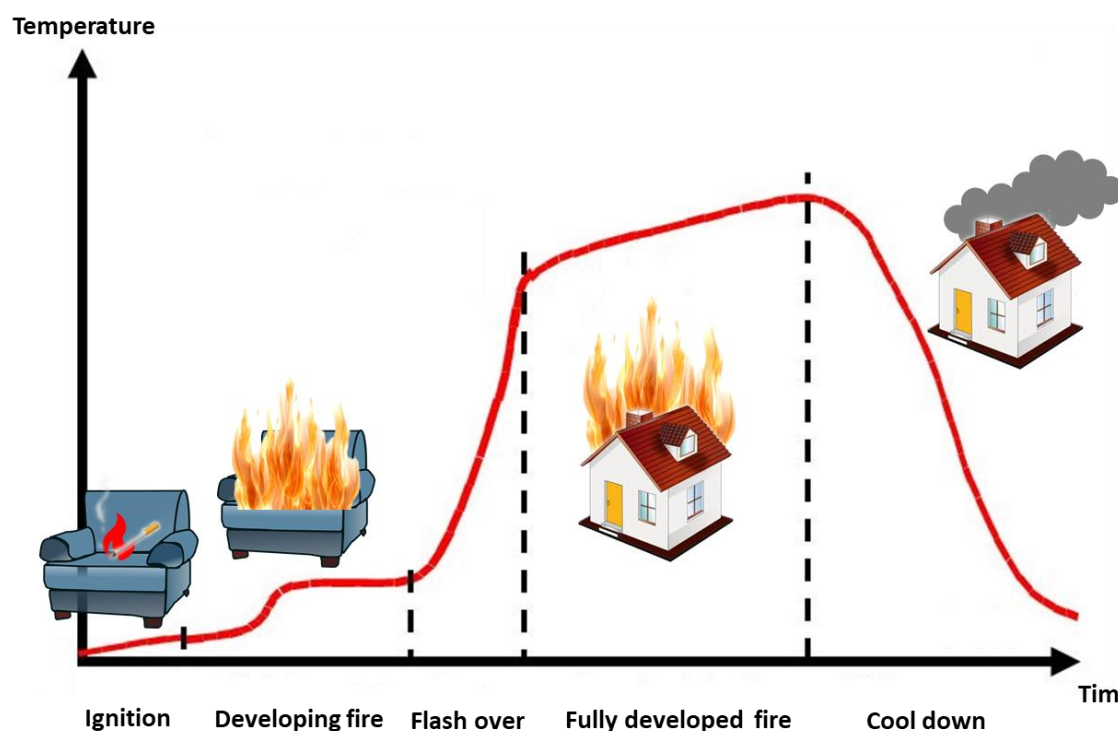


Figure 6: Fire developing curve showing the different stages of a fire in dependency of temperature (y-axes) and time (x-axes)

1.2.2. General mechanism of flame retardants

The application of flame retardant compounds (FRC) influence the first two steps of the developing of the fire. They can prevent the ignition or lead to self-extinguishing of the flame due to their properties which are described later in this paragraph.

Flame retardants are compounds which are added to surfaces as pre-treatment or post-treatment of organic materials like textiles and plastics. Their purpose is the inhibition of combustion by blocking the ignition, interfering with the heating of surfaces as well as preventing the degradation of the material. Even when a fire already started, flame retardants can help to prevent the spreading of the flames and provide extra time to extinguish the fire in the early stage of development.

Taking a look inside an average household, one can see the different use of flame retardants. They are used in furniture, wall insulations, curtains, flooring, clothing but also in technical devices like the housing of TV's, computers and many more.

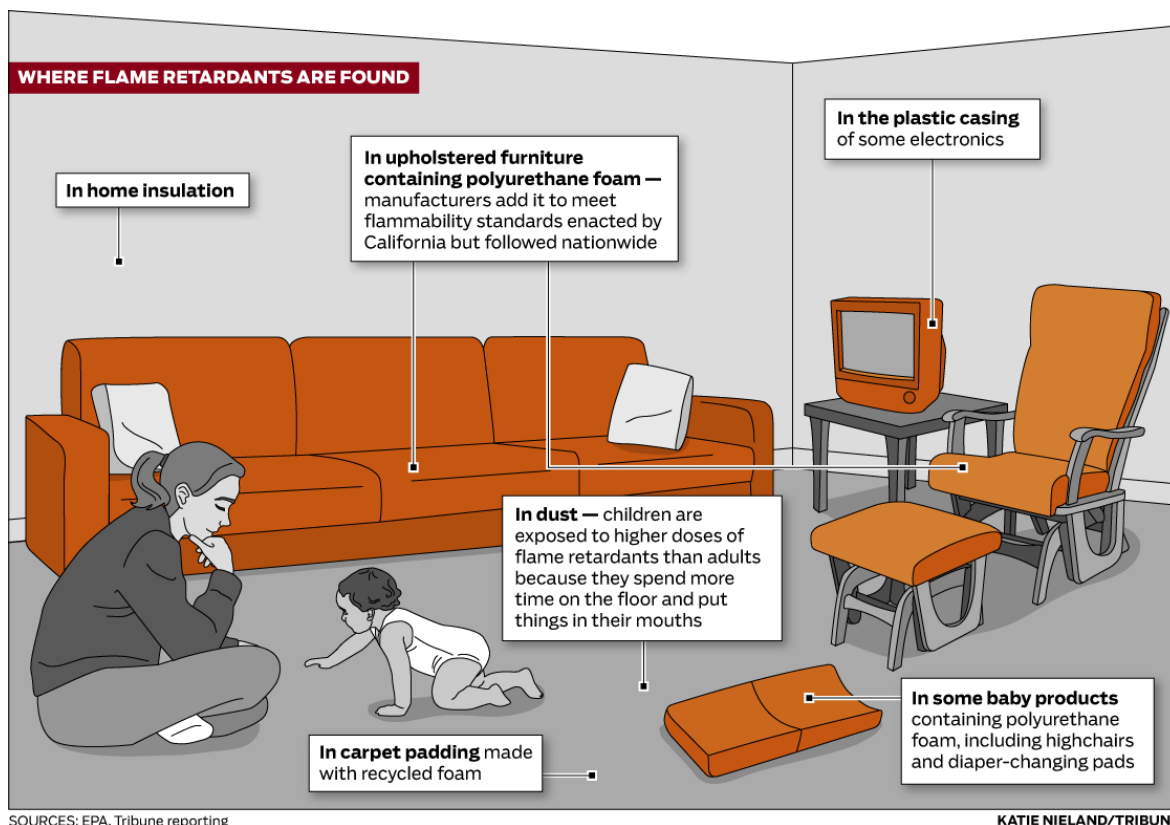


Figure 7: Flame retardants in an average living room

In general, there are three different ways of physical interaction. A first action is the reduction of temperature during combustion, by the release of water due to evaporation or by endothermic reactions. Another way of physical interaction is the release of inert gases during combustion, which leads to the dilution of the oxygen and the extinguishing of the flame due to a too low oxygen concentration. The third mode involves the formation of a solid layer which covers the combustible material and therefor blocks it for the combustion process. In the chemical modes of action, flame retardants can interfere in the gas and condensed phase where they favour the char formation which leads also to the extinguishing of the fire⁷.

1.2.3. Chemical structure and properties of FRC

1.2.3.1. Inorganic flame retardants

The most often used inorganic flame retardants are metal hydroxides with aluminium and magnesium compounds like aluminium trihydrate ($\text{Al}(\text{OH})_3$), bauxite (AlOOH) and magnesium hydroxide ($\text{Mg}(\text{OH})_2$). These compounds release water during endothermically degradation which leads to a cooling effect, as well as to a dilution in the gas phase. Another effect during the combustion of these compounds is the formation of a ceramic layer on the surface⁷.

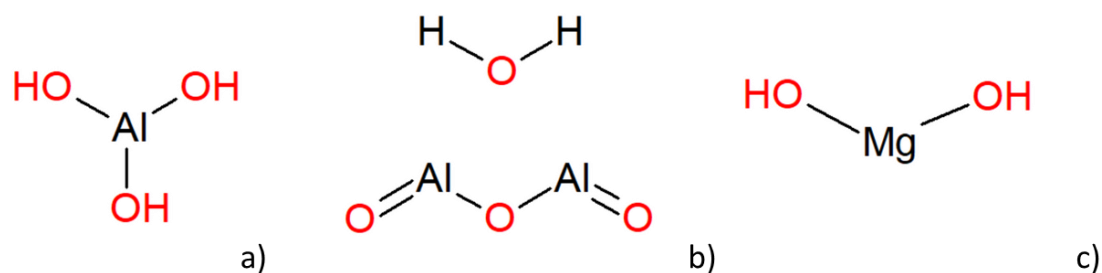
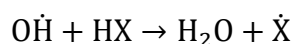


Figure 8: Chemical structures of inorganic flame retardants: a) aluminium trihydrate, b) bauxite and c) magnesium hydroxide

1.2.3.2. Halogenated flame retardants

Within the class of halogenated flame retardants, chlorine and bromine compounds are the most prominent and often used. The main reaction of halogenated flame retardants occurs in the gas phase, in which they remove H and OH radicals and therefore prevent further heat formation and thermal combustion. The inhibition reaction (1) is described in the following, where X represents the halogen atom.



Due to the high toxicity and environmental impact, as described later, the use of these kinds of flame retardants has drastically decreased. Furthermore, since 2003 the EU declared them as dangerous for the environment and very toxic to aquatic organisms⁸.

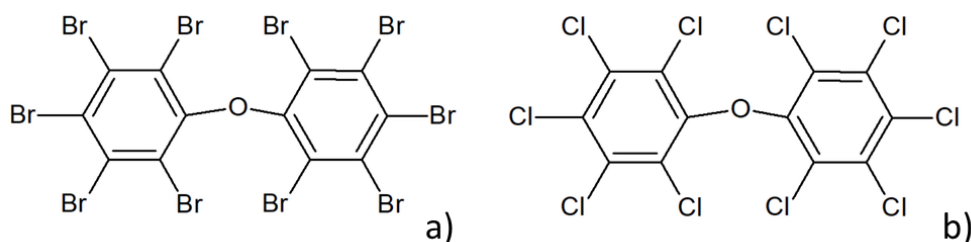
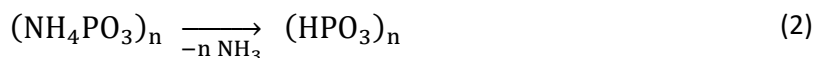


Figure 9: Chemical structure of brominated and chlorinated flame-retardant compounds: a) decabromodiphenyl ether, b) decachlordiphenyl ether

1.2.3.3. Phosphorus-based flame retardants

This class of flame retardants is most often used for natural and synthetic fibres and fabrics. Their main mode of action is during the solid phase of combustible material in which the phosphorus, when heated, reacts to form phosphoric acid (2). The

phosphoric acid leads to char formation and inhibits the pyrolysis necessary for the growth of the flame. They can be applied to the materials during the polymerization of plastics or by coating of the surface, where they can be chemically bound.



In combination with phosphorus containing flame retardants, often nitrogen compounds are applied. These compounds can release ammonia during combustion (2), which can lead to a dilution in the gas phase, resulting in the extinguishing of the flame.

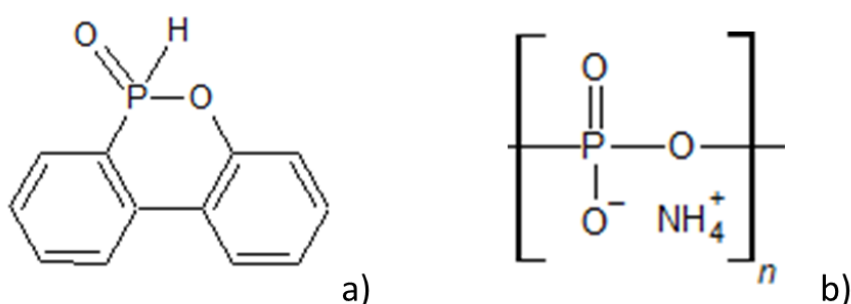


Figure 10: Structure of phosphorus and nitrogen containing flame retardants: a) 9,10-Dihydro-9-oxa-10-phosphaphenanthren-10-oxide (DOPO), b) ammonium polyphosphate

1.2.4. Environmental impact of commercial flame retardants

The impact to the environment is rather low for the inorganic and phosphorus/nitrogen containing flame retardants compared to the high toxicity and environmental pollution caused by brominated and chlorinated ones. Watanabe and co-workers⁹ showed that the major emission of brominated and chlorinated compounds is caused by factories producing brominated (BFR's) and chlorinated (CFR's) flame retardants, as well as electronic equipment, where flame retardants are used to protect their housing from burning. Furthermore, during the burning of waste, containing BFRs and CFRs in waste incineration plants these compounds are released, which causes major problems for the environment (Figure 11). The thermal breakdown leads to lower brominated and chlorinated compounds, which are more soluble in water, volatile and bio-accumulative compared to the higher ones. The fact of water-solubility and bio-accumulation causes major health risks and problems for aquatic organisms and as consequence also for humans due to their dietary.

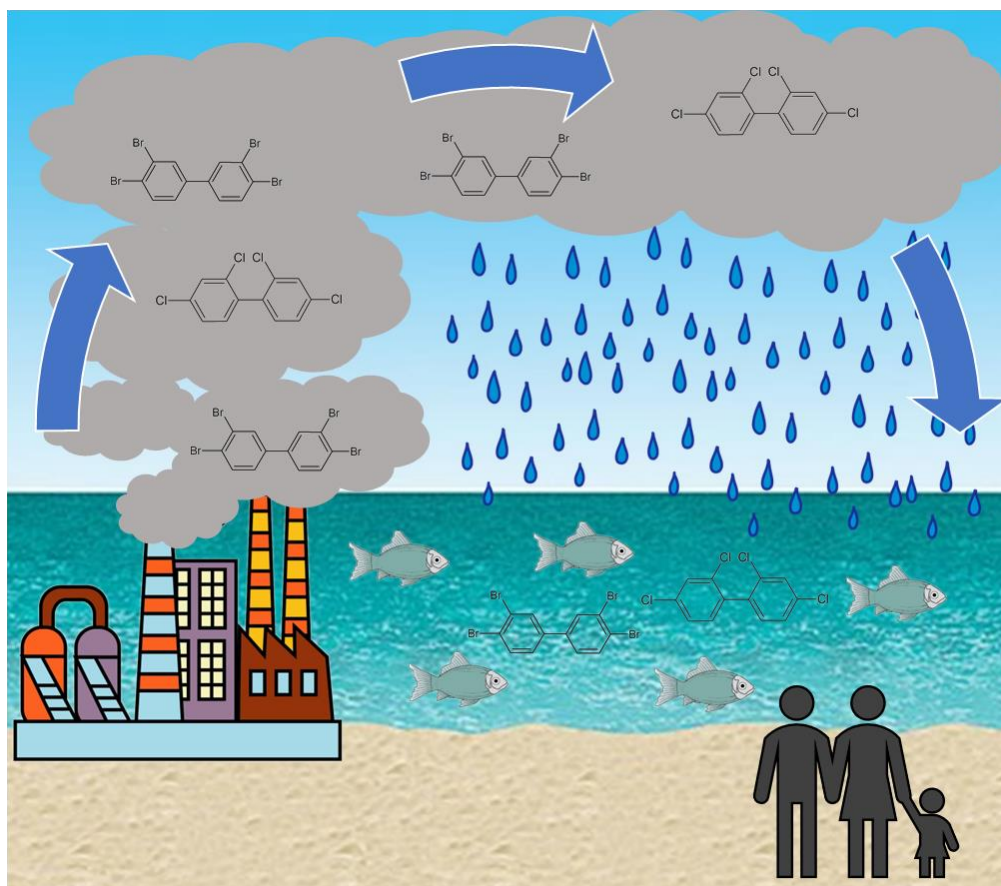


Figure 11: The way of BFRs and CFRs from the production facility into the aquatic environment and how they came in contact with humans.

Swedish scientists¹⁰ for example found polybrominated diphenyl ethers (PBDEs) in a concentration ranging from 27 mg/kg fat in the muscle to 110 mg/kg fat in the liver of fish. The most cases of PBDEs found in humans are reported in North America and were significantly higher compared to Europe and Japan. Betts and co-workers¹¹ found a concentration of PBDEs in human milk of about 200 ng/g lipid in Austin, Texas and Denver, Colorado. PBDEs can have critical effects like neurotoxicity and altered thyroid hormone homeostasis¹⁰. Due to the negative environmental and health impacts, the use of brominated and chlorinated flame retardants has already been banned in the EU and the world health organisation (WHO) also concluded that humans and environment should be protected from these compounds⁸.

1.2.5. Novel and green flame retardants

As results of the negative impact of the mentioned FRC, the research of eco-friendly alternatives is needed. The strong interest of new sustainable chemistry technologies increased since the beginning of the twenty-first century. In this sense,

biotechnologies proved to be a useful resource of tool and methodologies for polymer chemistry applications.

1.2.5.1. Proteins

Whey proteins, which make about 20 % of the total protein content in milk, consist to a high extend of α -helical structures and are available in 3 major forms, which are whey protein concentrate (WPC), whey protein isolate (WPI) and whey protein hydrolysate (WPH). WPI coatings were already successfully applied on cellulose fibres and cotton where they could inhibit the thermal degradation due to their moisture adsorption features and dilution of the gas phase¹².

Another class of proteins, which have successfully been used as flame retardant coating, are caseins. They represent the biggest fraction of milk proteins and are produced during the production of skim milk. Among the different classes of caseins, α - and β -caseins show the most prominent flame-retardant properties. The highly phosphorylated compounds in α -caseins, leading to the formation of phosphoric acid during combustion, as well as the glutamine-rich β -caseins which can release ammonia, make caseins interesting as flame-retardant coating for different fabrics¹².

Hydrophobins, produced by filamentous fungi, are a group of small proteins with low molecular weight, consisting of 70 – 350 amino acids. They self-assemble at the surface between medium and air to lower the water surface tension, allowing the hyphae of the fungi to reach the medium-air interface. Hydrophobins can be divided in 2 classes, the class I proteins (HFB I) which form highly insoluble aggregates and the class II hydrophobins (HFB II) forming aggregates which are highly soluble in aqueous solutions. Both classes consist of a four-stranded β -barrel core surrounded either by β -sheets and α -helixes connected *via* relatively unstructured loop regions (HFB I) or only α -helixes and are more structured (HFB II)¹³. They already find application as coating agent, in surface modification and other functions like as flame-retardant substances. During combustion, hydrophobins can release sulfuric acid due to the thermal breakdown of the disulphide bonds between the cysteine residues, which leads to char formation. It has already been reported that

hydrophobins could increase the total burning time and decrease the total burning rate of fabric on the other hand¹².

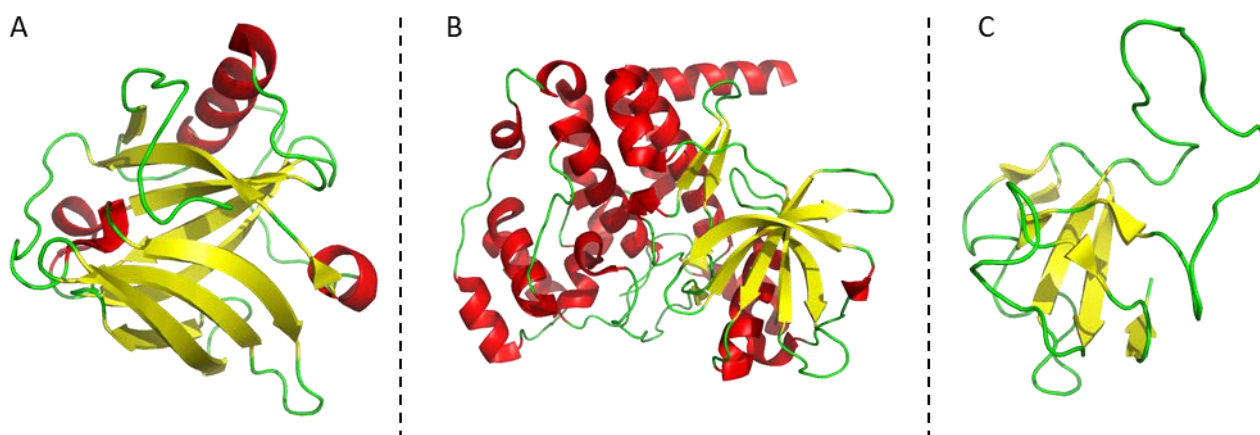


Figure 12: Different types of proteins used as flame retardant compound with secondary structures coloured in yellow (β -sheets), red (α -helices) and green (loop regions): A) Whey protein (2R73), B) alpha-casein (5TS8) and C) Hydrophobin class I (2FMC). Modelled *via* pymol (pymol.org)

1.2.5.2. DNA as flame retardant

The DNA double helix consists of two single strands of nucleotides. Each nucleotide contains one of the four nitrogen-containing bases adenine, guanine, cytosine or thymine. Together with a deoxyribose unit and a phosphate group, they built up the sugar phosphate backbone of the DNA. The two antiparallel single strands are connected *via* hydrogen bonds to form the well-known α -helical structure with minor and major groove in between (Figure 13). The availability of DNA has already become competitive to those of other chemicals as described by Grote and co-workers, which developed a large-scale method for the extraction of DNA out of salmon milt and roe sacks in waste products of Japanese fishing industry¹⁴. Furthermore, alternative sources of waste like spend brewer's yeast¹⁵ and vegetable waste¹⁶ have been proven to be potential sources for DNA and can present a cheap alternative to chemical flame retardants. Several studies already proved the potential of DNA as flame retardant for example on cotton and wool fabrics¹⁷. By comparing DNA with the commercial available flame retardants, DNA provides all requirements to be used as a flame-retardant compound in only one molecule. The nitrogen present in adenine, guanine, cytosine and thymine as well as deoxyribose units acting as carbon source, have the potential to release ammonia and carbon dioxide upon heating, which are non-combustible gases and can lead to self-extinguishing by displacing the oxygen. Furthermore, the sugar-phosphate

backbone can release phosphoric acid during combustion, which leads to degradation and char formation and in further consequence to the barrier of the combustible material¹⁷. Another advantage of using DNA is that a high purity is not necessary because also impurities like proteins can have positive effects due to their nitrogen content.

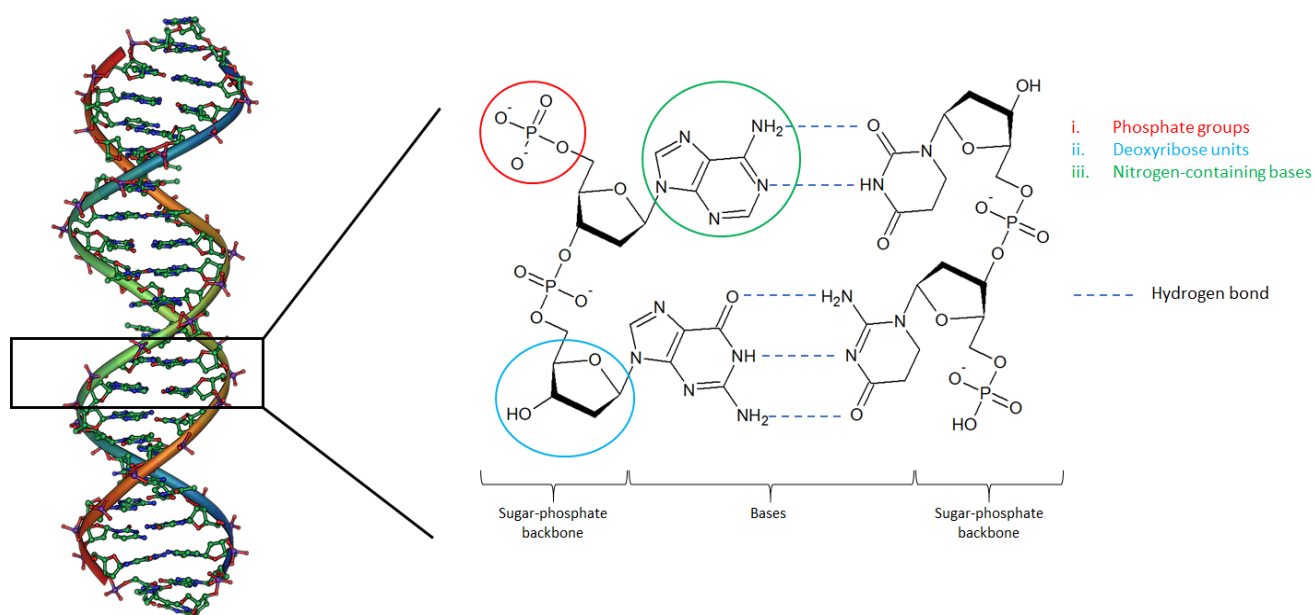


Figure 13: DNA double helix (left) and the close up of two single strands connected *via* hydrogen bonds (right). Compounds with flame retardant properties marked in red, blue and green (right).

1.3. Surface functionalization of PET and Nylon

Due to the crystallinity and hydrophobicity of synthetic fibres, it is hard for chemicals to penetrate into or bind to the surface of the fabric. In order to increase the surface reactivity, the main goal of functionalization is the introduction of more carboxylic (-COOH) and amine (-NH₂) groups. By the introduction of these groups, biomolecules like proteins, DNA and enzymes can easier bind to them or interact with the surface of the polymer. There are different methods for the pre-treatment of these polymers like alkaline, plasma or enzymatic treatment.

1.3.1. Alkaline treatment

The alkaline treatment of PET and Nylon is performed at high temperatures with sodium hydroxide (NaOH), which leads to the hydrolysis of the polyester bonds increasing the hydrophobicity of the fabric. Drawback of this treatment is the loss of bulk properties of the fabric, especially the strength is negatively affected.

Furthermore, the hydrolysis with NaOH is more chemical consumption (water and acid solutions) since it requires the neutralization of the pH⁴.

1.3.2. Plasma treatment

A technique which is not completely accepted by the textile industry is the treatment of PET and Nylon fabric with plasma. This method is rather expensive, difficult to control. Moreover, the non-specific behavior of this process can cause ageing of the polyester, as possible results for the rearrangement and different orientation of the polar groups⁴.

1.3.3. Enzymatic treatment

Enzymatic treatment of PET and Nylon fibres and fabric has been investigated by scientists in the last decades. The advantages of enzyme application is the rather mild and eco-friendly conditions, in terms of pH, temperature and chemicals which need to be added, made enzymes a green alternative to the alkaline and plasma treatment. The most promising results in surface modification were reported in literature among the enzyme classes of laccases (EC 1.10.3.2), lipases (EC 3.1.1.3), esterases (EC 3.1.1) and cutinases (EC 3.1.1.74). Main advantage of the enzymatic treatment is that pitting corrosion, like in alkaline treatment, does not occur and that the surface treatment of PET and Nylon is homogenous⁴.

1.3.3.1. Cutinase

Cutinases belong to the class of α/β Hydrolases, a class of relative small (20-30 kDa) enzymes which cleave esters into an acidic part and an alcoholic part.

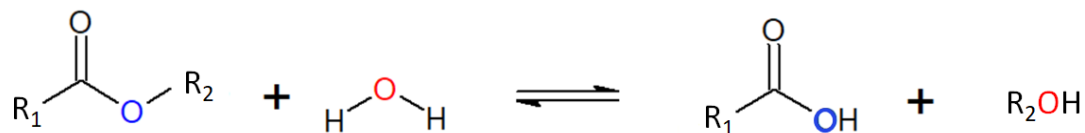


Figure 14: Hydrolysis reaction mechanism

A characteristic that all esterases have in common is a classical Ser-His-Asp catalytic triad (Figure 15, 16) where the catalytic serine is exposed to the solvent. Within the class of esterases, lipases are one of the most important biotechnological enzymes involved in hydrolysis, esterification and transesterification reactions. Lipases, in difference to esterases, have an additional “lid” structure covering the

active site when the enzyme is in aqueous solution. In presence of an interface (e.g. oil-water emulsion) the conformation changes to the open form in a mechanism called “interfacial activation” which leads to an increase in activity¹⁸. Cutinases do not have a hydrophobic lid which covers the active site and therefore the active site is large enough to accommodate also high molecular weight synthetic polymers like PET. The catalytic reaction in cutinases is performed in two steps with a covalent intermediate, linking the serine of the catalytic triad to the carbonyl group of the ester which is going to be hydrolysed. For the stabilisation of the transition state in the enzyme mechanism, an oxyanion hole consisting of a serine and a glutamine is for importance¹⁹.

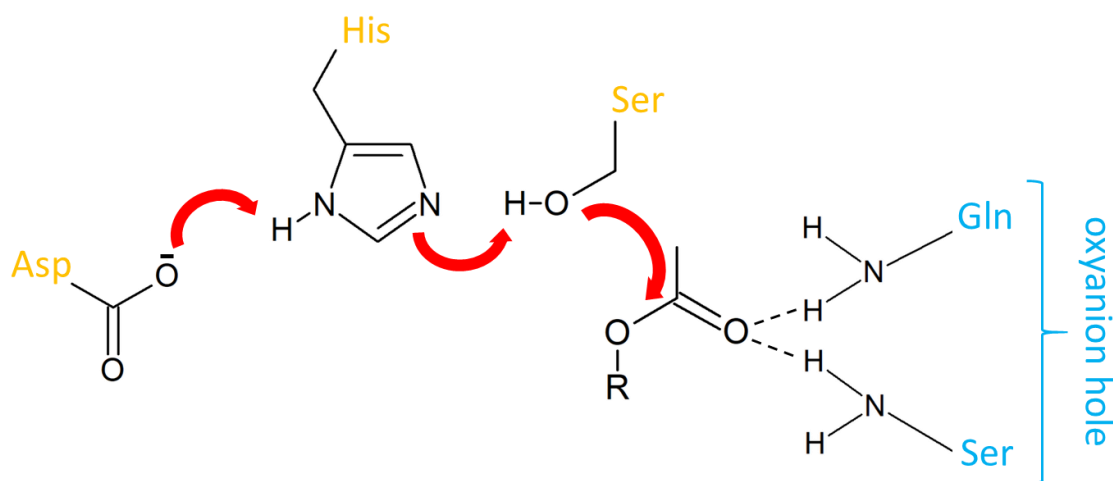


Figure 15: Reaction within the catalytic triad of *Humicola insolens* cutinase and the stabilizing oxyanion hole

In this work we used a cutinase from *Humicola insolens* (HiC) (CAS 9001-62-1) which is a thermophilic fungus able to grow at temperatures up to 60 °C and neutral pH (pH 7). HiC is built up of a 5 parallel β -sheets, surrounded by α -helices on both sides and has a molecular weight of about 20 kDa. The catalytic triad is formed by three amino acids (S105-H173-D160)²⁰.

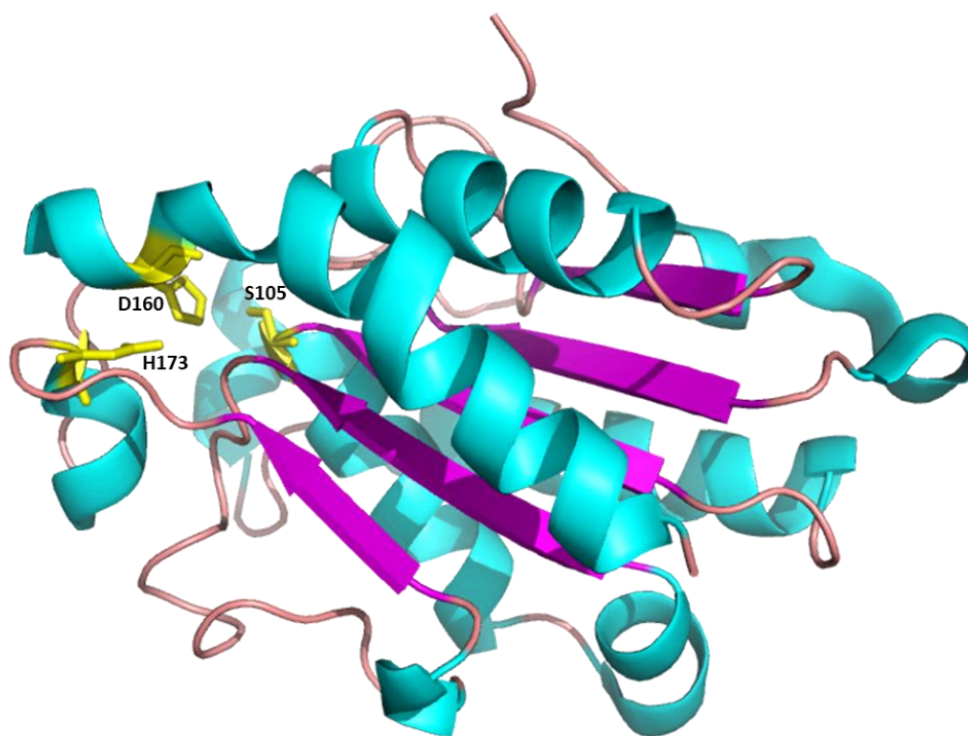


Figure 16: Tertiary structure of *Humicola insolens* cutinase (4OYL) with the β -sheet structure (purple), the α -helices (light blue) and the catalytic triad (yellow). Modelled *via* pymol (pymol.org)

1.3.3.2. Dihydropyrimidase (DHPase)

The enzyme belongs also to the class of hydrolases described before. The degradation of pyrimidines as thymine and uracil to β -alanine is done in four enzymatic steps, involving the enzyme Dihydropyrimidas (EC 3.5.2.2). In a first step of the reductive pathway, pyrimidines are converted to dihydropyridines by the enzyme dihydropyridine dehydrogenase (EC 1.3.1.2.) followed by hydrolytic ring opening and the conversion to ureidopropionic/ureidoisobutyric acid by DHPase as the second step. The enzyme β -ureidopropionase (EC 3.5.1.6.) catalyses the third step of the reaction by converting β -ureidopropionic/ β -ureidoisobutyric acid into (R)-3-amino-2-methylpropanoate followed by the last step in which the enzyme (R)-3-amino-2-methylpropionate-pyruvate transaminase (EC 2.6.1.40) catalyses the reaction to the amino acid L-alanine²¹.

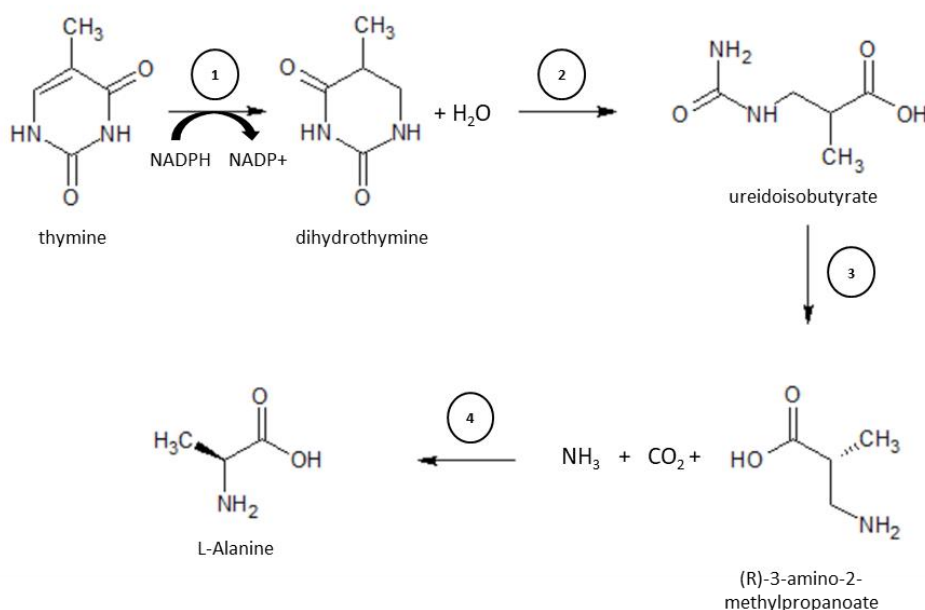


Figure 17: Degradation pathway of pyrimidines involving four enzymatic reaction steps including DHPase

The DHPase used in this study is from the yeast *Saccharomyces kluyveri*, which naturally uses this enzyme for the biosynthesis of pantothenate and coenzyme A at neutral pH (pH 7) and 50 °C. *S. kluyveri* DHPase is made out of 4 chains with a total length of 559 amino acids and a molecular weight of approximately 250 kDa. The structure is similar for different DHPase's, consisting of a dizinc catalytic centre in each subunit which is located inside a (β/α)₈-barrel structured core, coming with a small β-sandwich domain at the side. Amino acids involved in the ligation of the dizinc centre are the His199, Asp255, Asp358, His62, His64 and the Lys167 which forms a bridge with the metal ions. Furthermore, the two zinc ions are linked with a hydrolytic water molecule²². The binding of substrate with the active site via hydrogen bonds, involves two amino acids (Asn392- Ser331) (Figure 18).

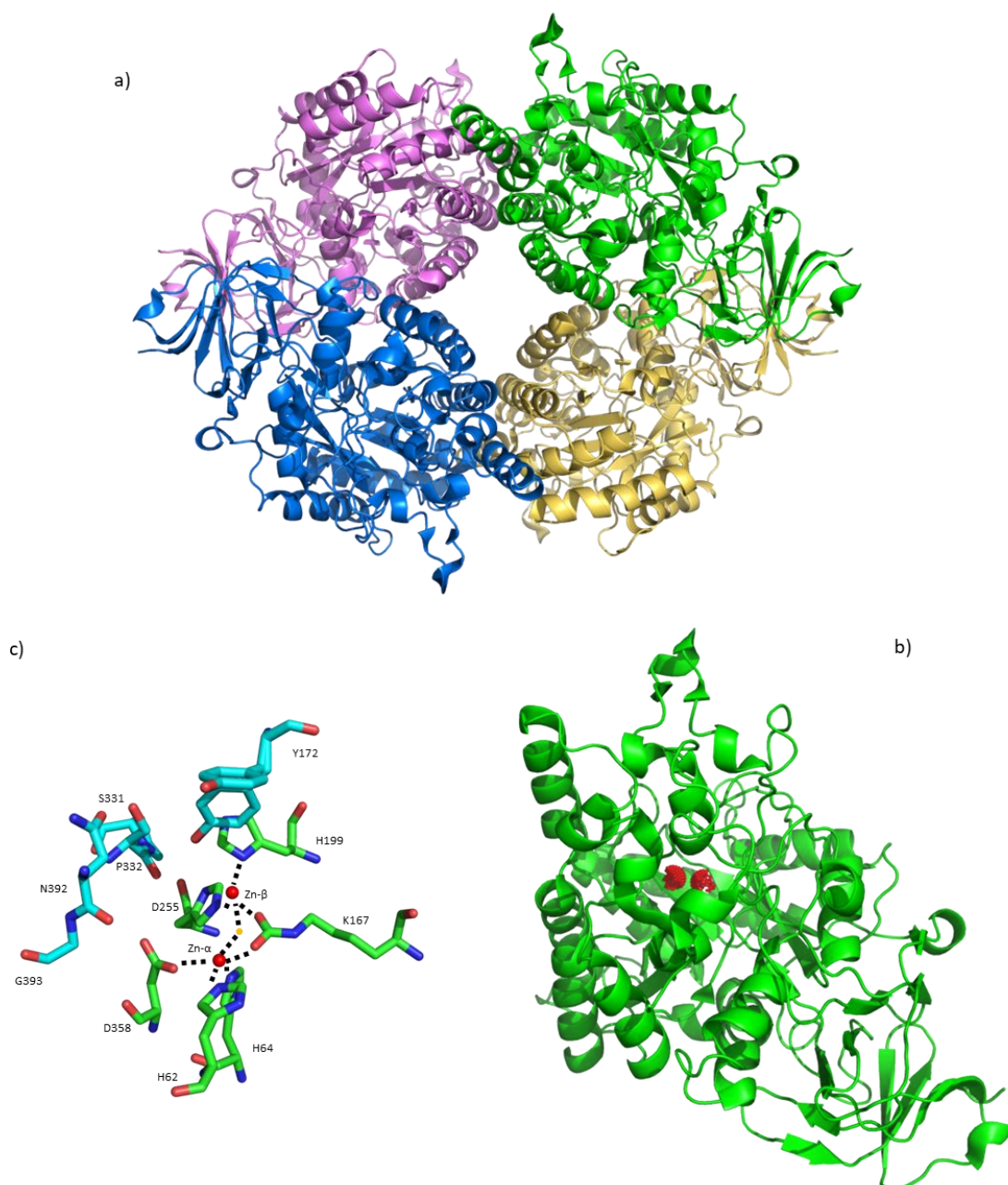


Figure 18: Structure of DHPase (2DTY): a) the overall tertiary structure consisting of four subunits (purple, green, gold and blue), b) single subunit with dizinc catalytic centre (red spheres), c) amino acids which are involved in the ligation of the catalytic zinc centre (green) and substrate binding (blue). Modelled *via* pymol (pymol.org)

1.4. Enzymatic functionalization of PET and Nylon

Cutinase and Dihydropyrimidase, used in this study, are enzymes which have already been investigated for their ability to degrade polymers like PET and Nylon. Haernvall and co-workers²³ for example showed that cutinases and lipases from wastewater organisms like *Pseudomonas pseudoalcaligenes* or *Pseudomonas pelagia* were able to degrade phthalic acid based polyesters like PET. In another study, different cutinases from *Thermobifida cellulosilytica* were used to create more carboxyl and hydroxyl groups on the surface of HLMS-Polyethylene terephthalate

fabrics, to improve the adhesion on rubber²⁴. Furthermore, HiC has already been investigated for its ability to functionalize and degrade poly lactic acid (PLA)²⁵.

One of the main goals of this thesis was to functionalize PET and Nylon fabric in order to improve the surface reactivity for the attachment of biomolecules, like DNA in this study. This can be achieved by enzymatic hydrolysis of the polymer chains leading either to more carboxyl (-COOH) and hydroxyl (-OH) groups on the surface of PET-fabrics or more -COOH and amine (-NH₂) groups in the case of Nylon (Figure 19). In hydrolysis reaction of both enzymes, polyester bonds are cleaved and the resulted release products can be measured *via* HPLC. In the case of PET, the hydrolysis causes fragmentation into terephthalic acid (Ta), mono-hydroxy ethylene terephthalate (MHET) and bis-hydroxy ethylene terephthalate (BHET). On the other hand, enzymatic hydrolysis of Nylon fabric leads to the formation of 6-aminocaproic acid (6-ACA), resulting in more -NH₂ and -OH reactive groups on the surface. Furthermore, 6-ACA undergoes a ring-closing reaction leading to the formation of caprolactam (CL) which can be measured via HPLC.

In this way generated reactive groups on PET and Nylon were then used to attach DNA with low molecular weight to the surface of the fabric either with linking molecules in between or directly to the reactive groups.

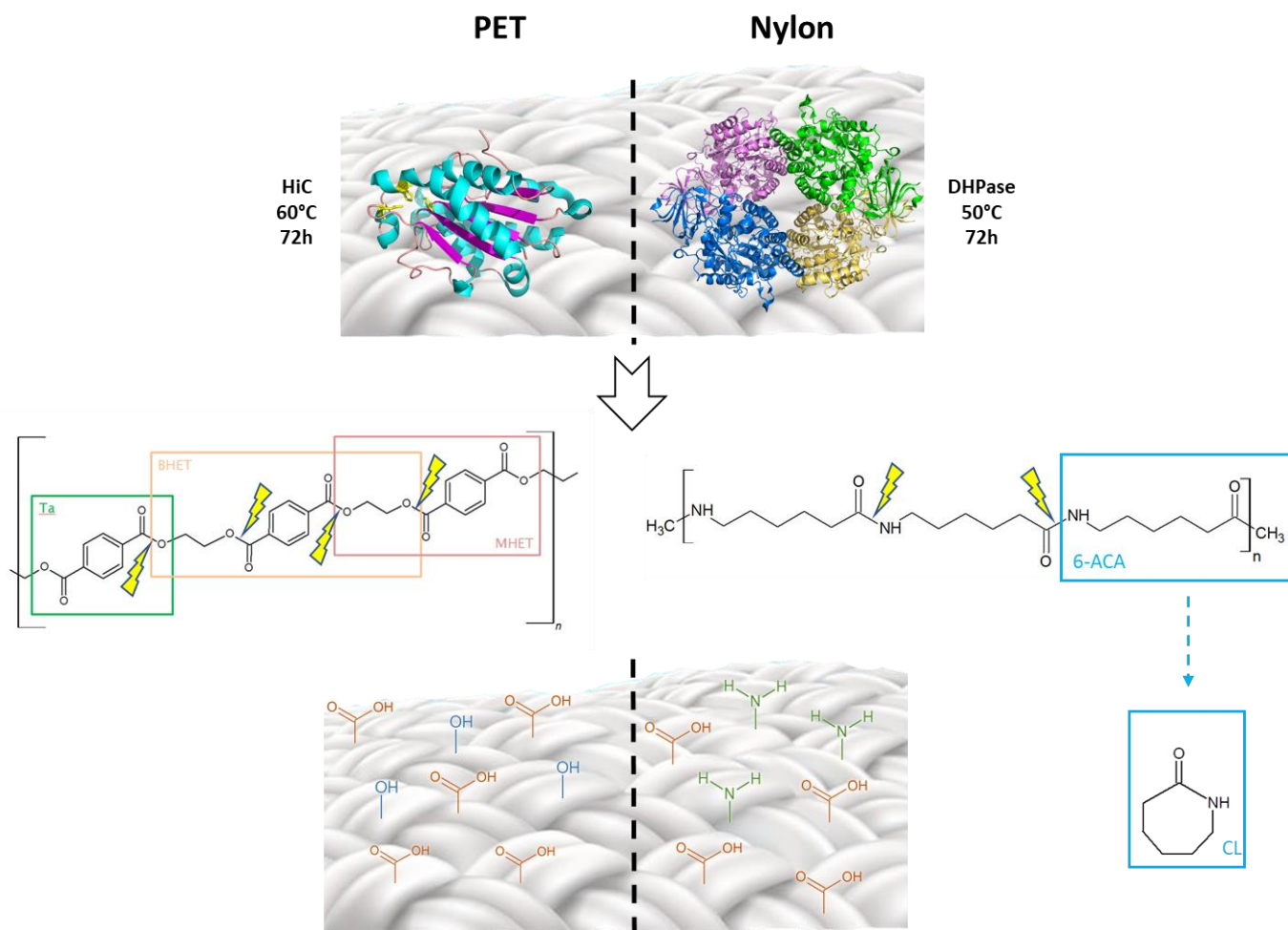


Figure 19: Enzymatic hydrolysis of PET and Nylon fabric with HiC (left) and DHPase (right). Yellow flashes representing the enzyme cleavage sites. Coloured squares indication the fractions which can be measured via HPLC.

1.5. DNA immobilisation

The immobilisation of biomolecules or chemicals on textiles can be done in different ways to give the material new and “smart” properties. The strategies of immobilisation can be classified into reversible and irreversible immobilisation, depending on the functionalization purpose. The use of crosslinking agents is one of the methods for irreversible attachment by binding the crosslinking molecules to the support surface and providing new functional groups. Another technique for irreversible immobilisation is the entrapment of biomolecules (e.g. enzymes) in gels or polymeric networks to enable the interaction with the surrounding environment and retaining tightly attached to the support at the same time²⁶. The most prominent way of irreversible binding proteins and other biomolecules to surfaces is covalent binding in which available functional groups like carboxylic- and amino-groups on

the surface are used to form covalent bonds between the support and the biomolecules²⁷. In case of DNA immobilisation, the irreversible binding of DNA to the polymer surface is favourable and will be described in more detail. When irreversible bound, the DNA cannot be detached from the surface without destroying the structure of support or DNA.

1.5.1. 1-Ethyl-3-(3-dimethylaminopropyl)carbodiimide/ N-Hydroxysuccinimide (EDC/NHS)

The EDC/NHS coupling system is a multistep reaction system to link carboxylic acid groups with primary amines. In this study, the EDC reacts in a first step with the obtained carboxylic groups on the PET and Nylon surface, leading to the formation of an o-acylisourea intermediate. This intermediate is unstable and reacts in the second step with the NHS to form an amine-reactive sulfo-NHS ester. In the last step of the reaction, the primary amine, in this case the DNA molecule, replaces the NHS and forms a stable amine bond with the carboxylic acid group.

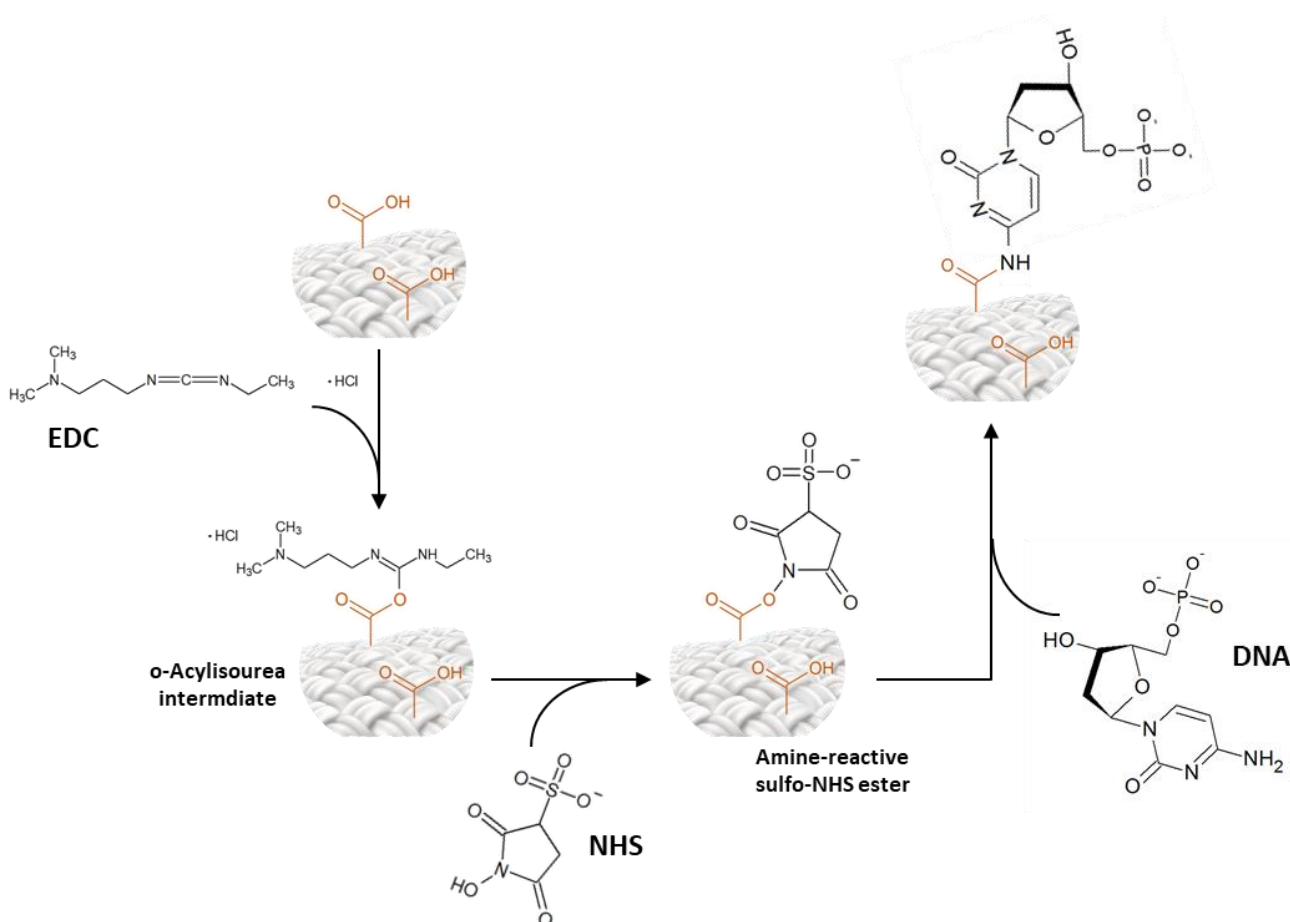


Figure 20: Reaction mechanism of EDC/NSH crosslinking system

1.5.2. Dopamine

Dopamine is a small catecholamine molecule formed by the decarboxylation of L- DOPA. It is a precursor for norepinephrine and epinephrine which function as neurotransmitter in the brain. It became interesting for scientists because of its amine and catechol functional groups which mimic the structure of mussel adhesive proteins.

In nature, these compounds are used by mussels for the attachment to wet surfaces²⁸. Due to its ability to form thin polydopamine layers on inorganic and organic surfaces at alkaline pH, dopamine has been investigated by several research groups. In literature are present different examples where polydopamine film shows application for binding macromolecules (like trypsin or other peptides) for polymer surface coating^{28,29}.

As well the coupling with EDC/NHS, after the enzymatic treatment, both polymers were coated with dopamine at alkaline pH. In a first step, the dopamine binds to the free carboxyl groups of the fabric surface leading to a dopamine coated polymer with catechol functional groups. Afterwards, DNA molecules bind to the dopamine and form stable amine bonds. This method leads to a brownish colour of the samples after dopamine coating which results from oxidation (as from the production of melanin).

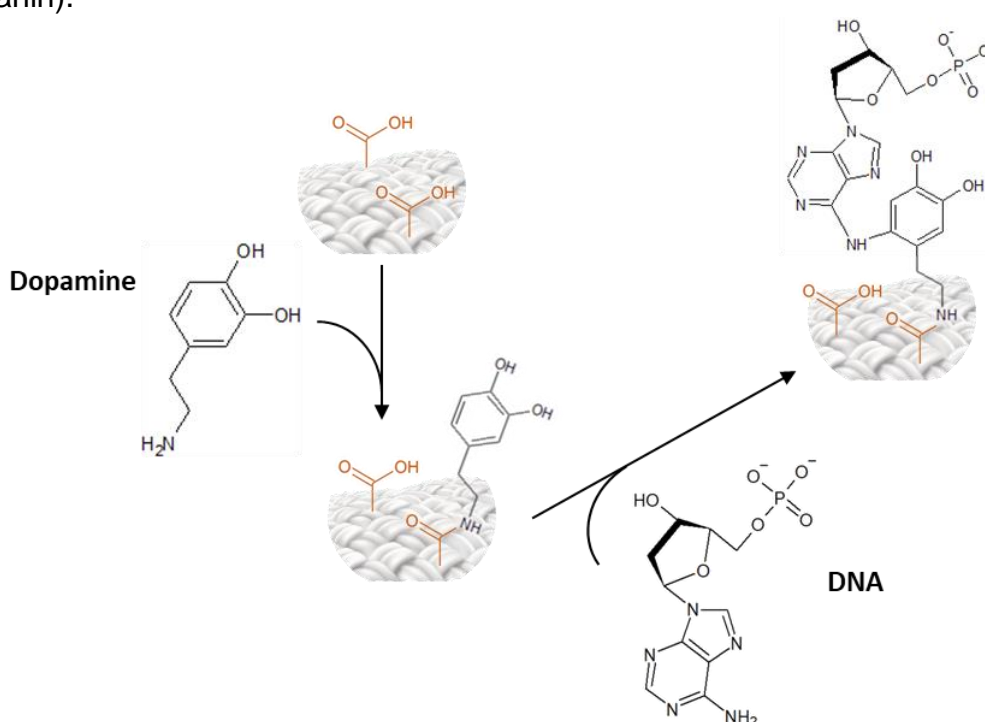


Figure 21: DNA immobilisation using dopamine as linker between the polymer surface and the DNA

1.5.3. Tyrosine

L-Tyrosine is a proteinogenic amino acid, with an aromatic ring and polar side group. It's a non-essential amino acid, since it's synthesized from phenylalanine (essential amino acid). It also represents the precursor of L-Dopa, necessary for dopamine production and after as neurotransmitter hormone.

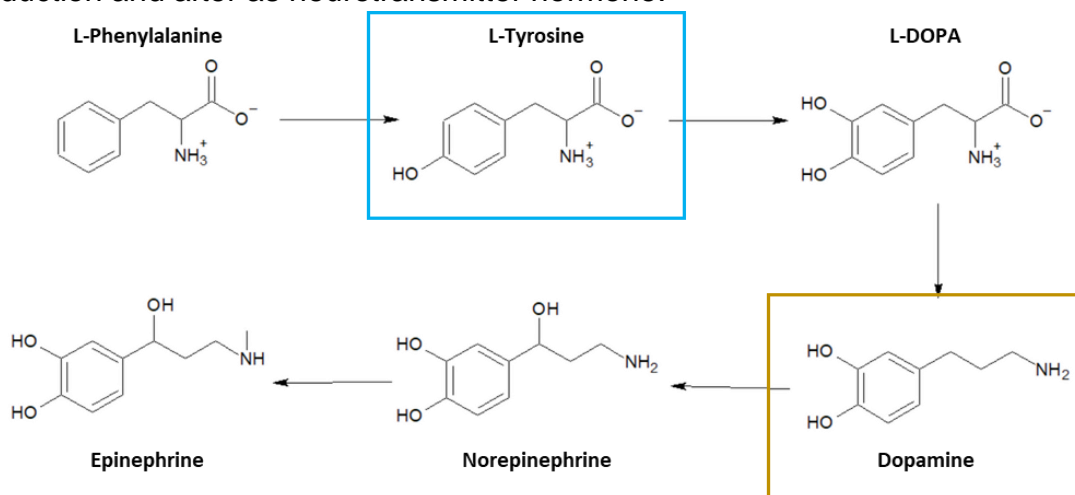


Figure 22: Synthesis pathway of neurotransmitters in the brain involving the precursors L-Tyrosine (blue square) and dopamine (brown square).

By looking on the structure, tyrosine provides two functional groups, an $-NH_2$ and an $-COOH$ group. This makes it possible for tyrosine to bind the free carboxyl groups on enzymatic treated PET and Nylon surfaces. Furthermore, tyrosine can be bound to free amide groups on the surface of Nylon via its $-COOH$ group.

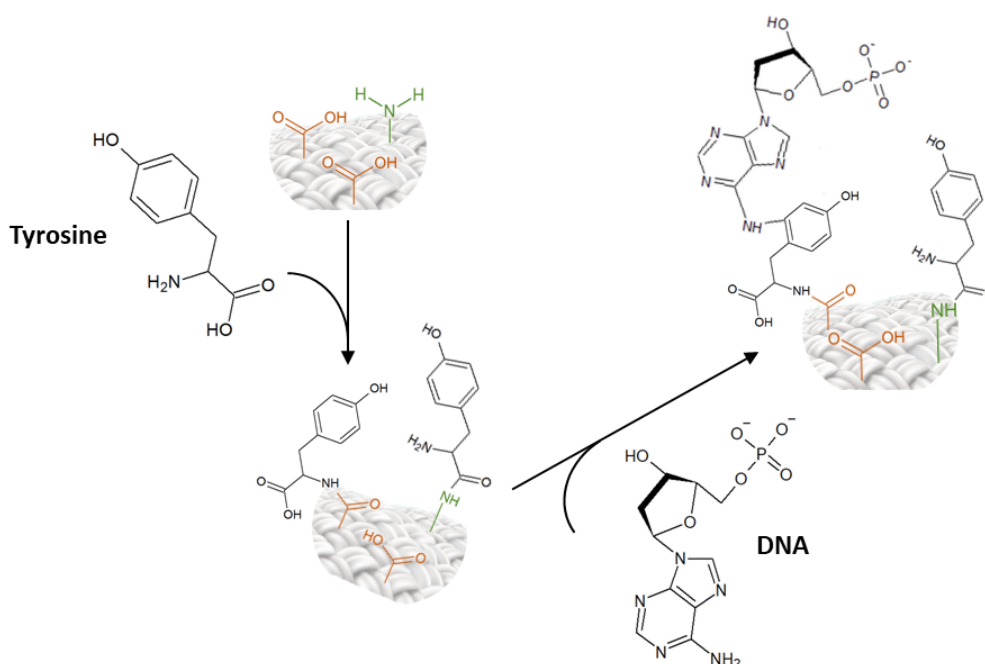


Figure 23: DNA immobilisation using tyrosine as linker between the polymer surface and the DNA

2. Material and Methods

2.1. List of Chemicals

2.1.1. Enzyme Characterization

- Bradford colour reagent 5x (SIGMA ALDRICH USA)
- Protein Standard BSA 2 mg/mL (SIGMA ALDRICH USA)
- Potassium Phosphate (SIGMA ALDRICH USA)
- MQ-H₂O (18.2 MΩcm, sartorius arium® pro GER)
- *p*-Nitrophenyl butyrate (SIGMA ALDRICH USA)
- DMSO (SIGMA ALDRICH USA)
- Glycerol (SIGMA ALDRICH USA)
- 2-mercaptoethanol (SIGMA ALDRICH USA)
- Sodium dodecyl sulfate (SDS) (SIGMA ALDRICH USA)
- Bromophenol blue (SIGMA ALDRICH USA)
- TRIS Hydrochloride (Carl ROTH GER)
- Running buffer (10x Tris/Glycine/SDS) (SIGMA ALDRICH USA)
- Protein Molecular Weight Marker (10-250 kDa) (MyBioSource USA)

2.1.2. Washing steps

- Triton™ X-100 (SIGMA ALDRICH USA)
- Sodium Carbonate (SIGMA ALDRICH USA)
- Thermo-shaker (IKA® KS 4000 GER)

2.1.3. Sample Characterization

- Methylene Blue (SIGMA ALDRICH USA)
- Coomassie Brilliant Blue (SIGMA ALDRICH USA)
- Methanol (EMD Millipore USA)
- Acetic Acid (SIGMA ALDRICH USA)

2.1.4. DNA Immobilisation

- DNA (low mol. weight, from salmon sperm) (SIGMA ALDRICH USA)
- Agarose (EMD Millipore USA)
- TAE buffer (50x Tris/Acetic Acid/EDTA (TAE)) (BIO RAD USA)
- 10000x SYBR® Green I nucleic acid gel stain (Molecular Probes USA)

- 6x Orange DNA Loading Dye (Thermo Fisher USA)
- O`RangeRuler 10 bp DNA Ladder (Thermo Fischer USA)
- 2-(N-morpholino)ethanesulfonic acid (MES) (SIGMA ALDRICH USA)
- 1-Ethyl-3-(3-dimethylaminopropyl)carbodiimide (EDC) (SIGMA ALDRICH USA)
- N-Hydroxysuccinimide (NHS) (SIGMA ALDRICH USA)
- Dopamine hydrochloride (SIGMA ALDRICH USA)
- L-Tyrosine (SIGMA ALDRICH USA)

2.2. Methods

2.2.1. Protein concentration

The protein concentration of HiC and DHPase was determined according to the method of Bradford³⁰. 20 μ L of the diluted samples were pipetted in triplicates in a 96-well plate (Greiner 96 flat transparent, SIGMA USA) and 200 μ L of Bradford colour reagent were added. The reaction was allowed to take place for 5 minutes at room temperature. The colour change from red to blue was measured in an infinite M200PRO Tecan plate reader photometer at 595 nm. For the determination of the protein concentration, a standard curve with bovine serum albumin (0.0125 – 0.1 mg/mL) was measured as well as a blank containing only buffer (potassium phosphate 0.1 M in MQ-H₂O, pH7) instead of protein.

2.2.2. Esterase activity assay

The activity was measured with a photometric assay using the substrate p-nitrophenyl butyrate which releases a chromophore (p-nitrophenolate) during hydrolysis, which can be measured spectrophotometrically at 405 nm. At first 11 mg of p-nitrophenyl butyrate were dissolved in 1 mL dimethyl sulfoxide (DMSO) resulting in solution A. 100 μ L of solution A were mixed with 900 μ L buffer (potassium phosphate 0.1 M, pH7) to produce solution B. As last step of the substrate preparation, 500 μ L of solution B were mixed with 22 mL buffer, resulting in substrate solution C. All the preparation steps have to be performed on ice and under absence of light. For the measurement in the photometer, 200 μ L of the substrate solution C were pipetted in a 96-well plate and 20 μ L of the protein solution was added afterwards. The release of the chromophore was measured for 10 min

with a cycle every 18 sec at 30 °C in an infinite M200PRO Tecan plate reader photometer (Tecan Trading AG, Switzerland) at 405 nm³¹.

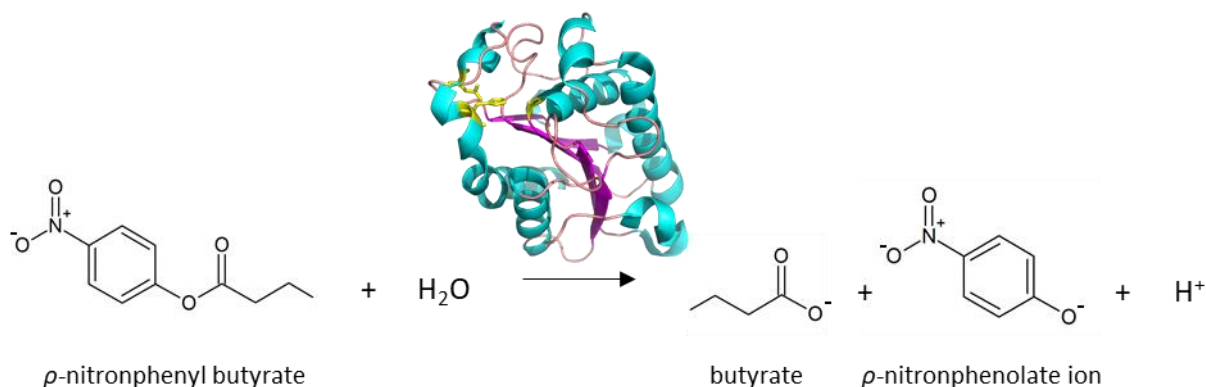


Figure 24: Reaction mechanism of the esterase activity assay

2.2.3. DHPase activity assay

Activity of DHPase was determined spectrophotometrically at 225 nm, by measuring the change in absorbance due to the hydrolysis of the Dihydrouracil (DHU) ring at 30 °C³². For the standard assay, the reaction mixture contained 200 µL of substrate solution (0.25 mM Dihydrouracil in 0.1 M potassium phosphate buffer, pH8) and 20 µL enzyme solution. The molar absorption coefficient for DHU at 225 nm is 1287 M⁻¹ cm⁻¹.

2.2.4. SDS-PAGE

To determine the size of the enzymes, a sodium dodecyl sulphate – polyacrylamide gel electrophoresis (SDS-PAGE) was performed. 20 µL of enzyme sample were mixed with 20 µL Laemmli buffer (20/10/4/0.004 (%), glycerol/2-mercaptoethanole/SDS/bromophenol blue in 0.125 M TRIS/HCl, pH6.8) and incubated for 5 min at 100 °C. For the electrophoresis, 4-15% Mini-PROTEAN™ TGX Stain-Free™ Protein Gels with 15 wells were purchased from BIO RAD. Gels were put into a Mini-PROTEAN® Tetra Vertical Electrophoresis Cell (BIO RAD) and filled with 1x running buffer (10x Tris/Glycine/SDS diluted 1:10 with distilled deionized water). 12 µL of sample and 5 µL of protein marker were pipetted into the wells. The cell was connected to the power supply (PowerPac™ HV High-Voltage Power Supply from BIO RAD) and the voltage was set to 180 V for about 30 min. Gels were afterwards imaged using a ChemiDoc™ MP imaging system from BIO RAD.

2.2.5. Enzyme recycling – Ultrafiltration

In order to re-use the enzyme after the enzymatic hydrolysis of PET and Nylon, an ultrafiltration step was performed. Therefore, a vivaflow 50 membrane from sartorius with a molecular weight cut-off of 5 kDa was connected to an ISMATEC® REGLO ICC pump (Figure 25). The ultrafiltration was performed at 100 rpm for up to 72 h. The fraction containing the enzyme was kept on ice all the time. Afterwards, the protein concentration and activity were measured again.



Figure 25: Vivaflow pump with 5 kDa cut-off membrane connected

2.2.6. Washing of PET and Nylon samples

Before the enzymatic treatment of PET and Nylon, fabric pieces of 1 cm² were cut with a hot wire and washed according the washing protocol. Briefly, samples were washed with a TRITON-X solution (5 g/L w/v) followed by a washing step with Na₂CO₃ (0.1 M) and MQ-H₂O as the last step. The complete washing procedure was performed at 50 °C, 30 min and 150 rpm on a thermo-shaker. Finally, samples were dried for 24 h at room temperature.

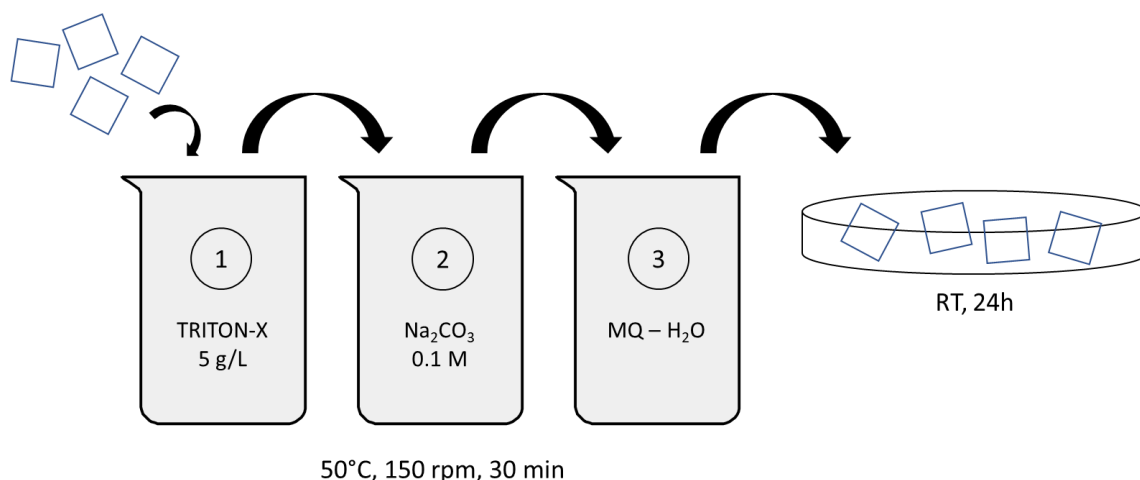


Figure 26: Washing procedure of PET and Nylon samples

2.2.7. Enzymatic hydrolysis of PET and Nylon

Fabric samples were incubated in triplicates with three different concentrations of HiC and DHPase (0.1, 0.25 and 0.5 mg/mL). The reaction was performed in 5 mL Eppendorf Tubes in a volume of 4 mL potassium phosphate buffer (0.1 M, pH7). Enzymatic hydrolysis was performed for 24, 48 and 72 hours at 150 rpm and 50 °C for DHPase or 60 °C for HiC. After the incubation, samples were washed according the washing protocol and dried for 24 h at room temperature. For the upscale, samples with a size of 8 x 20 cm were incubated with an enzyme concentration of 0.25 mg/mL in a 2 L Erlenmeyer shaking flask for 72 h at 150 rpm with the same temperatures.

2.2.8. Detection of surface reactive groups – Colorimetric method

To detect newly formed carboxyl (-COOH) and amino (-NH₂) groups on the surface of PET and Nylon fabric after the enzymatic hydrolysis, a colorimetric method, using two different colour reagents, was used.

For the determination of -COOH groups, the basic dye Methylene Blue was used. PET samples with the size of 1x1 cm were incubated with 1.5 mL basic dye (0.5% in MQ-H₂O) at 80 °C for 60 min. After incubation, samples were washed according to the washing protocol and dried for 24 h at room temperature³³.

To detect -NH₂ groups on the surface of Nylon, samples with the same size as PET were treated with the acid dye Coomassie Brilliant Blue. The samples were incubated in 1.5 mL of acid dye (0.5 mg/mL) in acid solution (MQ-H₂O/methanol/acetic acid 85:10:5 v/v, pH 2.2) for 5 minutes at room temperature. To wash off the unbound dye, samples were intensively rinsed with acid solution³⁴. After washing, samples were dried for 24 h at room temperature.

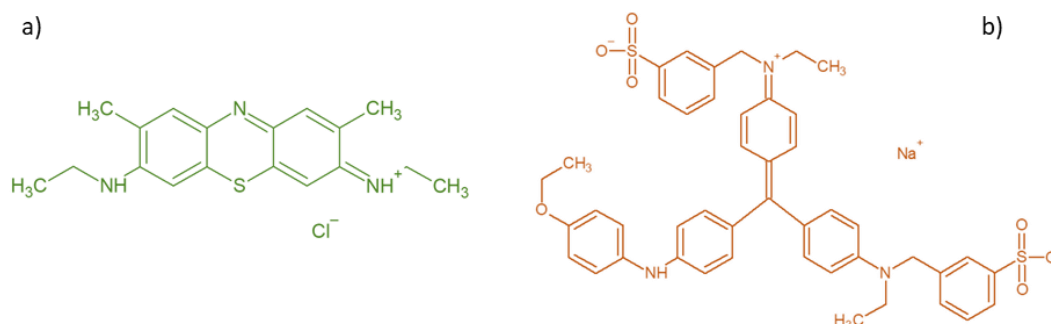


Figure 27: Chemical structure of Methylene Blue a) and Coomassie Brilliant Blue b)

In order to determine the difference in colour intensity of the PET and Nylon samples after the treatment with acid/basic dye, a ColorLite sph850 Spectrophotometer – Colour Measuring Instrument was used. Using this instrument, makes it possible to determine the colour difference between the blank (no enzymatic treatment) and the treated samples using the L*, a* and b* coordinates. The interpretation of the measurement is based on the theory defined by the Commission Internationale de l'Eclairage (CIE), that two colours cannot be red and green or yellow and blue on the same time. The coordinates L*, a* and b* indicate the lightness, red/green and yellow/blue difference. Enzymatic treated PET and Nylon samples were measured in triplicates (5 measurements per sample) against the non-treated blanks. To determine the colour difference, one has to calculate the delta (Δ) L*, a* and b*(3).

$$\begin{aligned}\Delta L^* &= (L^*_{\text{sample}} - L^*_{\text{blank}}) \\ \Delta a^* &= (a^*_{\text{sample}} - a^*_{\text{blank}}) \\ \Delta b^* &= (b^*_{\text{sample}} - b^*_{\text{blank}})\end{aligned}\tag{3}$$

The values for ΔL^* , a* and b* can be positive or negative. ΔL^* indicates the difference in lightness (+ = lighter, - = darker), Δa^* the difference in red and green (+ = redder, - = greener) and Δb^* the difference in yellow and blue (+ = yellower, - = bluer)



Figure 28: ColorLite sph850 Spectrophotometer

2.2.9. High Performance Liquid Chromatography (HPLC)

The release products after enzymatic hydrolysis of PET and Nylon were measured *via* HPLC. To remove protein impurities from the sample, a methanol precipitation step was performed with ice cold methanol (1:1 sample/methanol). Afterwards, samples were centrifuged at 12700 rpm for 15 min. at 4 °C (5920 R Centrifuge from Eppendorf) followed by an acidification step with 6 N HCl (6 μ L per sample) to reach a pH-value between 3 and 3.5. Before pipetting the samples into the HPLC-vials, a filtration step with a 0.45 μ M PTFE filter was performed, to remove further impurities which could damage the HPLC.

For the measurements of the PET hydrolysates Ta and BHET, an Agilent LC-MS system was used with a Poroshell 120 column (InfinityLab Poroshell 120 EC-C18, 4.6 x 50 mm, 4 μ M, Agilent), a flow of 0.35 mL/min and a non-linear gradient (Table 1). The released products were detected at 241 nm *via* UV-Vis spectroscopy.

Table 1: HPLC gradient for the measurement of PET hydrolysates

Time [min]	A (H ₂ O + 0.1 % Formic Acid) [% v/v]	B (MeOH + 0.1 % Formic Acid) [% v/v]
2	50	50
9	0	100
12	0	100
14	70	30

Caprolactam release was measured using an Agilent LC-MS system with a phenomex[®] column (Aqua[®] 5 µm C18, 125 Å, LC Column, 250 x 4.6 mm) with an isocratic gradient (H₂O/MeOH, 60/40 [% v/v]) and flow of 0.5 mL/min for 50 min. Hydrolysates were measured at 210 nm *via* UV-Vis spectroscopy.

2.2.10. DNA – Agarose Gel Electrophoresis

To determine the length of the DNA molecules, an agarose gel electrophoresis was performed. Therefore a 3% agarose gel was produced by dissolving 1.2 g of agarose in 40 mL of 1x TAE-Buffer (50x Tris/Acetic Acid/EDTA (TAE), diluted with distilled deionized water) by heating it up in a microwave. For staining of the DNA, 4 µL nucleic acid gel stain were added to the gel. After casting the gel, it was allowed to solidify for 30 min and was put into a Mini-Sub cell GT cell from BIO RAD. For the preparation of the DNA samples, 5 µL of a DNA loading dye were added to 25 µL of sample. 12 µL of the samples and 5 µL of a 10 bp DNA ladder were pipetted on the gel and allowed to run for about 30 min at 120 V. Gels were afterwards imaged using a ChemiDoc[™] MP imaging system from BIO RAD.

2.2.11. Nanodrop

For the measurement of the DNA content, an Implen NanoPhotometer[®] was used. Therefore, the photometer was blanked, using only MES-buffer and afterwards the samples were measured in triplicates at 260 nm.

2.2.12. DNA – Immobilisation

To find the right concentration of DNA, 3 different amounts of DNA were dissolved in MES-Buffer (2-(N-morpholino)ethanesulfonic acid, 0.1 M, pH4.6) at 150 rpm and room temperature for 3 h, to produce 2, 5 and 7 % DNA solutions. The linkage between the salmon DNA and the pre-treated PET or Nylon samples was performed in three different ways using 1-Ethyl-3-(3-dimethylaminopropyl)carbodiimide (EDC)/N-Hydroxysuccinimide (NHS), dopamine or tyrosine as crosslinking agents.

2.2.12.1. EDC/NHS

For the crosslinking of DNA using the EDC/NHS system, an EDC stock solution with 200 mg/mL and a NHS stock solution with 400 mg/mL were produced in MES-Buffer (0.1 M, pH4.6). Crosslinking reactions were performed in 12-well plates in a volume of 3 mL at 150 rpm and room temperature. MES-Buffer, EDC, NHS and DNA stock solutions were added in suitable amounts to reach final concentrations in the reaction mixture of 50 mg/mL EDC, 100 mg/mL NHS and 2, 5 and 7 % DNA. At first the right amount of MES buffer was added to the fabric, followed by 750 μ L EDC stock solution. After 10 min, 750 μ L NHS stock were added and after another 10 min incubation time, 1260 μ L (7%), 900 μ L (5%) or 360 μ L (2%) DNA stock solution was pipetted to the reaction mixture. The DNA was allowed to bind for 24 h at 250 rpm and room temperature. After incubation, samples were dried for 24 h at room temperature (Figure 29 A).

2.2.12.2. Dopamine/Tyrosine

To use dopamine or tyrosine as crosslinking agents, a 2 mg/mL dopamine hydrochloride solution and a 2 mg/mL tyrosine solution were prepared in TRIS/HCl buffer (0.1 M, pH8.5). For the coating with either dopamine or tyrosine, 3 mL of the solutions were pipetted to enzymatic treated PET and Nylon samples and incubated for 24 h at 250 rpm and room temperature. After incubation, samples were washed by dipping them 3 times in MQ-H₂O. DNA immobilisation reaction was done with a 7% DNA solution (in MES-buffer) which was directly pipetted to the dopamine or tyrosine samples. The incubation with DNA was performed for 24h at 250 rpm and room temperature. After the incubation, the samples were dried for 24h at room temperature (Figure 29 B & C).

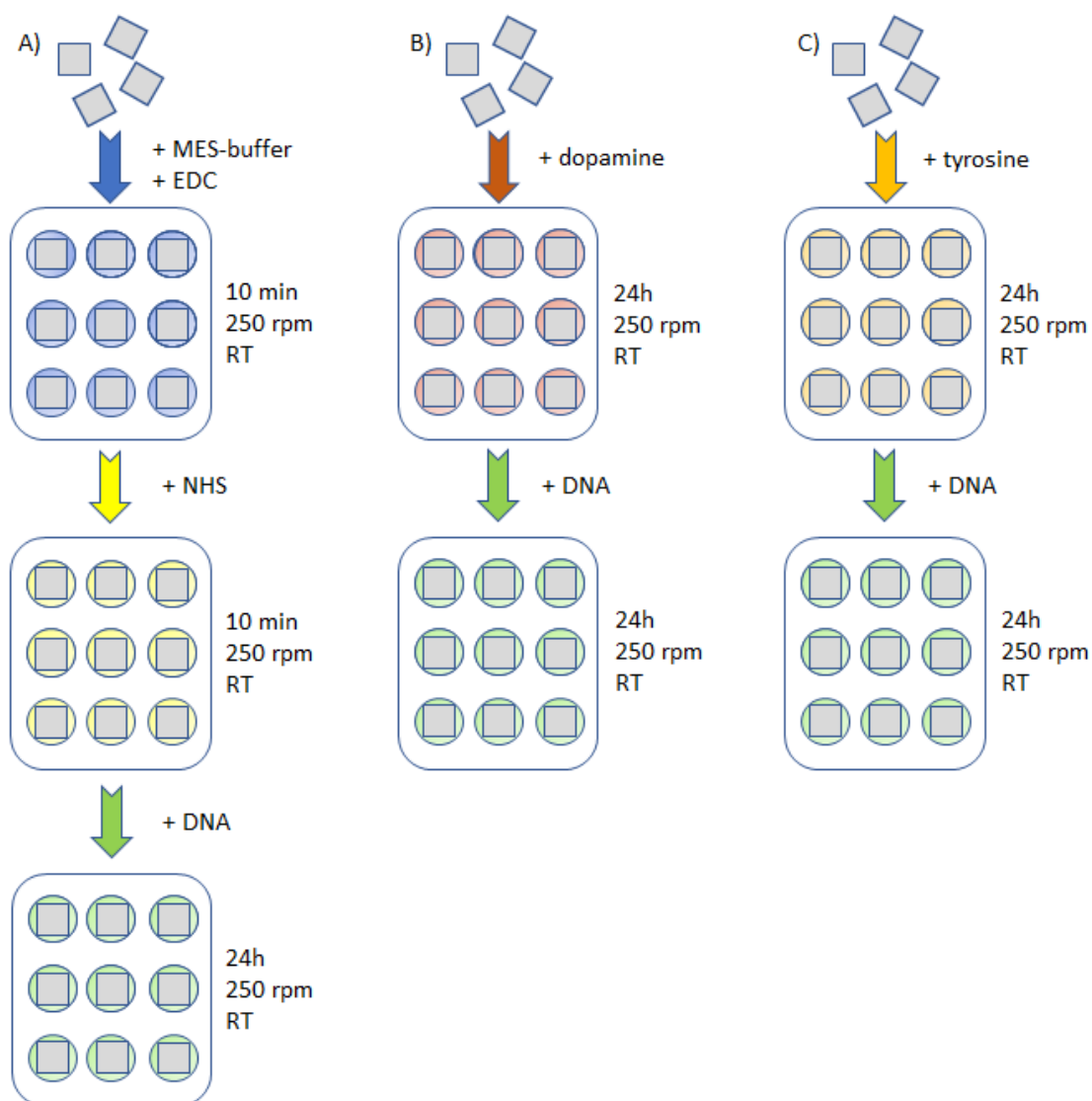


Figure 29: Scheme of PET and Nylon coating and DNA immobilisation

2.2.13. Fourier-transformed Infrared Spectroscopy (FT-IR)

To measure changes on the surface of PET and Nylon after enzymatic treatment and the different coating steps, a PerkinElmer Spectrum 100 FT-IR Spectrometer was used. Spectra were recorded from $4000\text{--}650\text{ cm}^{-1}$. Normalization of the recorded spectra was done at the band occurring in the 1410 cm^{-1} region (CH in plane bending and CC stretching), which has been already proven to be a suitable reference band³⁵. To achieve comparable results, the Transmittance (%T) was kept constant (%T=70-72 for PET and %T=68-72 for Nylon) for all measurements. Each spectrum stated in this study is the result of the average of at least 3 measurements.

2.2.14. Environmental Scanning Electron Microscopy (ESEM)

For imaging the surface of untreated and treated PET and Nylon fabric, a Quanta™ SEM FEG 250 from Thermo Scientific™ was used (Figure). First, samples were stacked to the specimen-holder and sputter coated with gold using a EDWARDS Scancoat Six sputter coater for 2 minutes. Imaging was done using magnifications from 100x to 25000x. Furthermore, elemental analysis was performed with Energy-dispersive X-ray spectroscopy (EDS), showing chemical characteristics of the samples by stimulation of the emission of characteristic X-rays from the specimen.

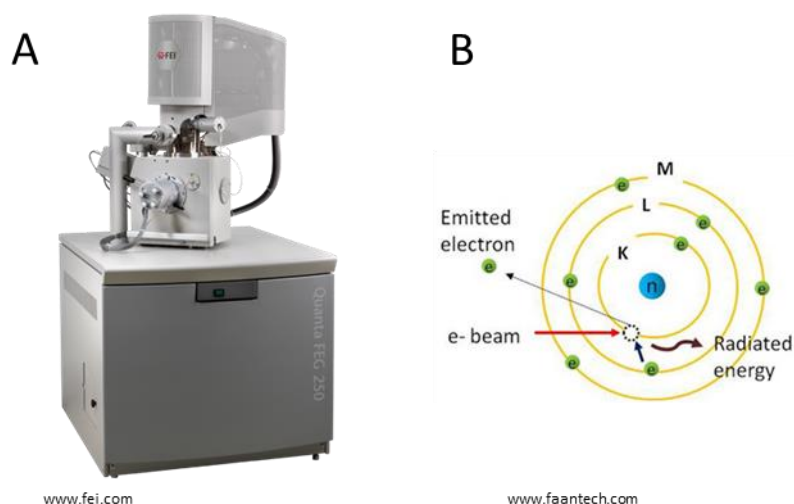


Figure 30: A: ESEM, B: Schematic principle of EDS

2.2.15. Flame-retardant Characterizations

2.2.15.1. Flammability test

Flammability tests were done according to the ISO 6940 for the determination of ease of ignition of vertically oriented specimens. Samples were cut in the size of 8x20 cm and fixed in the apparatus (Figure 30 B). For the ignition of the sample, the flame of the burner was set to a vertical height of 4 cm (Figure 30 C). Tests were performed in bottom edge ignition (Figure 30 A), in which the flame was applied to the sample to the shortest time to cause ignition. The whole experiment was recorded on video and the time was measured from the time of ignition until self-extinguishing was reached or the sample completely burned. This test gives information about the burning time, burning length and the resulting burning rate. Furthermore, one can gain information about self-extinguishing, char-formation and the ease of ignition.

An increase in flame-retardancy would result in longer burning time, a decrease of the burning length and a lower burning rate.

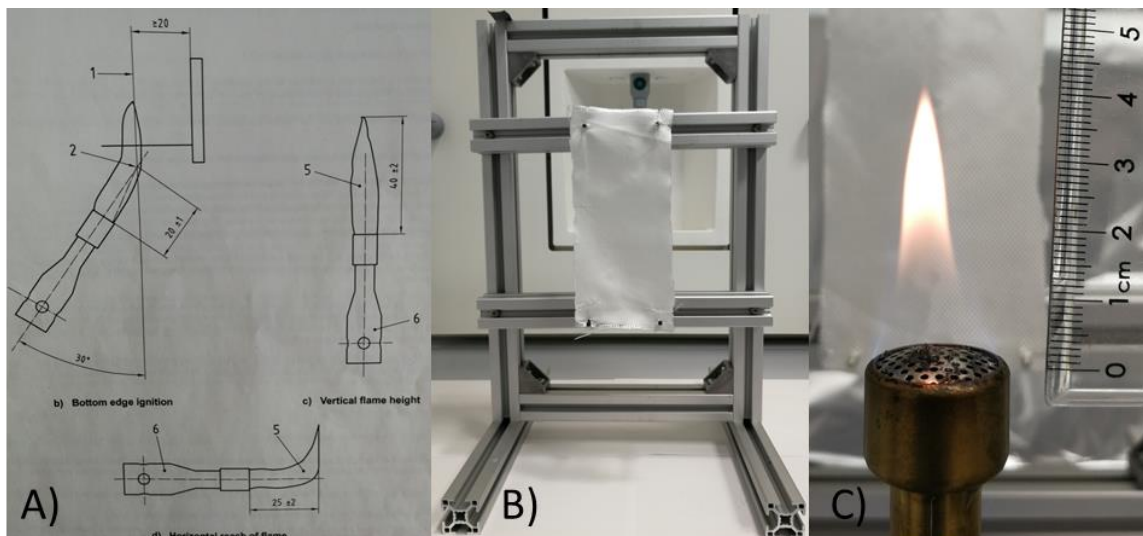


Figure 31: A) Flame position during bottom edge ignition, B) fixed fabric sample in the apparatus and C) flame of the burner set to a height of 4 cm

2.2.15.2. Thermogravimetric Analysis (TGA)

In TGA, a sample in the range of 5 – 20 mg is fixed in a pan and put inside a furnace (Figure 31), where it is heated with defined heating rates or at a specific temperature (isothermal test). The atmosphere within the furnace can be inert (N_2), oxidative (O_2) or reducing (H_2). This technique is used to measure the weight change of the sample due to the loss of water, thermal degradation, pyrolysis and oxidation. Due to these measurements, results according the thermal and thermo-oxidative behaviour of the material and the rate of thermal degradation can be obtained.

TGA was performed on a PL Thermal Sciences STA 625 thermal analyser, using ~ 10 mg of sample in an aluminium pan. The flow of N_2 or O_2 was set to $100 \text{ mL} \cdot \text{min}^{-1}$ and samples were heated from 21 to 625°C at a heating rate of $10^\circ\text{C} \cdot \text{min}^{-1}$. The temperatures at 5% and 50% mass loss (TD5 and TD50) were subsequently determined.

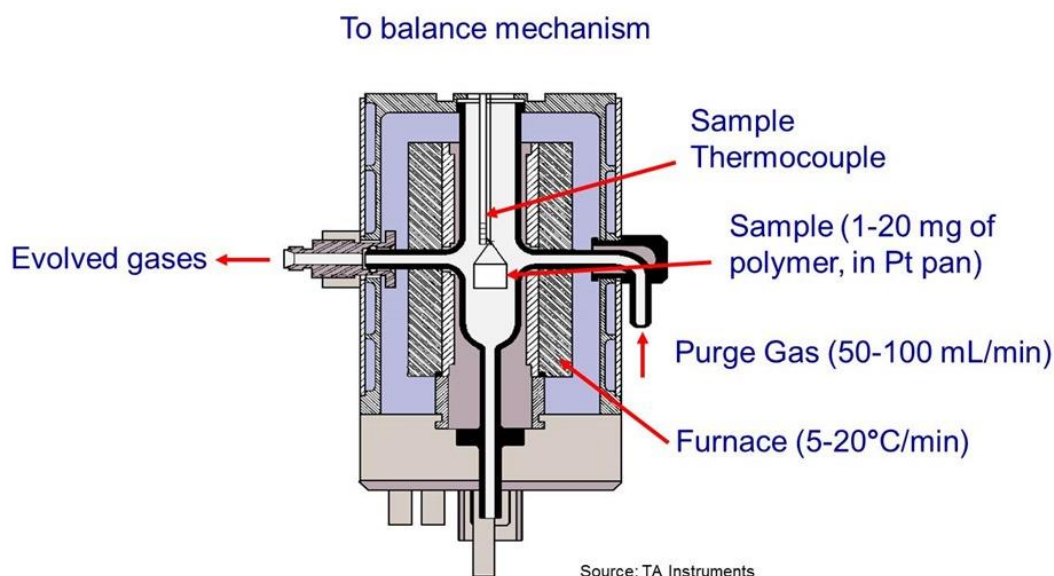


Figure 32: Apparatus for the thermogravimetric analysis

3. Results and Discussion

3.1. Enzyme Characterization

The protein concentrations of HiC and DHPase were determined according to the method of Bradford, resulting in a concentration of 8.90 mg/mL and 2.50 mg/mL for HiC and DHPase. Volumetric enzyme activity of HiC was measured *via* esterase activity assay, using p-nitrophenyl butyrate as substrate. Colour change was determined at 405 nm and activity was calculated in units, where 1 unit is the amount of enzyme which is required to hydrolyse 1 μ mol of substrate resulting in a volumetric activity of 360 U/mL.

The activity of DHPase was measured by detection of the change in absorbance at 225 nm due to the hydrolysis of the DHU ring and calculated in units, where 1 unit of DHPase catalysed the hydrolysis of 1 μ mol of DHU per minute at 30 °C. The resulting volumetric activity was ~2.9 U/mL, which was comparably low to the activity of the Cutinase.

An SDS-PAGE was done with both enzymes showing a clear and thick band in the range of 20 kDa in case of HiC and around 60 kDa for DHPase (Figure 33). This confirmed the size of HiC as mentioned in the introduction and showed that the DHPase was degraded into its 4 subunits, each in the size of 60 kDa. This could happen by the treatment with Laemmli-buffer in which the detergents β -mercaptoethanol and SDS can lead to the breakage of the disulphide bonds, connecting the 4 subunits.

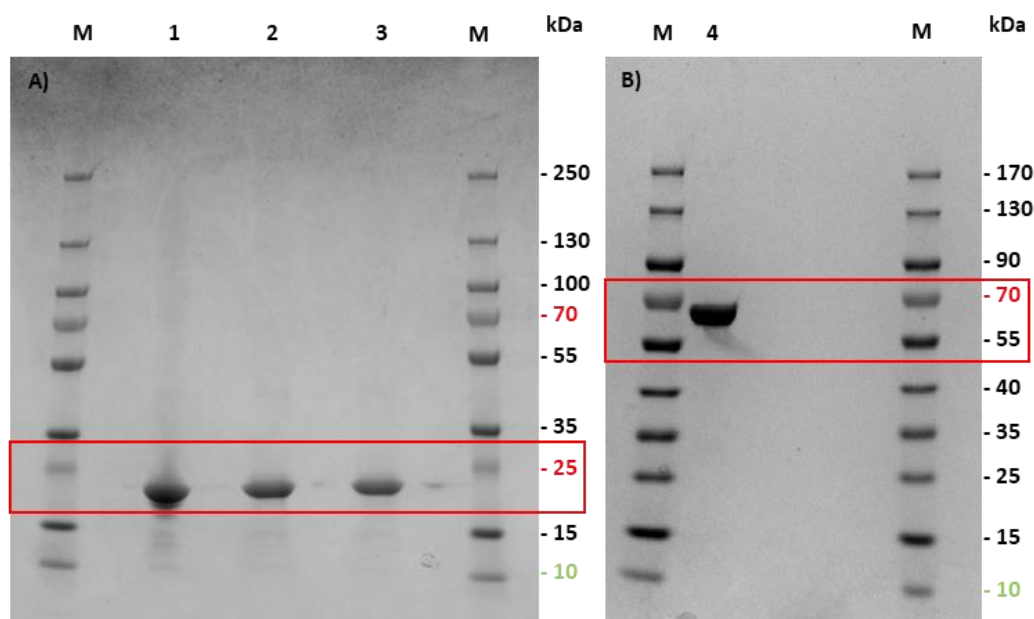


Figure 33: SDS-PAGE of HiC (A) and DHPase (B): A) M: Marker form 10 – 250 kDa, 1: HiC (1:100), 2: HiC after incubation with PET, 3: HiC after incubation with Nylon; B) M: Marker form 10 – 170 kDa, 4: DHPase (1:10)

Enzyme recycling – Ultrafiltration

The ultrafiltration step was done in order to re-use the enzyme after the hydrolysis of PET and Nylon. Therefore, the ultrafiltration was running up to 72 h and afterwards the activity and the protein content was measured again, resulted in a protein concentration of 1.30 mg/mL and a volumetric activity of around 26 U/mL after the hydrolysis of PET and 1 mg/mL and 12 U/mL after the Nylon hydrolysis. The specific activity after PET and Nylon hydrolysis was therefore around 20 U/mg and 12 U/mg of enzyme, respectively. Compared to the initial activity of fresh HiC (~ 360 U/mL), after the ultrafiltration the activity was reduced of around 1/10 of the fresh enzyme. By reducing the volume and concentrating the enzyme solution after hydrolysis reaction *via* ultrafiltration, it was possible to re-use the enzyme in another hydrolysis reaction. Therefore, the amount of fresh enzyme which needed to be

added to the new reaction mixture could be reduced, providing economic and costs-saving potential. In the case of the hydrolysis of the big PET stripes (8x20 cm), 160 mL of the “recycled” enzyme solution was used, resulting in a protein concentration of 0.14 mg/mL in the big reaction mixture (1500 mL). To reach a final concentration of 0.25 mg/mL, 18 mL of fresh HiC were added. For Nylon hydrolysis, 200 mL of enzyme solution was added to reach a concentration of 0.13 mg/mL in the reaction mixture. Additionally, 20 mL of fresh enzyme was added. Compared to the amount of HiC needed in the first incubation of the big stripes (~ 84 mL) the portion of fresh enzyme could be reduced to more than half of the initial value.

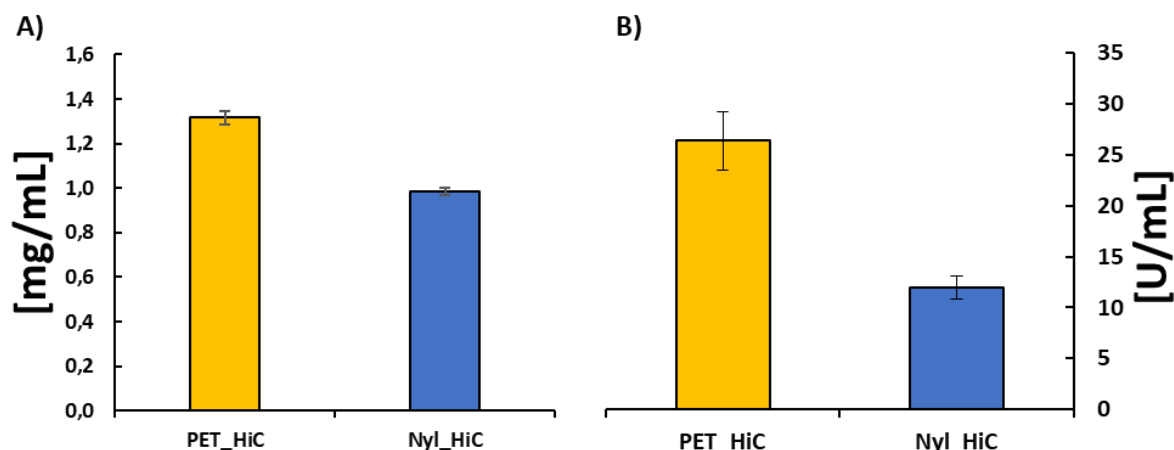


Figure 34: A) Protein concentration of HiC after PET (orange) and Nylon (blue) hydrolysis; B) Volumetric activity of HiC after PET (orange) and Nylon (blue) hydrolysis

3.2. Enzymatic Hydrolysis

HPLC

To determine the optimal conditions for the hydrolysis reaction in terms of enzyme concentration and incubation time, the two enzymes with three different concentrations (0.1, 0.25 and 0.5 mg/mL) were incubated with 1 cm² fabric pieces of PET and Nylon for up to 72 h. In the case of PET, the concentration of hydrolysis products (Ta and BHET) was measured *via* HPLC after 24, 48 and 72 h, showing the highest concentration of terephthalic acid (~ 0.045 mM) after 72 h with the highest enzyme concentration of HiC (Figure 35).

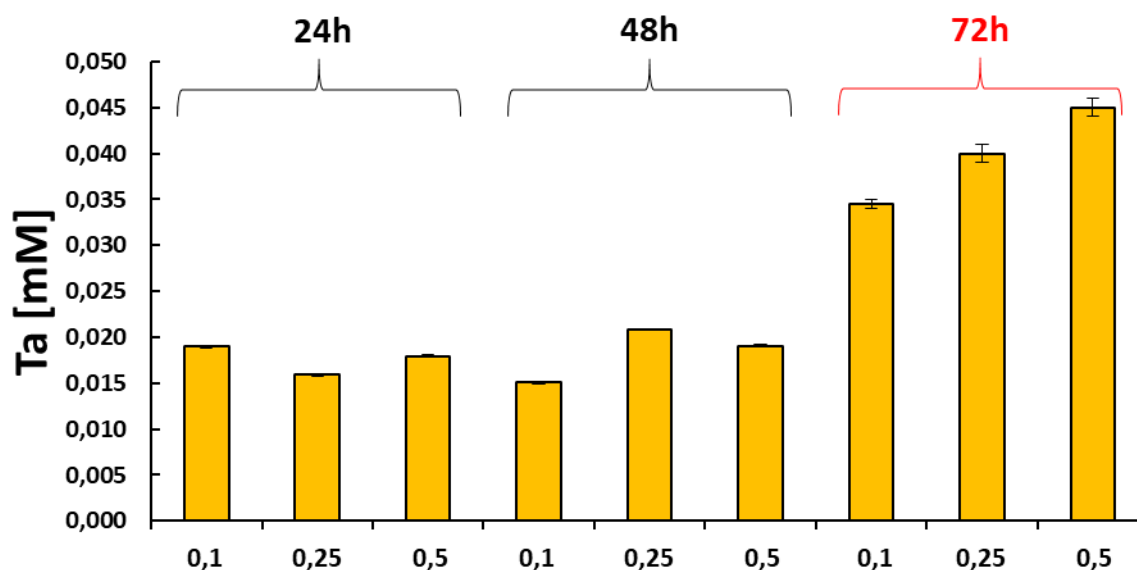


Figure 35: Release of terephthalic acid from PET hydrolysis during 72h with three different concentrations of HiC at each time point.

The concentration of caprolactam during 72 h of Nylon hydrolysis reaction was as well determined *via* HPLC (~ 2.3 mg/L), showing results only after 72 h with the highest enzyme concentration of DHPase. To test the hydrolysis activity of HiC on Nylon fabric too, Nylon pieces were also incubated with the different concentrations of enzyme, resulting in caprolactam concentrations of up to 7.5 mg/L after 72 h and 0.25 mg/mL HiC. Since the concentration of caprolactam was nearly 3-times higher with HiC compared to DHPase and the easier availability of the cutinase, we decided to use only *Humicola insolens* cutinase for the incubation of the big stripes. The conditions for the hydrolysis of big Nylon and PET stripes was therefore set to an enzyme concentration of 0.25 mg/mL for 72 h and 60°C.

To follow the hydrolysis reaction of big PET and Nylon stripes, samples were taken at 1, 3, 24, 48 and 72 h and analysed *via* HPL resulting in a concentration of ~ 1 mM BHET in the case of PET and ~ 7.5 mg/L (~ 0.07 mM) of caprolactam for Nylon, both after 72 h (Figure 36).

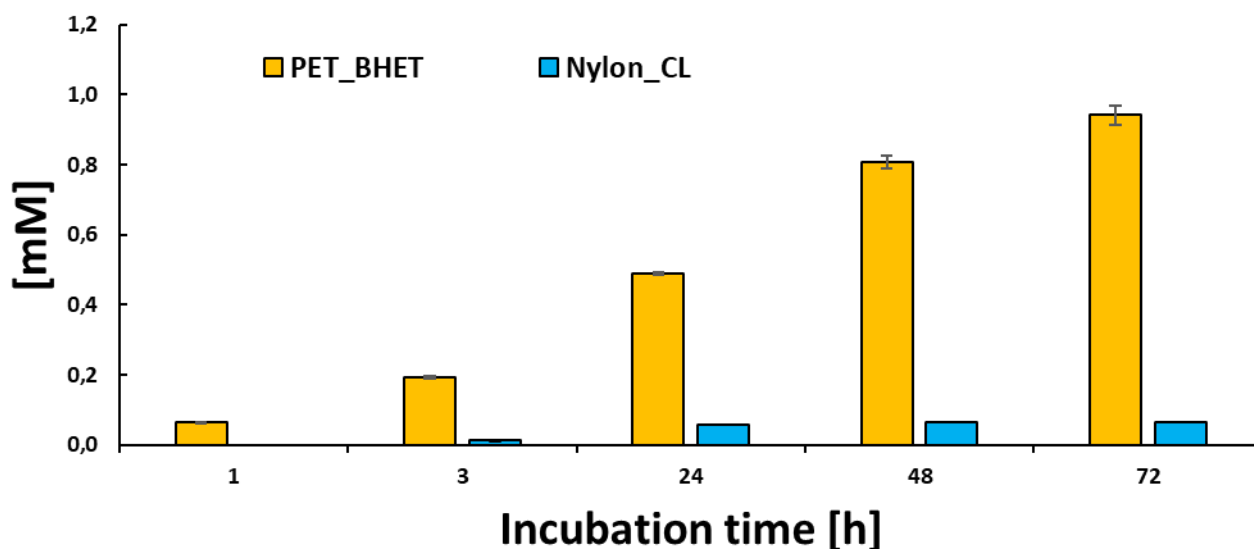


Figure 36: Concentration of BHET (orange) and CL (blue) during hydrolysis with HiC over 72 h

Colour measurement

To confirm the hydrolysis of PET and Nylon, newly formed carboxyl (-COOH) and amide (-NH₂) groups were detected using basic (Methylene Blue) and acid (Coomassie Brilliant Blue) dye. The difference in blue colour between blank and enzymatic treated fabric after 72 h (Figure 37) indicates that new carboxyl and amide groups on PET and Nylon surface have been generated by the hydrolytic cleavage of the polymer.

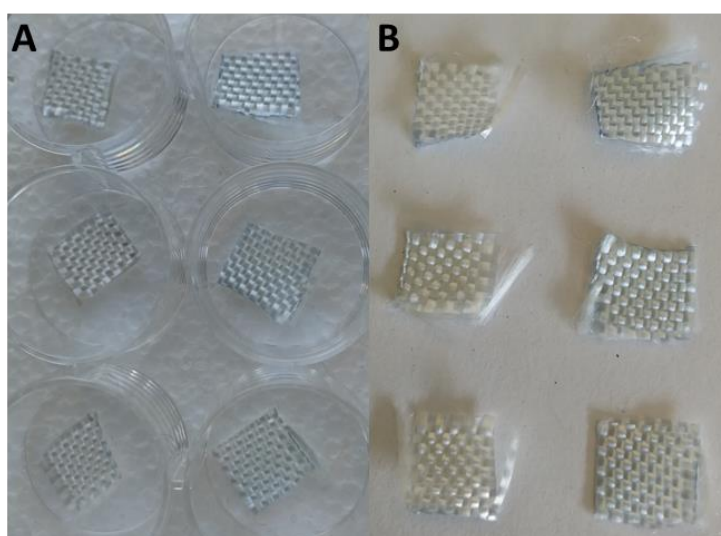


Figure 37: Samples after treatment with acid and basic dye: A) PET blank (left) and enzymatic-treated (right) after staining with Methylene Blue; B) Nylon blank (left) and enzymatic-treated (right) after Coomassie Brilliant Blue staining

These colour difference was also measured, using a ColorLite Spectrophotometer resulting in different values for both polymers (Table 2). In case of PET, the difference (Δ) between the values of L^* , a^* , b^* and E^* for blank and enzymatic-treated fabric indicates that the samples became darker, greener and bluer, compared to the blank. The same trend can be observed with Nylon but to a lower extend (Table 2). This can be explained by looking at the data obtained *via* HPLC. There, the concentration of caprolactam after 72 h hydrolysis, was about 100-fold lower compared to the concentration of BHET, indicating that the hydrolysis of PET was more efficient. Nevertheless, the increase of blue and green colour, as well as darkness of the samples, confirmed that on the surface of PET and Nylon fabric more surface reactive groups could be generated *via* enzymatic hydrolysis of HiC.

Table 2: Results of the measurement of colour difference (Δ) between PET (orange) and Nylon (blue), blank and enzymatic-treated (HiC) sample

PET - Methylene Blue				
	L^*	a^*	b^*	ΔE^*
Blank	104,15	8,75	31,70	0,06
HiC	101,38	7	28,27	4,80
delta (Δ)	-2,77	-1,75	-3,43	4,74

Nylon - Coomassie Brilliant Blue				
	L^*	a^*	b^*	ΔE^*
Blank	73,04	-1,31	-8,44	0,02
HiC	66,36	-1,42	-9,55	8,59
delta (Δ)	-6,68	-0,11	-1,11	8,57

Fourier transformed Infrared Spectroscopy (FT-IR)

To further proof the generation of new surface reactive groups, FT-IR was used before and after the enzymatic hydrolysis. The spectra recorded were normalized at the 1410 cm^{-1} band (CH in plane bending and CC stretching) which was already used in further studies and proofed as internal reference band³⁵. The spectra of PET-Blank in the region of $1800 - 650\text{ cm}^{-1}$ (Figure 39) shows bands at 1471 cm^{-1} (CH_2 bending), 1340 cm^{-1} (CH_2 wagging), 1120 cm^{-1} (O- CH_2 and ring CC stretching), 970 cm^{-1} (O- CH_2 and C=O stretching) and 847 cm^{-1} (bending of benzene rings) which are characteristic for semi crystalline structure of PET. Furthermore, the more intense band at 1100 cm^{-1} (C-O stretching) and the smaller band at 1120 cm^{-1} (compared to PET-crystalline) indicating also the structure of

amorphous PET³⁶. The interpretation of the whole spectra confirms that the fabric is made of a mixture of semi-crystalline and amorphous PET.

The enzymatic hydrolysis with HiC (Figure 38) showed only minor changes compared to the blank. The intensity of the band at 1721 cm^{-1} , representing the carbonyl stretching band, decreased and was shifted after enzymatic treatment. Furthermore, the band at 1240 cm^{-1} (C(=O)-O stretching and CC stretching) showed lower intensity after hydrolysis. The change of shape and intensity upon the bands at 1240 cm^{-1} and 1100 cm^{-1} confirmed that the enzyme could cleave the ester bonds within the PET structure.

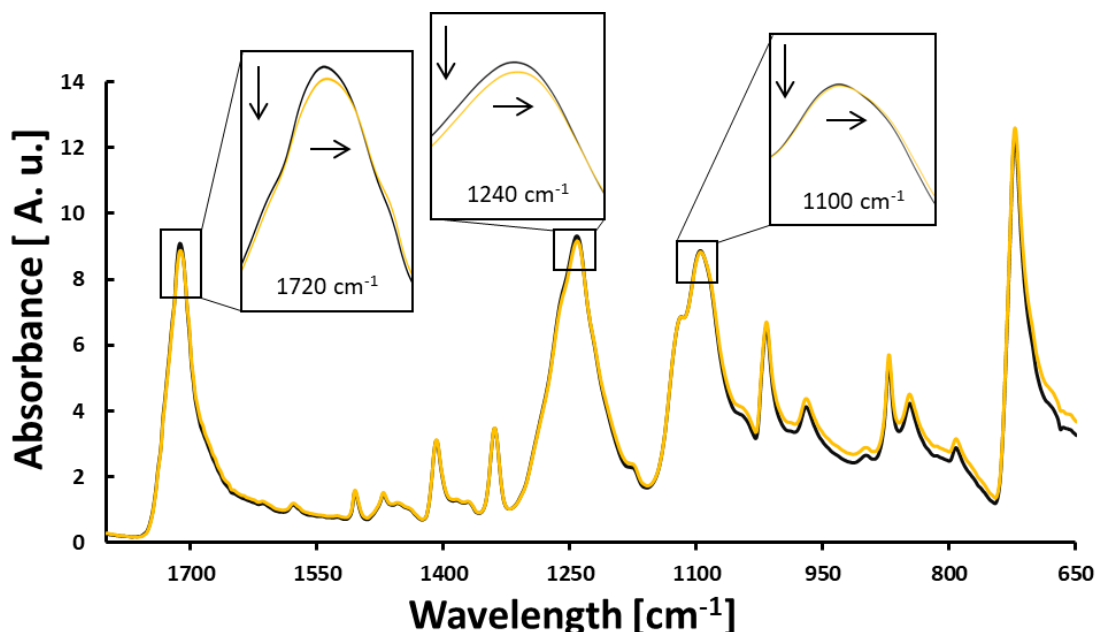


Figure 38: FT-IR Spectra of PET-Blank (black) and PET after enzymatic treatment (orange). In the boxes: enlarged view of characteristic peaks which changed after hydrolysis (arrows indicating a shift and decrease in intensity)

Nylon spectra of the blank showed bands at 3300 cm^{-1} (N-H stretching and bending vibrations of secondary amide), 1640 cm^{-1} (N-H bending of Amide I) and 1540 cm^{-1} (C=O stretching vibration of Amide II) which can be found in all polyamides. Furthermore, bands at approximately 1460 cm^{-1} (CH_2 bending vibration), 1250 cm^{-1} (C-N stretching vibration), 960 cm^{-1} and 930 cm^{-1} (C-H out of plane bending) can be found in the spectra, confirming the characteristic bands of polyamide 6 (Nylon 6) (Figure 39).

The FT-IR spectra of Nylon after the enzymatic treatment with HiC showed major differences, compared to the blank. Bands in the region of $2800 - 3300\text{ cm}^{-1}$ showed a shift and decrease in the intensity which results from the breakage of peptide bonds. Additionally, due to the breakage of peptide bonds, bands at 1640 and

1540 cm^{-1} decreased dramatically resulting in the appearance of bands at 1711 cm^{-1} (C=O vibration) and 723 cm^{-1} (NH_2 vibration) which clearly indicate the formation of new carboxylic groups ($-\text{COOH}$). This is also confirmed by the newly appearing band at 1340 cm^{-1} (C-O stretching of carboxylic acids) as well as the greatly intensified and shifted bands in the region of 1100 – 1300 cm^{-1} and the newly formed bands at 870 and 850 cm^{-1} (C-H out of plane bending)³⁷.

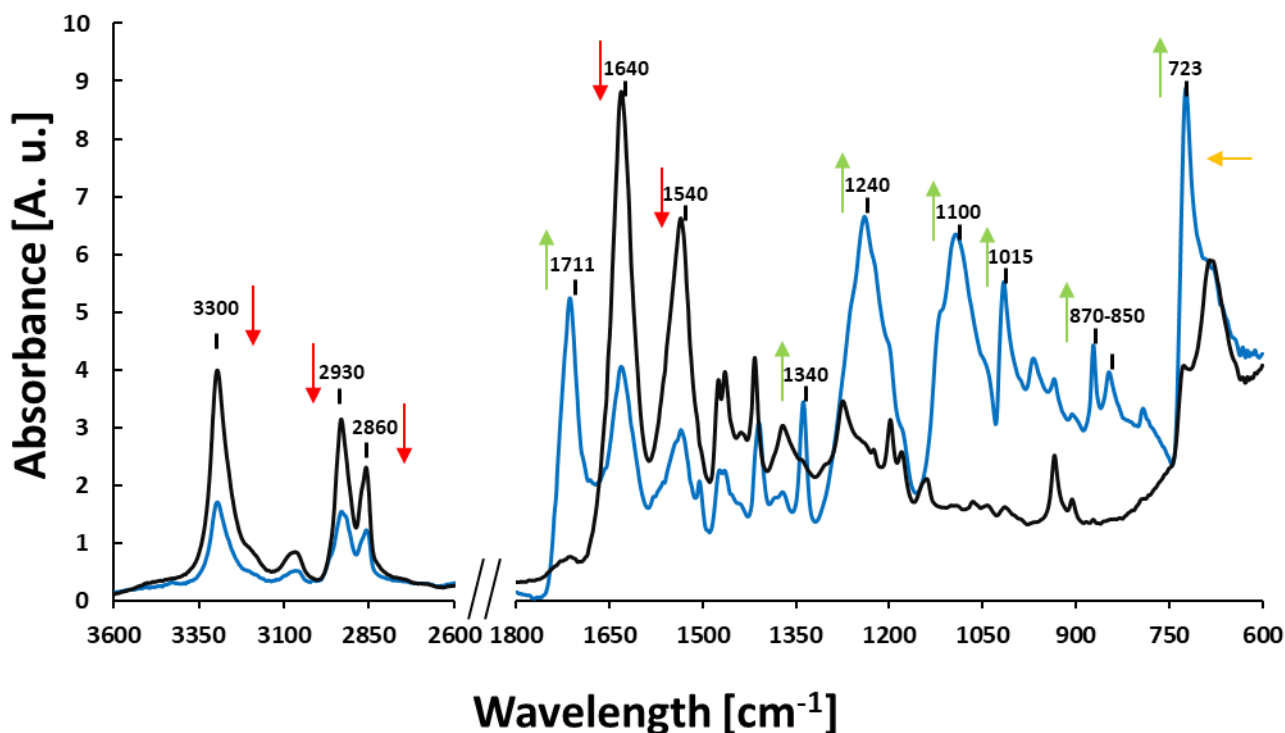


Figure 39: FT-IR Spectra of Nylon blank (black) and after enzymatic hydrolysis (blue). Characteristic peaks labelled; arrow indicating decrease (red), increase (green) and shift (orange) of the band after enzymatic treatment.

ESEM

Imaging the surface of PET and Nylon *via* ESEM showed distinct changes between the untreated and enzymatic treated fabric. As expected, the surface of the untreated samples showed a rather smooth and plain structure. In contrast, after enzymatic hydrolysis, the surface of both polymers showed scratches and small holes resulting from the hydrolytic attack, indicating that HiC could cleave ester-bonds within both polymers (Figure 40).

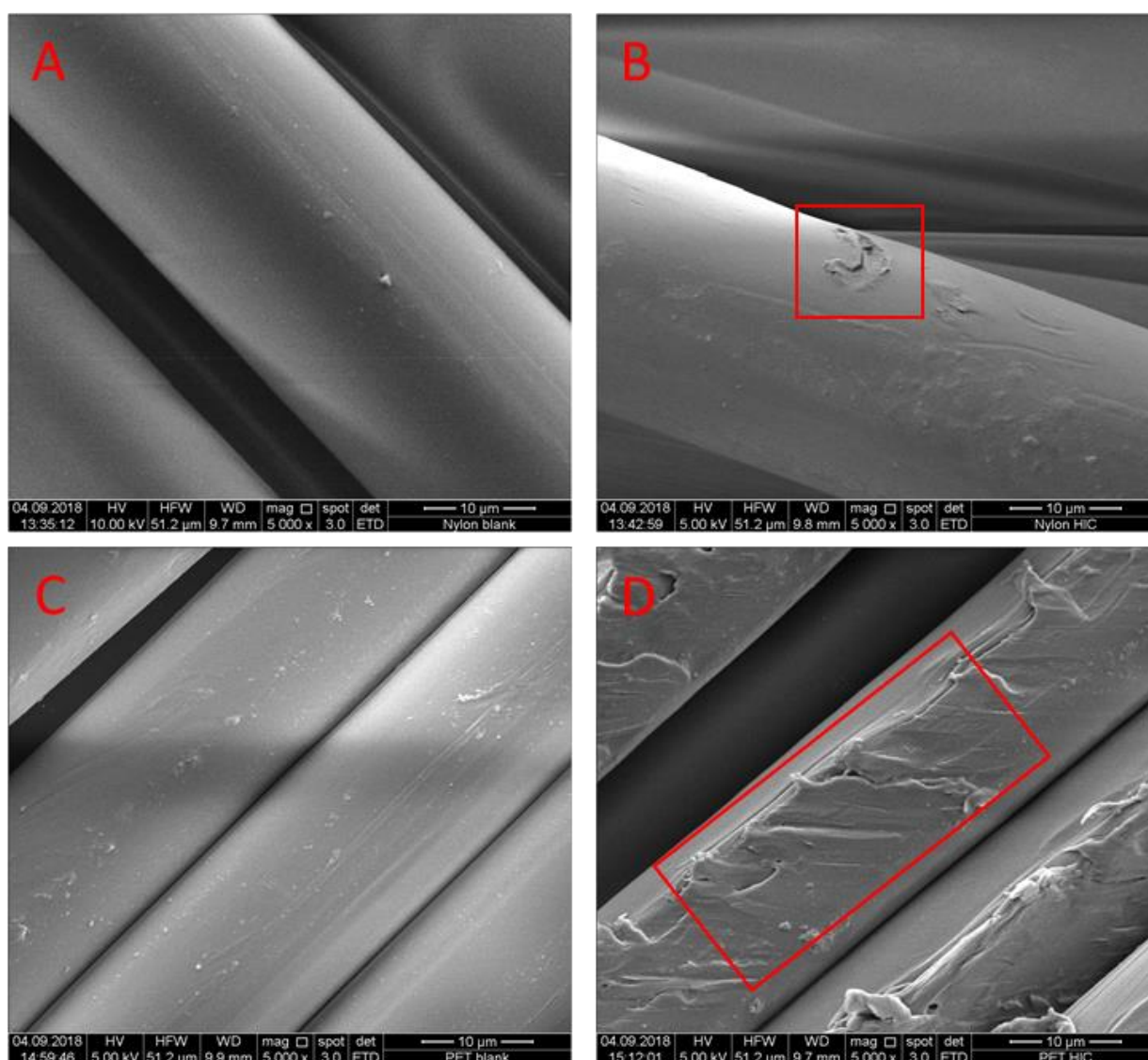


Figure 40: ESEM image of untreated (A) and enzymatic treated (B) Nylon in the upper part and untreated (C) and enzymatic treated (D) PET. Red squares showing holes and scratches after hydrolysis

3.3. DNA – Immobilisation

DNA

Deoxyribose Nucleic Acid (DNA) with low molecular weight form salmon sperm, was used in this study. To determine the length of the DNA fragments (bp), an agarose gel electrophoresis was done (Figure 41). The results obtained showed that the DNA is in the size range of 20 – 30 bp which is thought to be a good size for immobilization trials. The rather small length of the DNA should favour the binding of the fragments with the surface reactive groups on the polymer. Longer DNA fragments could hinder the proper and sufficient binding due to steric hindrance.

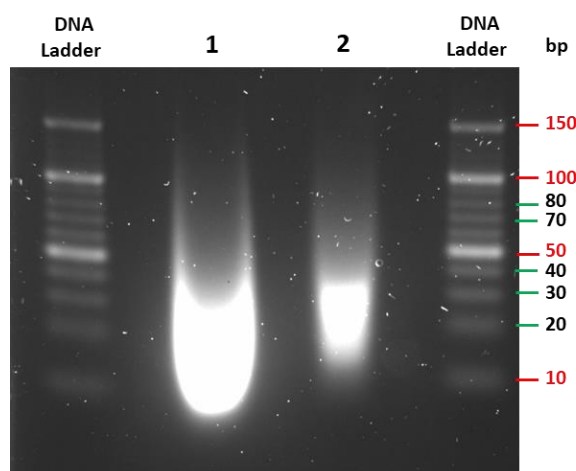


Figure 41: Agarose gel electrophoresis of DNA from salmon sperm: DNA Ladder 10 – 150 bp, 1: undiluted 5% DNA solution, 2: 1:10 diluted DNA solution

For the incubation of big PET and Nylon stripes, a 5% (w/v) DNA solution was produced. The concentration was measured using a Nanodrop photometer, resulting in a concentration of 50 mg/mL (in 1500 mL buffer) which corresponds to the 5%.

An FT-IR spectrum of the salmon DNA was recorded as well, to determine the peaks, characteristic for interpretation of the polymer spectra after immobilisation. Characteristic peaks are located at bands 1680 cm^{-1} (P=O) with formation of a little shoulder (C=O vibration of guanine, cytosine and thymine), 1220 and 1060 cm^{-1} (asymmetric and symmetric PO_2^- vibrations)¹⁷. Furthermore, bands at 967 cm^{-1} (phosphodiester) as well as 832 and 782 cm^{-1} representing the deoxyribose-phosphate and sugar-phosphate of the DNA could be recorded (Figure 42).

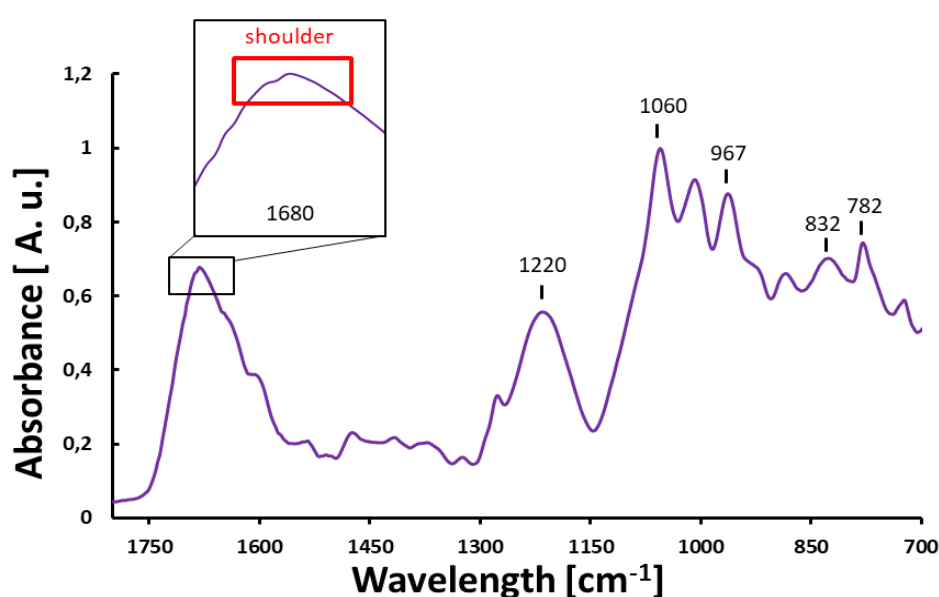


Figure 42: FT-IR spectrum of salmon sperm DNA. Box: Band at 1680 cm^{-1} and shoulder formation; characteristic peaks labelled.

EDC/NHS crosslinking system

The first technique which was used to immobilise the DNA on the surface of PET and Nylon was the EDC/NHS coupling system. Samples were treated with EDC solution, followed by NHS and DNA and incubated for 24 h at RT and 250 rpm. After drying the samples for 24 h, FT-IR spectra were recorded for PET and Nylon. Spectra of PET after EDC/NHS/DNA coating showed only minor changes. Bands at $\sim 1710\text{ cm}^{-1}$ showed an increase and shift which is maybe due to P=O band of the DNA. Furthermore, bands at ~ 1230 and $\sim 1090\text{ cm}^{-1}$ increased and were shifted due to the bands, characteristic for asymmetric and symmetric PO_2^- vibrations of the DNA, indicating that DNA was immobilised to a small extend (Figure 43).

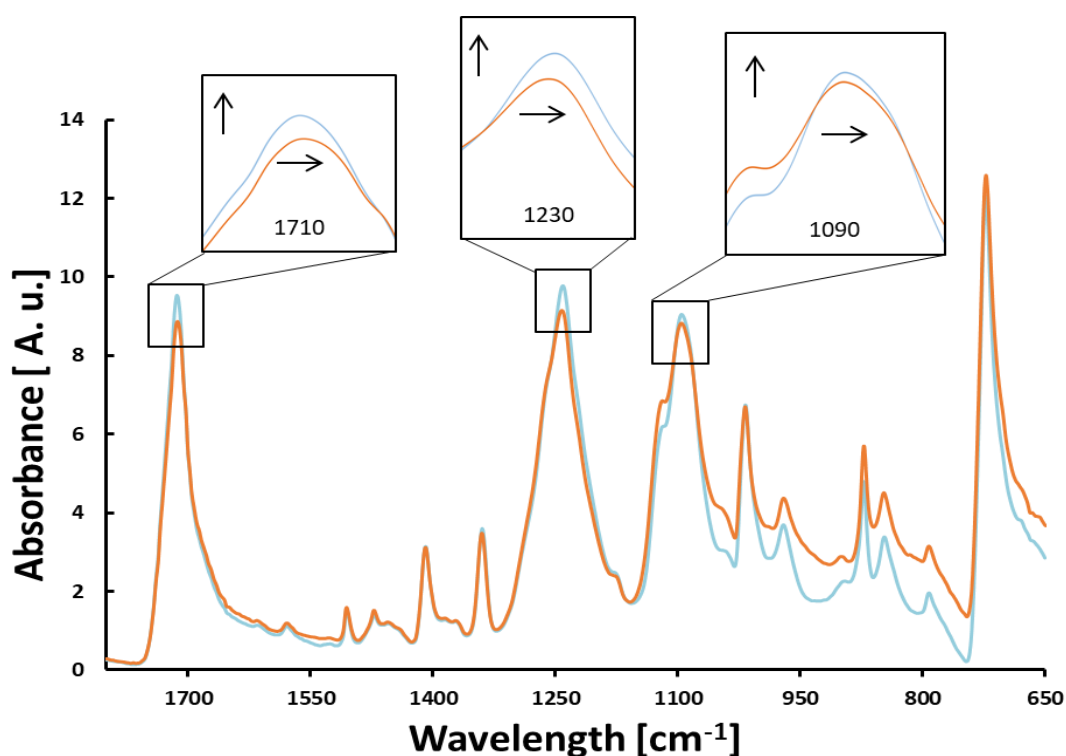


Figure 43: FT-IR spectra of PET blank (orange) and after EDC/NHS/DNA crosslinking (light-blue). Boxes: showing changes of intensity and position (arrows) of peaks characteristic for DNA.

In the case of Nylon, more distinct differences can be seen after EDC/NHS/DNA crosslinking compared to PET. The band at $\sim 1630\text{ cm}^{-1}$ is intensified and shifted into the direction of the P=O band of DNA. The band at $\sim 1530\text{ cm}^{-1}$ indicates the present of pyrimidine and purine bases due to their C=N and C=C stretching modes at approximately 1540 cm^{-1} ¹⁷. The shift and increase in intensity at $\sim 1270\text{ cm}^{-1}$ after DNA crosslinking can be explained by the presence of bands between 1220 and 1280 cm^{-1} (PO_2^-) in the spectra of salmon DNA. Furthermore, changes in intensity of peaks in the area $960 - 1060\text{ cm}^{-1}$, characteristic for PO_2^- and phosphodiester

bonds as well as between 780 and 890 cm^{-1} (deoxyribose-phosphate and sugar-phosphate), indicate the presence of DNA. By comparing the spectra of PET and Nylon after immobilisation with EDC/NHS crosslinking system, it is clearly visible that the immobilisation of DNA was successful even if the amount of DNA seems not to be very high.

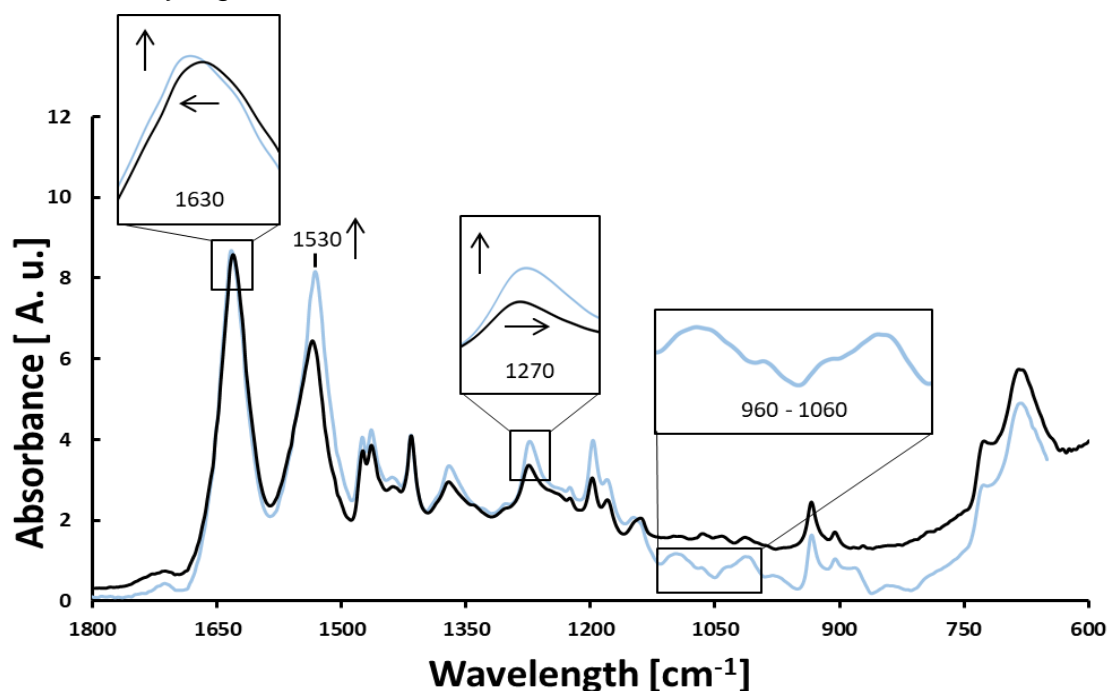


Figure 44: FT-IR spectra of Nylon blank (black) and after EDC/NHS/DNA crosslinking (light-blue). Boxes: shifted and intensified bands, characteristic for DNA

Dopamine

As dopamine has already been proven to be a useful molecule, providing surface reactive groups for the immobilisation of different kind of biomolecules (see introduction), PET and Nylon samples were coated with dopamine hydrochloride (material and methods) to provide a linker-molecule (material and methods) for the DNA.

FT-IR spectra of PET after dopamine coating were recorded, showing broad and intensified bands between 2900 and 3600 cm^{-1} due to hydrogen bonds which are formed between neighbouring hydroxyl groups. Intensified bands in the area of 1450 – 1650 cm^{-1} due to N-H bending vibrations and aromatic C-C stretching vibrations clearly confirm the presence of dopamine after coating³⁸. Further characteristic peaks of dopamine -1265 cm^{-1} (aromatic amine C-N stretching vibrations) and

1050 cm^{-1} (C-N bending vibrations between the benzene ring and the hydroxyl groups)- are overlaid in the spectra by peaks characteristic for PET.

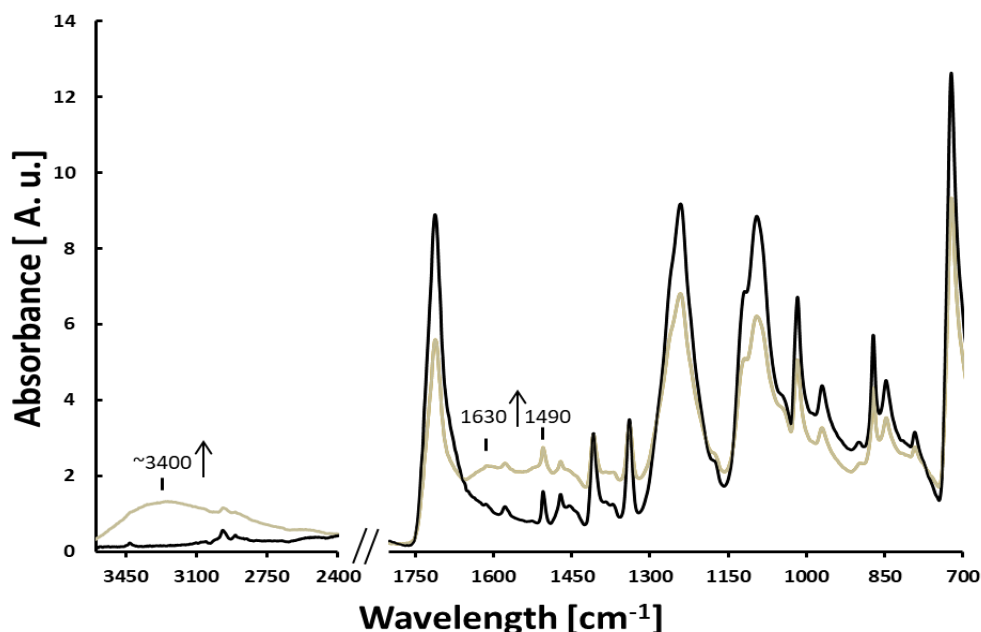


Figure 45: FT-IR spectra of PET blank (black) and after dopamine coating (brown). Characteristic peaks for dopamine labelled; arrows indicating the increase of intensity.

After coating with DNA for 24 h, PET/Dopamine/DNA samples were dried for 24 h at RT and measured again *via* FT-IR (Figure 46). A new band at around 1680 cm^{-1} (P=O), as well as intensified and shifted bands at 1220 cm^{-1} and 1060 cm^{-1} (asymmetric and symmetric PO_2^- vibrations) clearly indicate the presence of immobilized DNA. This is also confirmed by intensified and shifted bands at 835 cm^{-1} and 780 cm^{-1} which contribute to C=C and C=N stretching modes of pyrimidines and purines¹⁷.

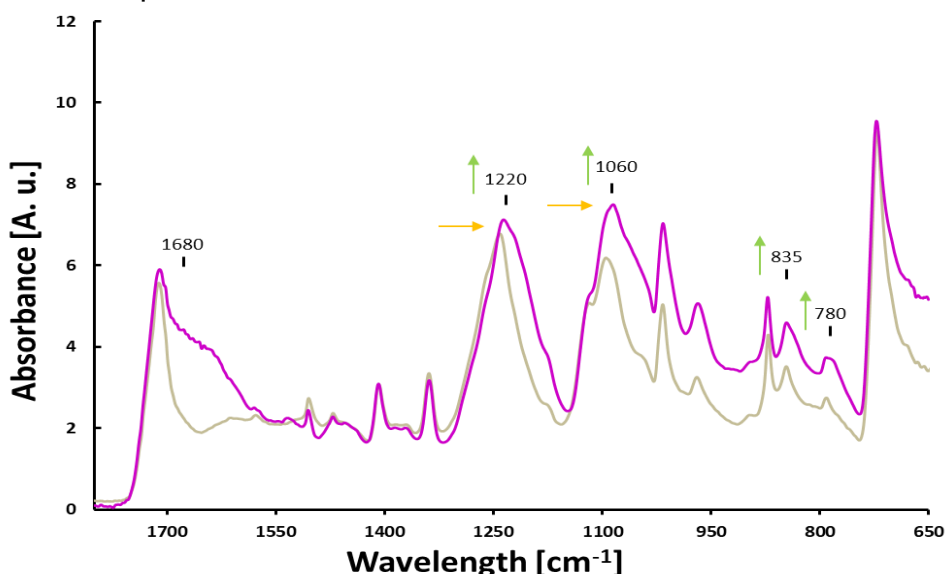


Figure 46: FT-IR spectra of PET/Dopamine (brown) and PET/Dopamine/DNA (pink). Peaks which were increased (green arrows) and shifted (orange arrows) after DNA immobilisation are labelled.

Compared to the EDC/NHS crosslinking system, FT-IR spectra of PET/Dopamine/DNA samples showed a significantly higher increase in signal peaks characteristic for DNA.

Dopamine coating of Nylon samples showed changes in the FT-IR spectra, which correspond to the ones recorded for PET/Dopamine. Peaks with a broader bandwidth in the range of $2800 - 3600\text{ cm}^{-1}$ indicate the formation of hydrogen bonds between the hydroxyl groups of dopamine. The band at 1493 cm^{-1} , characteristic for aromatic C-C stretching vibrations of dopamine, is overlaid by the amide II band of Nylon but there is a shift into the direction of dopamine. A brighter and intensified peak at approximately 1265 cm^{-1} as well as a clearly visible peak at around 1050 cm^{-1} further confirms the presence of dopamine on the surface of Nylon fabrics (Figure 47).

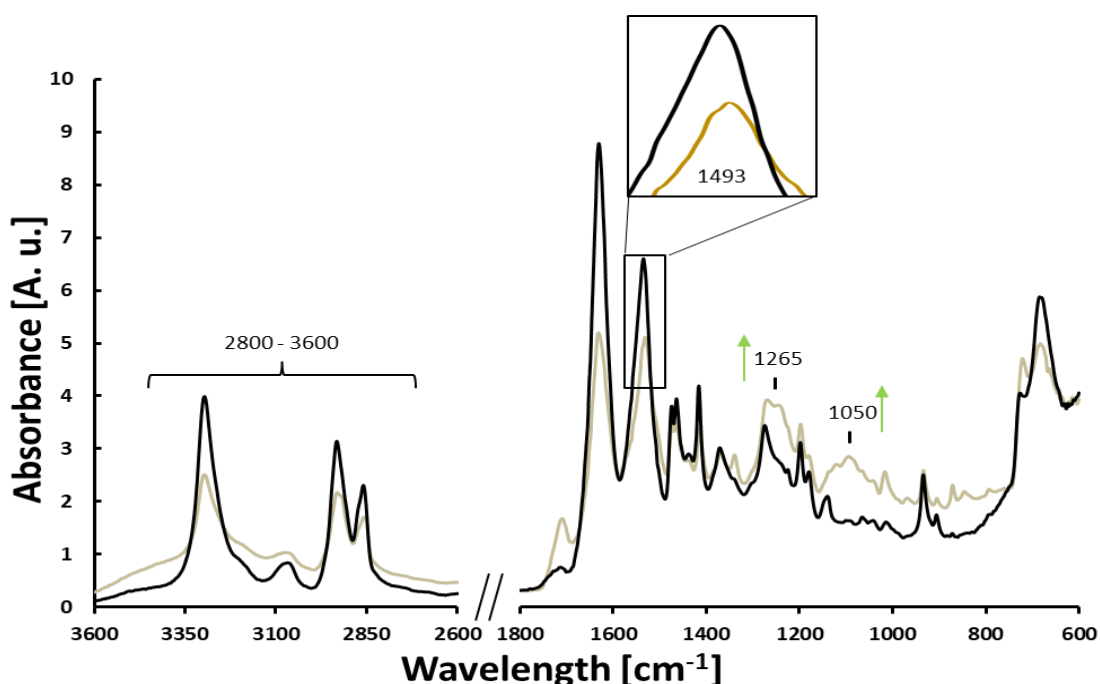


Figure 47: FT-IR spectra of Nylon blank (black) and Nylon/Dopamine (brown). Characteristic peaks of dopamine are labelled.

Spectra of Nylon/Dopamine/DNA samples were recorded *via* FT-IR (Figure 48) after 24 h of drying, showing an intensified, shifted peak which also forms a small shoulder at $\sim 1540\text{ cm}^{-1}$. Furthermore, sharper and in some cases more intensified peaks were recorded between $1420 - 1470\text{ cm}^{-1}$. A shift of the band at $\sim 1006\text{ cm}^{-1}$ and a broader bandwidth of the peak at around 835 cm^{-1} which are characteristic for C=C and C-N stretching modes, again confirm that also the DNA immobilisation on

dopamine coated Nylon fabric was successful. Compared to PET/Dopamine/DNA, the intensity of the bands indicating the presence of DNA was smaller, which leads to the assumption that dopamine works better as crosslinking agent on PET.

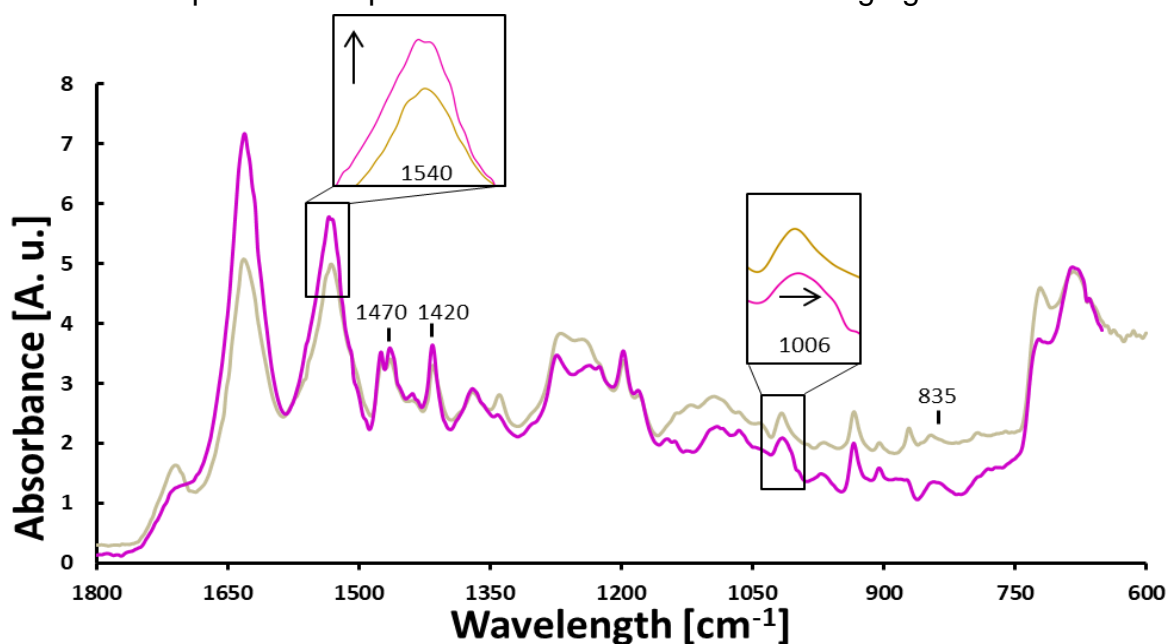


Figure 48: FT-IR spectra of Nylon/Dopamine (brown) and Nylon/Dopamine/DNA (pink). Peaks characteristic for DNA are labelled. Increase of intensity and shift of peaks are shown with black arrows.

ESEM

Scanning electron microscopy was again used to image the surface of PET and Nylon after the coating with dopamine and DNA. On the surface of Nylon fabric, dopamine forms scurf-like particles which are attached to the fibres (Figure 49). There is no homogenous coating of DNA visible which is also confirmed by the FT-IR spectra, showing only low bands in the characteristic region of DNA. After DNA-immobilization the elemental composition of the surface should show an increase in the peak characteristic for phosphorus (~ 1.9 KeV). In case of Nylon, only a small peak is visible in the EDS spectra which further confirms that the DNA immobilisation was not homogenous.

Imaging of PET after Dopamine/DNA coating showed again the scurf formation of dopamine on the fibre. In contrast to Nylon, spots with immobilized DNA are visible which is also confirmed by the changes in the FT-IR spectra of PET/Dopamine/DNA but also in the case of PET a homogenous coating was not achieved. The appearance of the phosphorus peak in the EDS spectra further confirms the presence of DNA on the fabric surface.

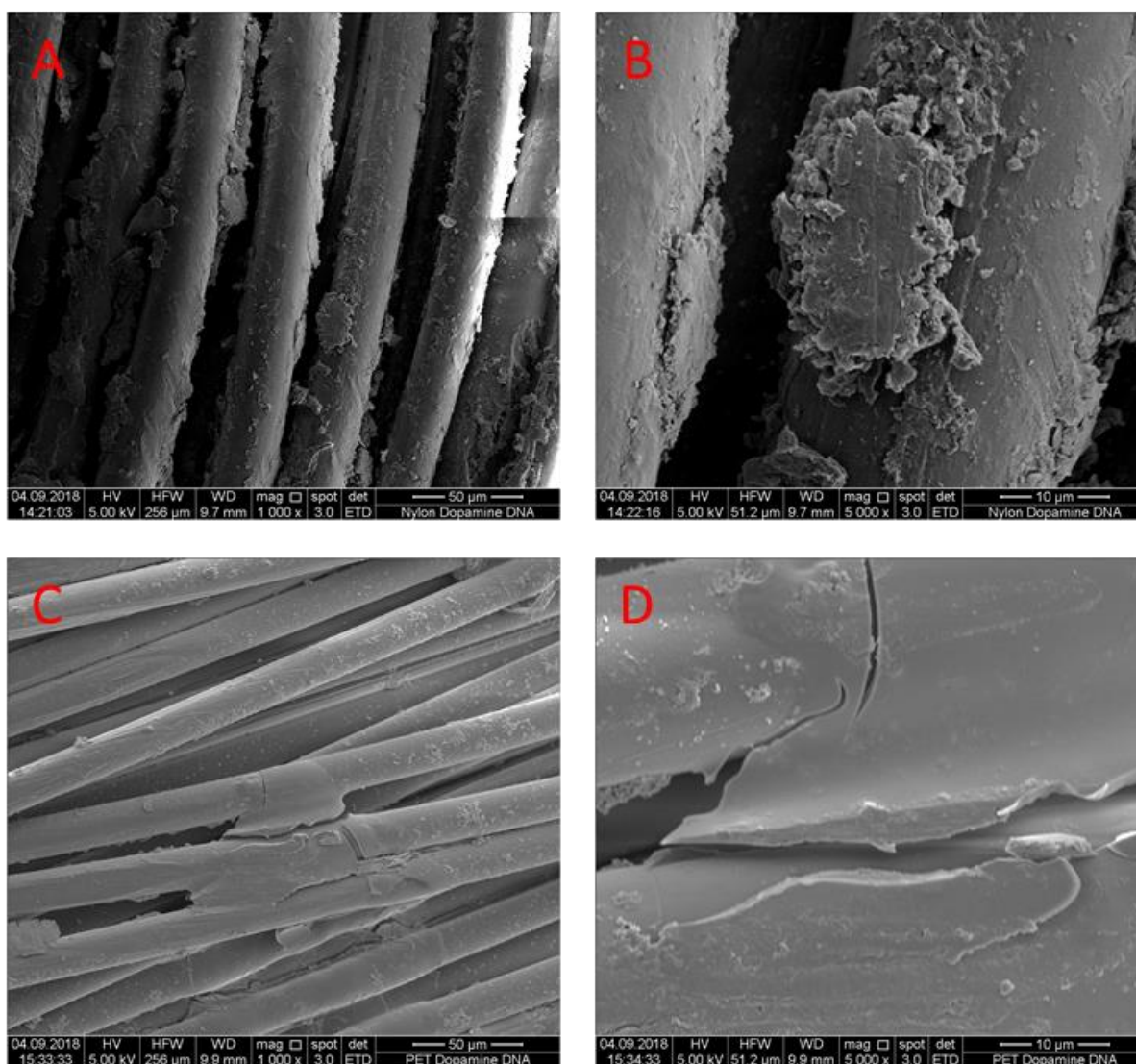


Figure 49: ESM image of Nylon/Dopamine/DNA (A&B) and PET/Dopamine/DNA (C&D)

Tyrosine

The last technique to immobilise the DNA on PET and Nylon surface was the use of L- Tyrosine as linker between the surface reactive groups and DNA. The coating with tyrosine and DNA was carried out according the protocol in the material and methods part. After 24 h of drying at RT, the samples were characterized according their FT-IR spectra as well as imaging with microscope and SEM.

Starting with the FT-IR spectra of PET/Tyrosine (Figure 50), bands at 3210 cm^{-1} and 3040 cm^{-1} (aromatic CH stretching), 1590 cm^{-1} (asymmetric stretching of NH_3^+) and 1450 cm^{-1} (scissoring vibration of Tyrosine), which are characteristic for Tyrosine, are visible after the treatment³⁹. This confirms that Tyrosine could be attached to the surface of PET to a certain extend.

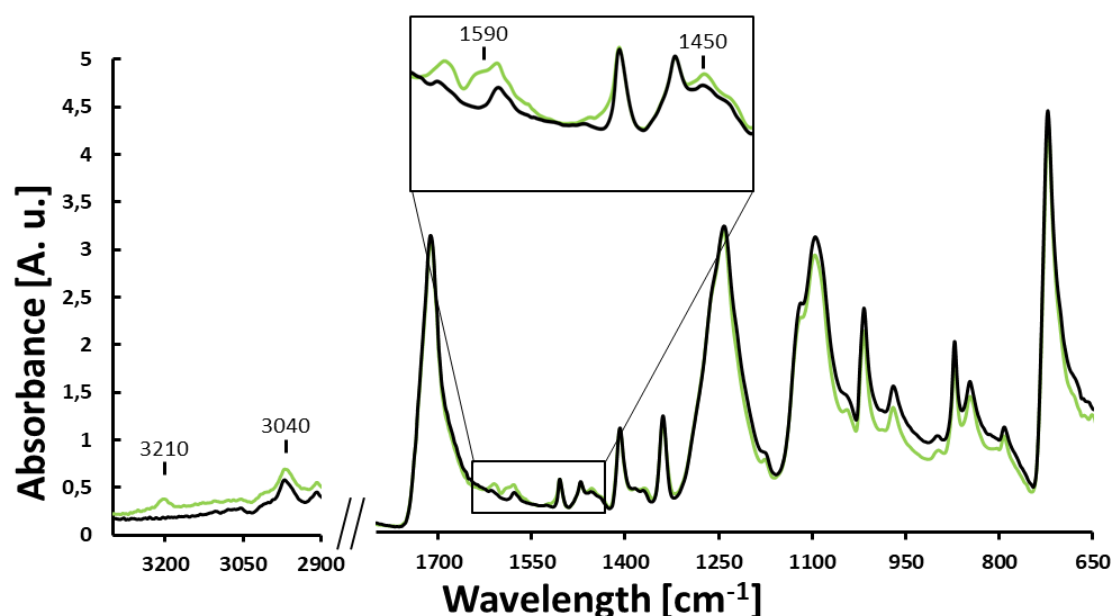


Figure 50: FT-IR spectra of PET blank (black) and PET/Tyrosine (green). Characteristic peaks of Tyrosine are labelled. In the box, zoomed spectra in the range of 1400 - 1650

After immobilization of the DNA, there are major changes visible in the FT-IR spectra. By comparing the spectra of PET/Tyrosine/DNA with the spectra of salmon DNA it is clearly visible that all peaks characteristic for DNA (1680, 1220, 1060, 967, 832 and 780 cm^{-1}) can be found, which confirms the presence of DNA on the PET fabric (Figure 51). Due to the intense and clearness of the bands it can be assumed that DNA was immobilized to a huge amount.

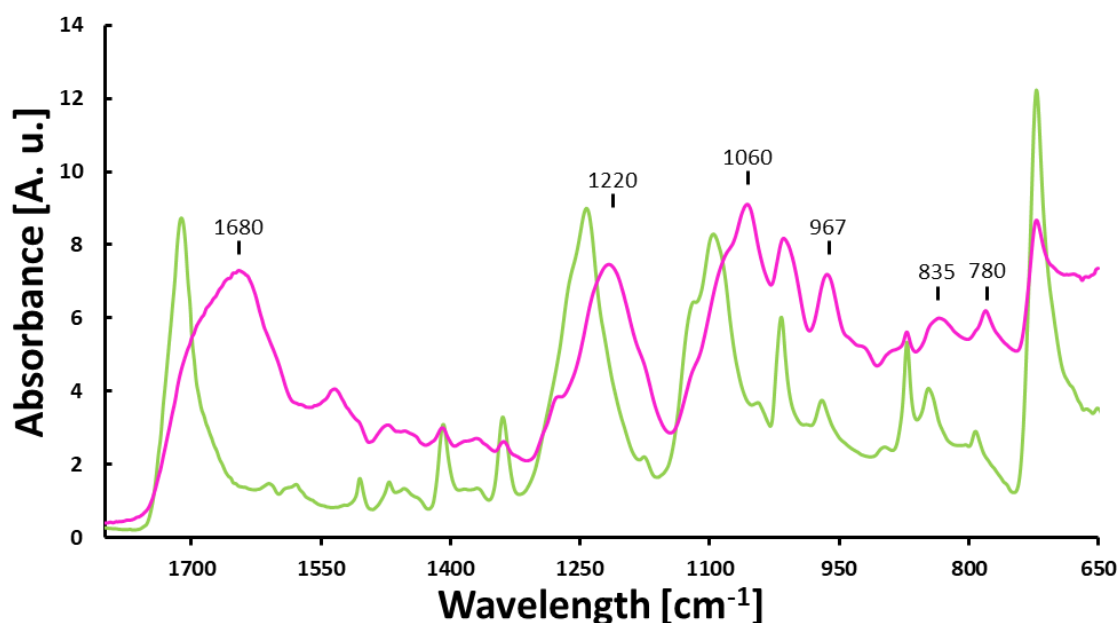


Figure 51: FT-IR spectra of PET/Tyrosine (green) and PET/Tyrosine/DNA (pink). Bands characteristic for DNA are labelled.

FT-IR spectra of Nylon/Tyrosine showed as well distinct changes compared to the blank. As described earlier, the reduction of the amide I and II bond (1657 and 1533 cm^{-1}) and the increase in the band at 1711 cm^{-1} is due to the hydrolysis of the polymer bonds which leads to an increase in carboxylic acid groups. This is also the reason for the intense band at $\sim 1100\text{ cm}^{-1}$ which results from newly formed carboxyl groups. Nevertheless, tyrosine characteristic peaks were also visible in the case of Nylon/Tyrosine. These peaks are again located at 3040 cm^{-1} , 1590 cm^{-1} (overlaid by the amide II band) and 1330 cm^{-1} . Furthermore, there is a very strong and wide peak at 1250 cm^{-1} (OH in plane deformation coupled to C-O stretching) and together with the peak at 840 cm^{-1} the spectra clearly confirm that L-Tyrosine could also be coupled to Nylon fabric (Figure 52).

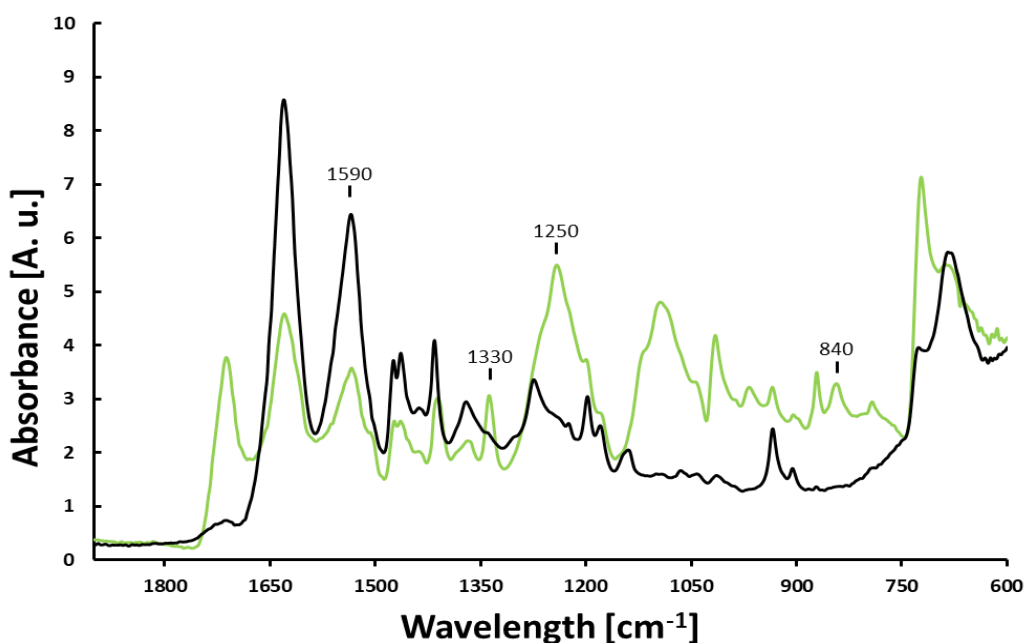


Figure 52: FT-IR spectra of Nylon blank (black) and Nylon/Tyrosine (green). Characteristic peaks of Tyrosine labelled.

The band at $\sim 1710\text{ cm}^{-1}$ was intensified and shifted towards the direction of the $\text{P}=\text{O}$ bonding after the immobilization of DNA. Furthermore, bands at 1220 and 1060 cm^{-1} were further intensified and show a slightly shift. At approximately 970 cm^{-1} the intensity of the band decreases which is due to ribose phosphate skeletal motions¹⁷. The shift of the bands at 1410 and 1340 cm^{-1} can be explained by the presence of purine and pyrimidine molecules ($1320 - 1470\text{ cm}^{-1}$).

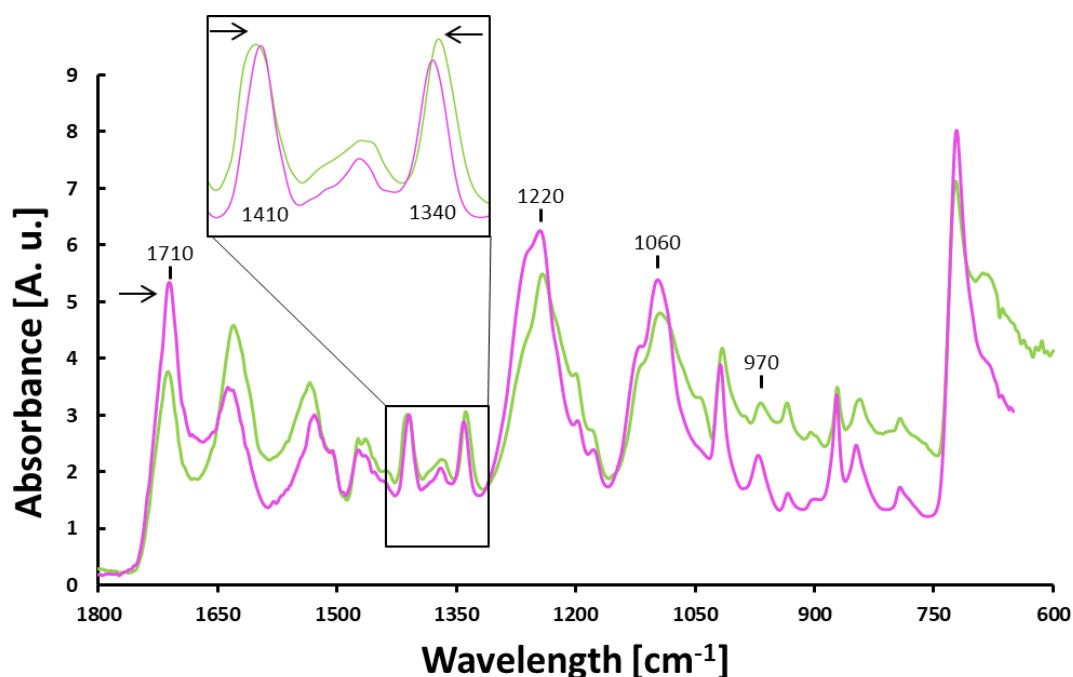


Figure 53: FT-IR spectra of Nylon/Tyrosine (green) and Nylon/Tyrosine/DNA (pink). Characteristic DNA peaks labelled. Region 1300 – 1450 cm^{-1} enlarged in the box.

ESEM

Imaging of Tyrosine and DNA coated samples showed major changes in the surface structure. In the case of Nylon, Tyrosine coating resulted in the formation of crystals which are attached to the fibre surface. After the DNA-immobilization Nylon surface is homogenously coated by a film of DNA, which is further confirmed by the EDS spectra showing a newly formed and intense peak of phosphorus.

Tyrosine coating of PET resulted in even more crystals which are attached to the fibres. Compared to Nylon, DNA-immobilization on PET was not homogenous, showing again spots of DNA distributed on the surface of the sample. This deviation to the FT-IR spectra of PET/Tyrosine/DNA, which showed the most intense bands for DNA, can be explained by the fact that FT-IR is a point measurement. It is therefore possible that the FT-IR measurement hit one of the spots visible on the ESEM image. Furthermore, the EDS spectra showed a smaller peak for phosphorus compared to Nylon/Tyrosine/DNA.

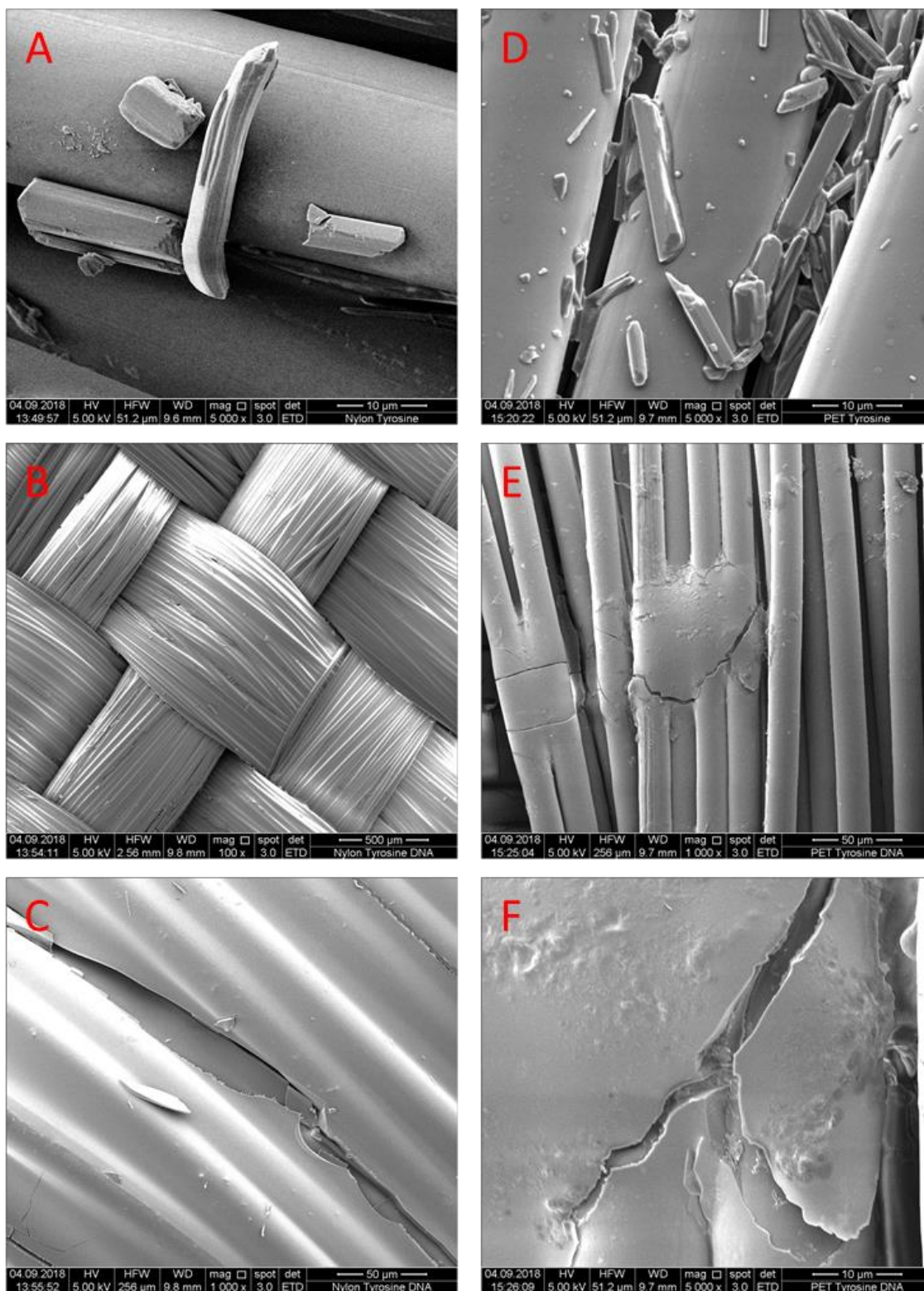


Figure 54: ESEM images of Nylon/Tyrosine (A) and Nylon/Tyrosine/DNA (B&C) on the left and PET/Tyrosine (D) and PET/Tyrosine/DNA (E&F) on the right

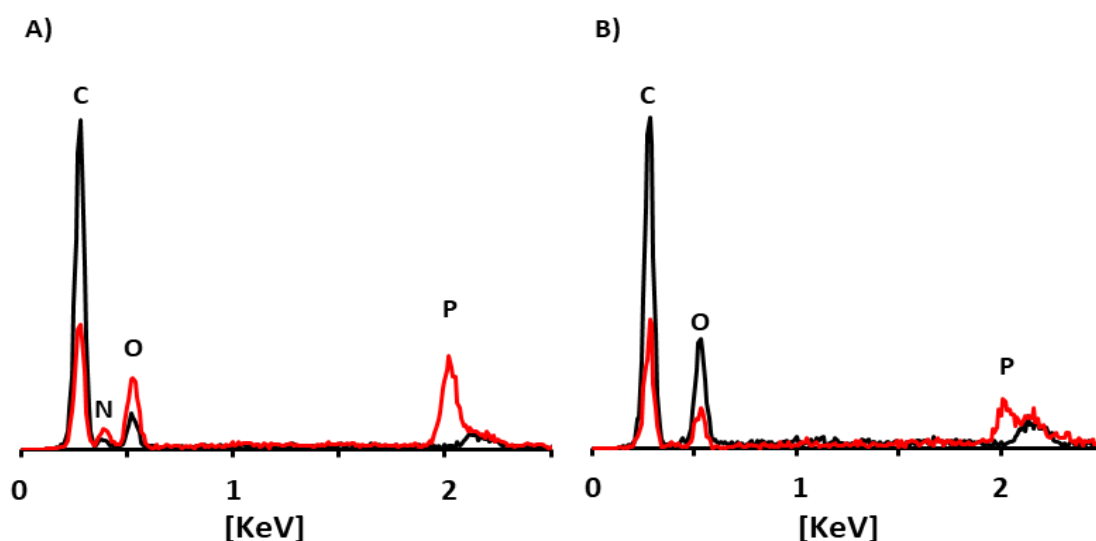


Figure 55: A: EDS spectra of Nylon/Blank (black) and Nylon/Tyrosine/DNA (red). B: EDS spectra of PET/Blank (black) and PET/Tyrosine/DNA (red)

By comparing the FT-IR spectra of all three immobilization techniques, it is clearly visible that there are differences according to the effectiveness of DNA-immobilisation. The EDC/NHS crosslinking system shows the lowest intensity in bands corresponding to DNA in the case of both polymer fabrics, making it not favourable for PET and Nylon functionalization. Polydopamine coating seems to be more effective on PET in terms of the coating itself and in serving as a linker between DNA and the polymer. The intensity of the bands characteristic for dopamine shows a higher intensity after PET coating compared to dopamine-coated Nylon fabric. This can be explained by looking at the hydrolysis of both polymers. In the case of PET, hydrolysis results in the formation of carboxylic groups to which dopamine can be bound *via* formation of amide bonds. The hydrolysis of Nylon generates also new amine groups which makes it harder for the dopamine molecules to bind. Tyrosine on the other hand provides two functional groups ($-\text{COOH}$ and $-\text{NH}_2$) which can bind to carboxylic groups on PET and Nylon *via* formation of amide bonds. Furthermore, it can bind also the newly formed amine groups on Nylon which makes it probably the best immobilization agent for DNA on both polymers. This is also confirmed by the FT-IR spectra which show the most intense bands of DNA after the coating with L-Tyrosine as well as the ESEM images showing inhomogeneous coating of PET and homogeneous coating of Nylon with Tyrosine as linker-molecule.

3.4. Flame retardant characterization

Flammability test

In a first trial, 8 x 20 cm stripes of all different treatments were used for flammability tests to determine the most sufficient treatment of PET and Nylon (shown in Table 3). In the case of PET, the three treatments showed a decrease in burning rate compared to the untreated (Blank) and enzymatic treated (HiC) samples. The total burning time (TBT) increased as well as the length of the burned sample, showing that the immobilization of the DNA could favour the flame-retardancy of PET fabric. Within the three different immobilization techniques, dopamine treated samples showed the longest burning time and the remaining, unburned fabric was about half of the original one. EDC/NHS and Tyrosine showed very similar behaviour in terms of TBT and burning rate but among all three treatments, Tyrosine/DNA coated samples showed the biggest fraction of unburned fabric.

Nylon fabric showed different behaviour compared to PET. The blank nearly completely burned with the longest TBT. In contrast, the enzymatic treated (Nylon_HiC) fabric showed an about 1/3 reduced TBT and burning length. This may be explained by the newly formed amine groups after enzymatic hydrolysis, which can release ammonia during combustion, leading to a dilution in the gas phase and an extinguishing of the flame. In case of dopamine, the sample completely burned and did not reach self-extinguishing of the flame. Among the three different treatments, Tyrosine/DNA seems to be the best also for Nylon fabric, due to the shortest TBT and burning length. Furthermore, the flame was self-extinguished nearly immediately after the flame was applied to the fabric.

Table 3: Results of flammability tests for all different treatments.

Sample	Total burning time [s]	burning lenght [mm]	Burning rate [mm/s ⁻¹]
PET Blank	6,75	57,5	8,5
PET_HiC	5	42,5	8,5
PET_EDC_NHS_DNA	13	70	5,4
PET_Dopamine_DNA	21,5	85	4,0
PET_Tyrosine_DNA	11	68	6,2
Nylon Blank	35	150	4,3
Nylon_HiC	10	60	6,0
Nylon_EDC_NHS_DNA	15	53	3,6
Nylon_Dopamine_DNA	33	200	6,1
Nylon_Tyrosine_DNA	3,5	17,5	5,0

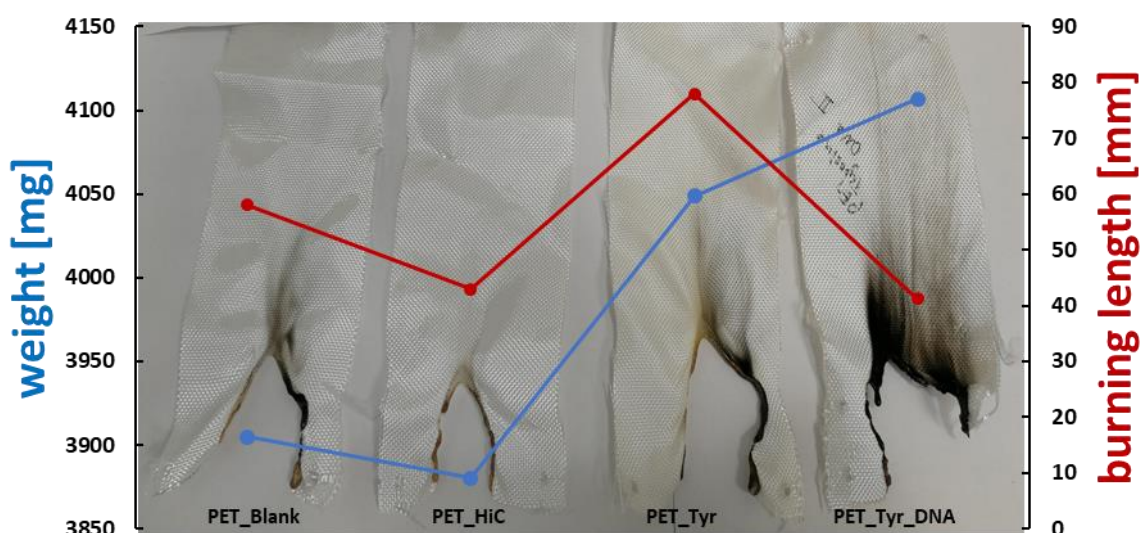


Figure 56: Results of flammability test of PET showing the weight-change (blue line) and the length of burned specimen (red line)

The best results for both polymers were obtained with Tyrosine/DNA coating, making it the best candidate for further flammability tests with more samples. Samples were again prepared according to the functionalization and immobilization procedure shown in the material and methods. This time blank, enzymatic treated (HiC), Tyrosine coated (Tyr) and Tyrosine/DNA coated samples were used to test the flammability behaviour. During the different coating steps, the weight-decrease and increase, resulting from hydrolysis and DNA immobilization, were measured.

PET samples showed a decrease in weight after enzymatic hydrolysis, confirming that the polymer was degraded during the functionalization with HiC. Coating with Tyrosine at first, followed by DNA resulted in a weight-increase indicating that it was possible to immobilize Tyrosine and DNA on the surface of PET. This was also confirmed by the flammability tests of Tyrosine/DNA treated PET samples, which resulted in a decreased burning rate and length of the burned specimen. An increase in the char formation during burning of the Tyrosine/DNA treated sample also indicates the presence of DNA (Figure 56). Compared to the untreated and enzymatic treated sample, it was possible to decrease the burning rate from 8.5 to 6.2 mm*s⁻¹, which further confirms that DNA provides flame retardant properties.

Table 4: Results of flammability tests of enzymatic, Tyrosine and Tyrosine/DNA treated PET

Sample	Total burning time [s]	burning length [mm]	Burning rate [mm*s ⁻¹]
PET Blank	6,8	57,5	8,5
PET_HiC	5,0	42,5	8,5
PET_Tyrosine	11,7	78,3	6,7
PET_Tyrosine_DNA	11,0	68,0	6,2

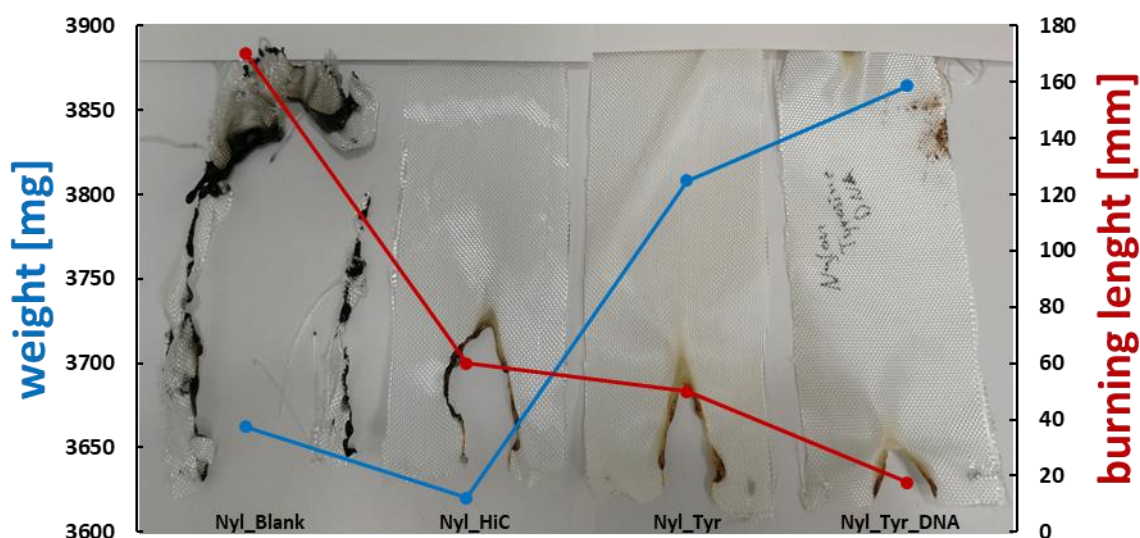


Figure 57: Results of flammability test of Nylon showing the weight-change (blue line) and the length of burned specimen (red line)

The same trend could be observed with Nylon fabric, showing a decrease of weight after enzymatic hydrolysis and an increase during Tyrosine and DNA coating. The flammability test showed very promising results. Starting with the untreated Nylon fabric which completely burned and did not manage to self-extinguish the flame, there is a clear trend in decreasing length of the burned sample visible throughout the different coating steps. After coating with Tyrosine and immobilization of the DNA, the flame was immediately self-extinguished after ~18 mm and a few seconds. The brownish colour of the burned parts, which results from sugars within the sugar-phosphate backbone of DNA, confirms the presence of DNA on the Nylon fabric (Figure 57).

Table 5: Results of flammability tests of enzymatic, Tyrosine and Tyrosine/DNA treated Nylon fabric

Sample	Total burning time [s]	burning lenght [mm]	Burning rate [mm*s ⁻¹]
Nylon Blank	35,0	200,0	5,7
Nylon_HiC	10,0	60,0	6,0
Nylon_Tyrosine	7,0	50,0	7,1
Nylon_Tyrosine_DNA	3,5	17,5	5,0

ESEM

Images of untreated (Blank) and Tyrosine/DNA coated PET and Nylon samples were recorded after the flammability tests to see distinct differences in burning behaviour and char formation. PET/Blank showed a melting behaviour of the fibres during combustion. In contrast, the Tyrosine/DNA coated samples showed more

intact fibres as well as char formation due to still attached DNA which serves as kind of protection layer during thermal decomposition of the polymer.

Untreated Nylon samples showed a very similar burning behaviour in terms of melting. In case of Tyrosine/DNA coated samples, the DNA seems to swell during combustion which indicates the release of non-combustible gases during thermal degradation of the DNA, leading to the very quick self-extinguishing of the flame. Beneath the DNA coating, Nylon fibres are still intact and have not been attacked by the heat.

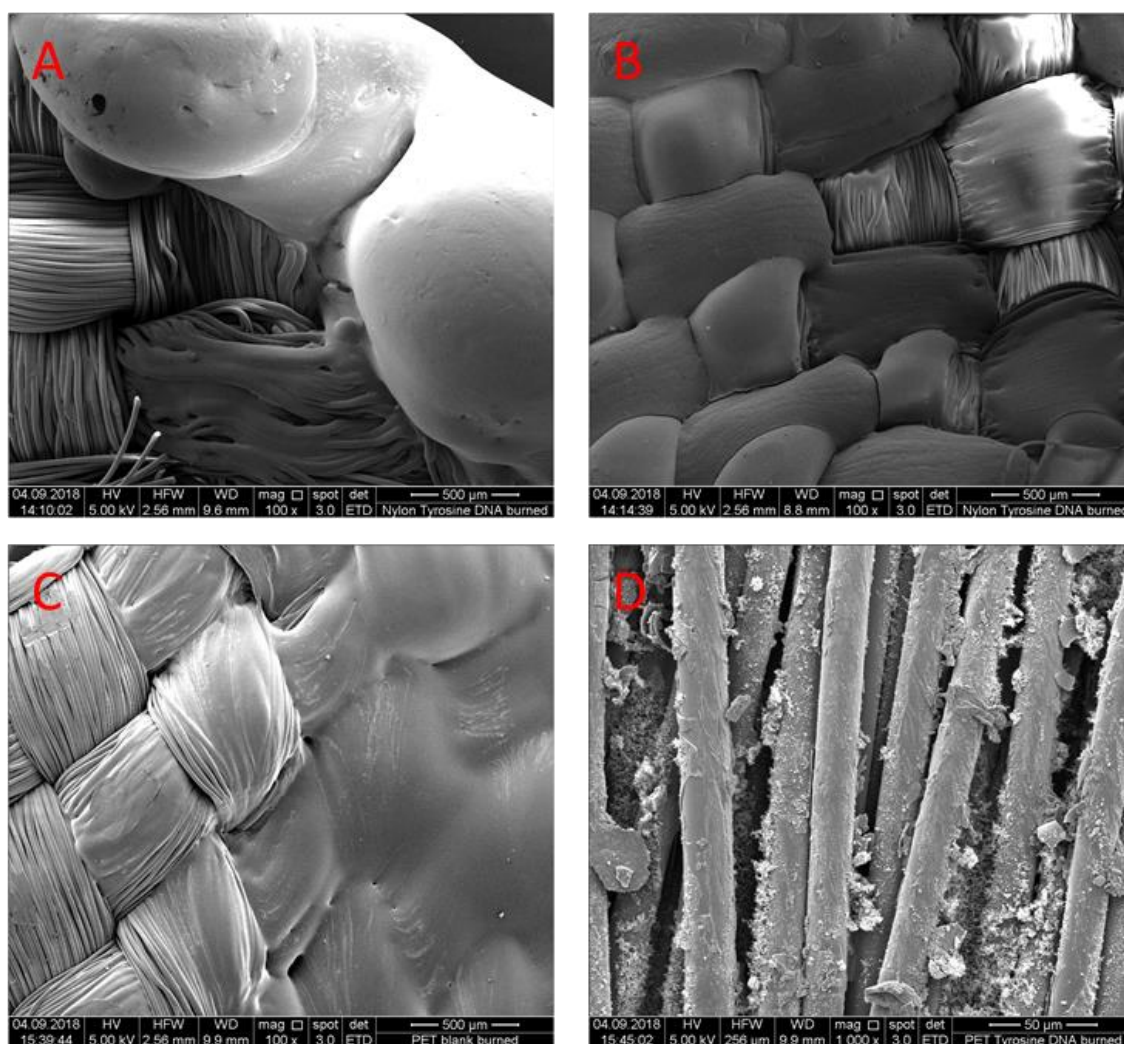


Figure 58: ESEM image of Nylon/Blank burned (A) and Nylon/Tyrosine/DNA burned (B) in the upper part and PET/Blank burned (C) and PET/Tyrosine/DNA burned (D)

TGA

Thermogravimetric analysis was performed with the two most promising samples after flammability tests and FT-IR. It shows changes in thermo-oxidative behaviour and thermal degradation of Tyrosine/DNA coated PET and Nylon. Tyrosine/DNA-coated PET showed a slower thermal degradation in the region between 500 – 600 °C indicating that DNA could favour the flame-resistance (Figure 59, A). In the case of Nylon, the coating with Tyrosine and DNA showed even higher effects in terms of thermal resistance. The weight-loss due to thermal degradation between 450 – 600 °C was significantly lower compared to the untreated Nylon sample and was not completely degraded at 600 °C (Figure 59, B). Compared to TGA curves of untreated, dopamine and EDC/NHS treated samples which show no significant changes in thermal degradation, this further confirms that the DNA-Immobilization on Nylon was more successful.

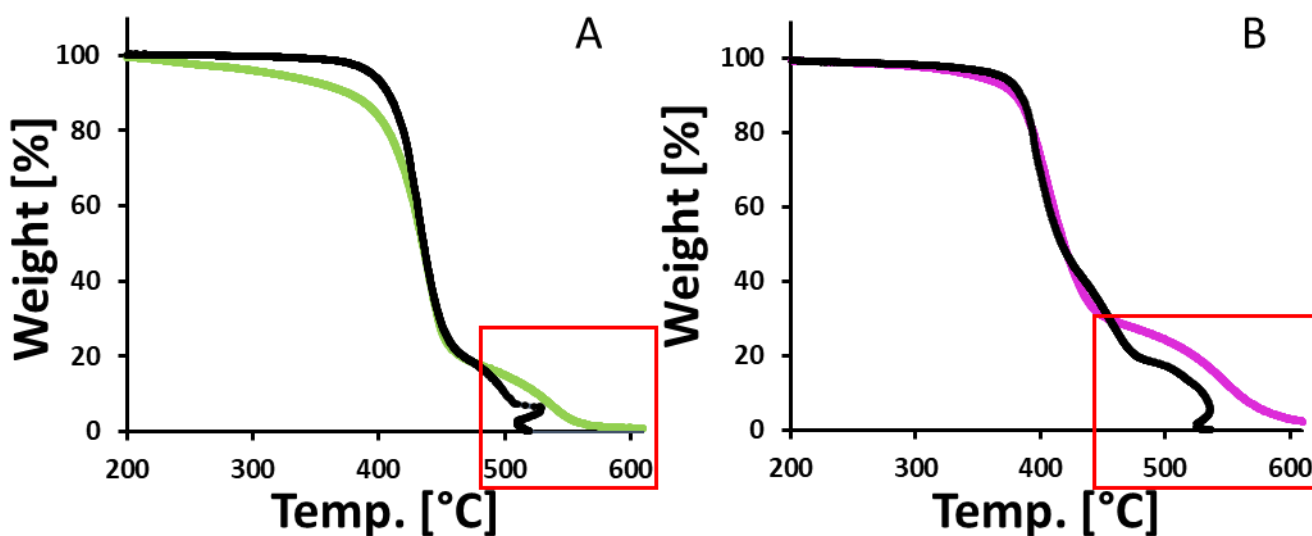


Figure 59: A: Thermal degradation curve of PET Blank (black) and PET/Tyrosine/DNA (green); B: Thermal degradation curve of Nylon Blank (black) and Nylon/Tyrosine/DNA (purple). The slower thermal degradation is shown in the red boxes.

4. Conclusion

The aim of this thesis was to develop a new and eco-friendly method to improve the flame-retardant properties of synthetic polymers like PET and Nylon. The properties of these kinds of materials (crystallinity, hydrophilicity, strength, etc) made it necessary to pre-treat the fabric in order to increase the surface reactivity for the attachment of biomolecules. A cutinase from *Humicola insolens* (~360 U/mL) has

been proven to provide hydrolytic activity towards PET and Nylon, resulting in the cleavage of the polyester bonds. HPLC analysis determined released products, Ta and BHET in the case of PET and CL in case of Nylon, in the range of 0.045 - 0.07 mM and 1 mM, respectively. Furthermore, measurements of the colour difference after staining with acid and basic dye confirmed the presence of newly formed -COOH and -NH₂ groups after enzymatic treatment ($\Delta E=4.80$ and 8.60 for PET and Nylon). FT-IR spectra of the samples showed the most promising results for the enzymatic treated Nylon fabric indicated by a decrease of the Amide I and II peak (1640 and 1540 cm^{-1}) and a corresponding increase of the carboxylic acid peak (1711 cm^{-1}). Scratches on the surface as well as an increase in roughness of the samples after enzymatic hydrolysis have been imaged *via* ESEM, which further confirms the action of the enzyme on the fibre surface. This results clearly indicate the successful hydrolysis of PET and Nylon fabric by HiC as pre-treatment to increase the surface reactivity.

DNA, which provides all properties of a flame-retardant compound (temperature reduction by the release of water, release of inert gases and formation of a solid layer), has already been investigated to be an eco-friendly alternative to commercial ones in meanings of availability and the rather mild operation conditions. To immobilise DNA on the surface of PET and Nylon, three different crosslinking agents have been applied (EDC/NHS, Dopamine and Tyrosine), in which Tyrosine has shown to be the most sufficient. FT-IR spectra showed characteristic and intense peaks at 1450 and 1250 cm^{-1} (scissoring vibration of Tyrosine and OH in plane deformation coupled to C-O stretching) confirming the presence of Tyrosine on the fabric. Imaging *via* ESEM further proved the presence of Tyrosine crystals attached to the fibres. FT-IR spectra of salmon DNA showed characteristic peaks at 1680 , 1220 and 1060 cm^{-1} (Phosphate groups of DNA) which were also found on the surface of Nylon and PET after Tyrosine/DNA treatment, confirming that DNA could be immobilised on the fabric. ESEM images of Nylon/Tyrosine/DNA treated samples showed a completely homogenous layer of DNA on the fabric surface.

To investigate the flame retardancy of DNA-coated fabric, flammability tests according to the ISO 6940 were performed, showing astonishing results for the Tyrosine/DNA treated Nylon fabric. Untreated Nylon fabric completely burned (200 mm) in a total burning time of 35 s and a resulting burning rate of $5.7\text{ mm}\cdot\text{s}^{-1}$

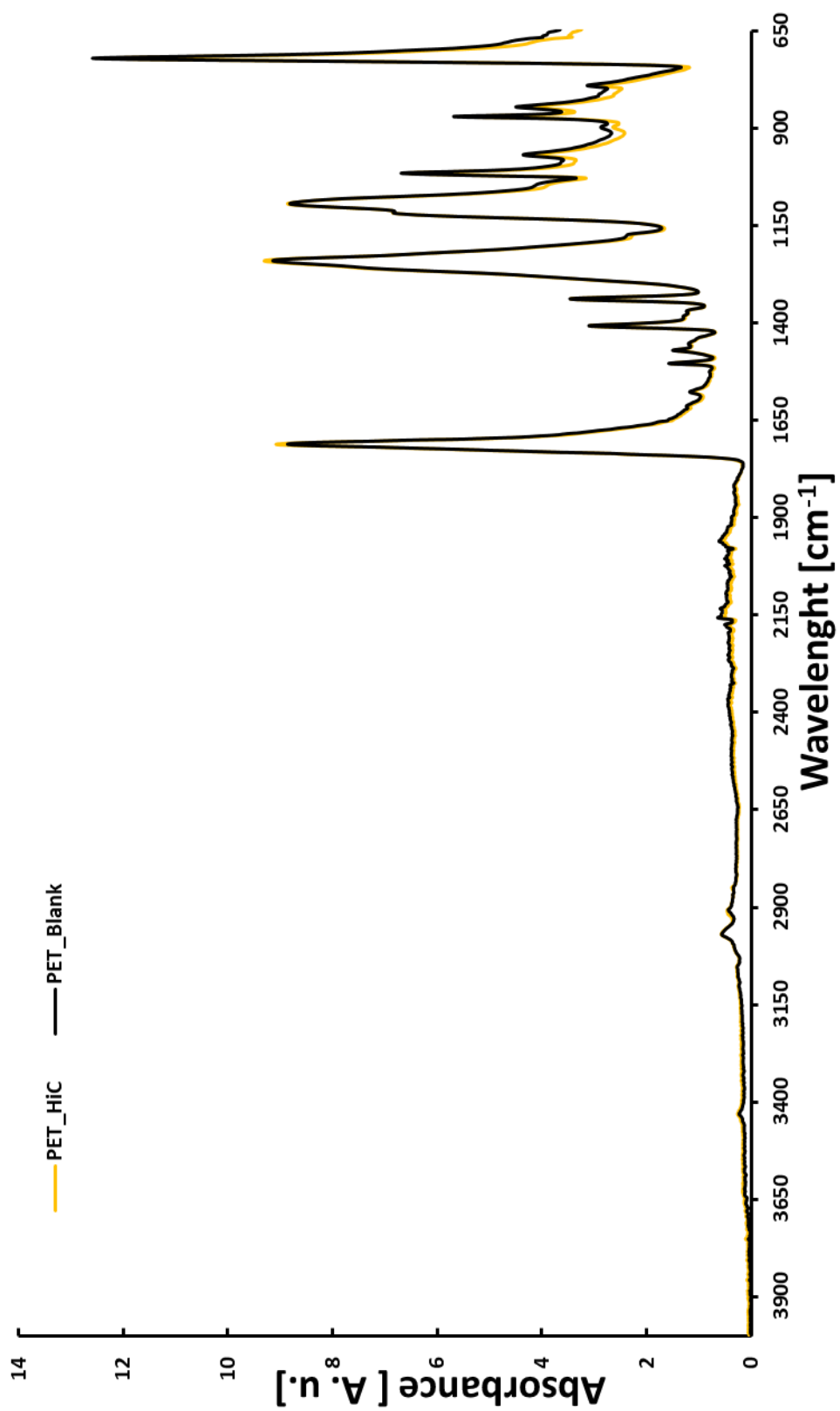
without self-extinguishing. In comparison, ~90% of DNA-coated Nylon fabric remained unburned and the flame was self-extinguished immediately after 3.5 s and 17.5 mm. The resulting burning rate also decreased to a value of $5.0 \text{ mm} \cdot \text{s}^{-1}$. The flame-retardant behaviour was also proved by ESEM imaging of the burned sample, showing a swelling of the DNA layer due to the release of non-combustible gases and water as well as char formation during burning.

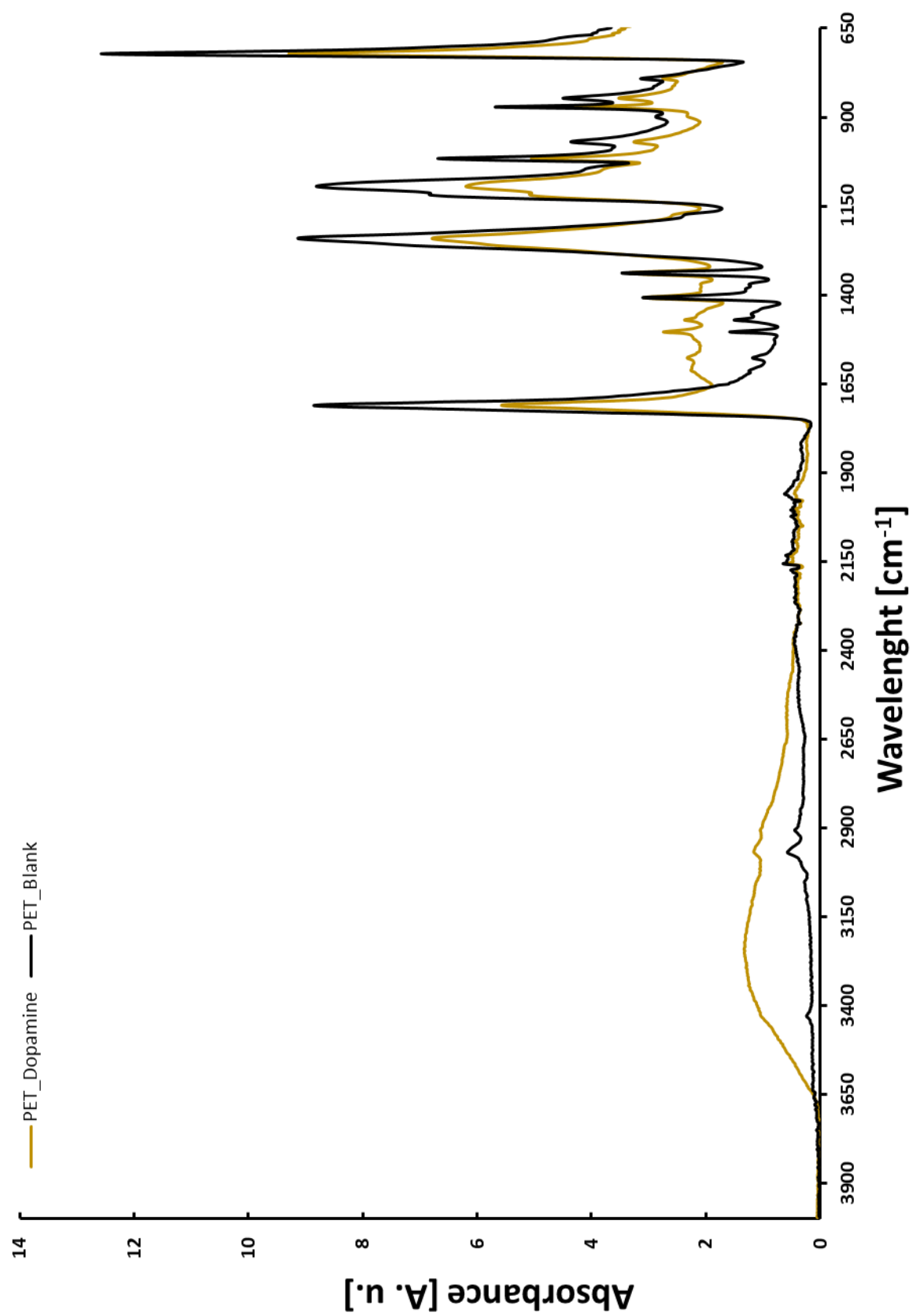
Thermogravimetric analysis of untreated and Tyrosine/DNA coated PET and Nylon could further confirm the flame-retardant properties of DNA by reducing the thermal degradation of the fabric between 450 – 600 °C.

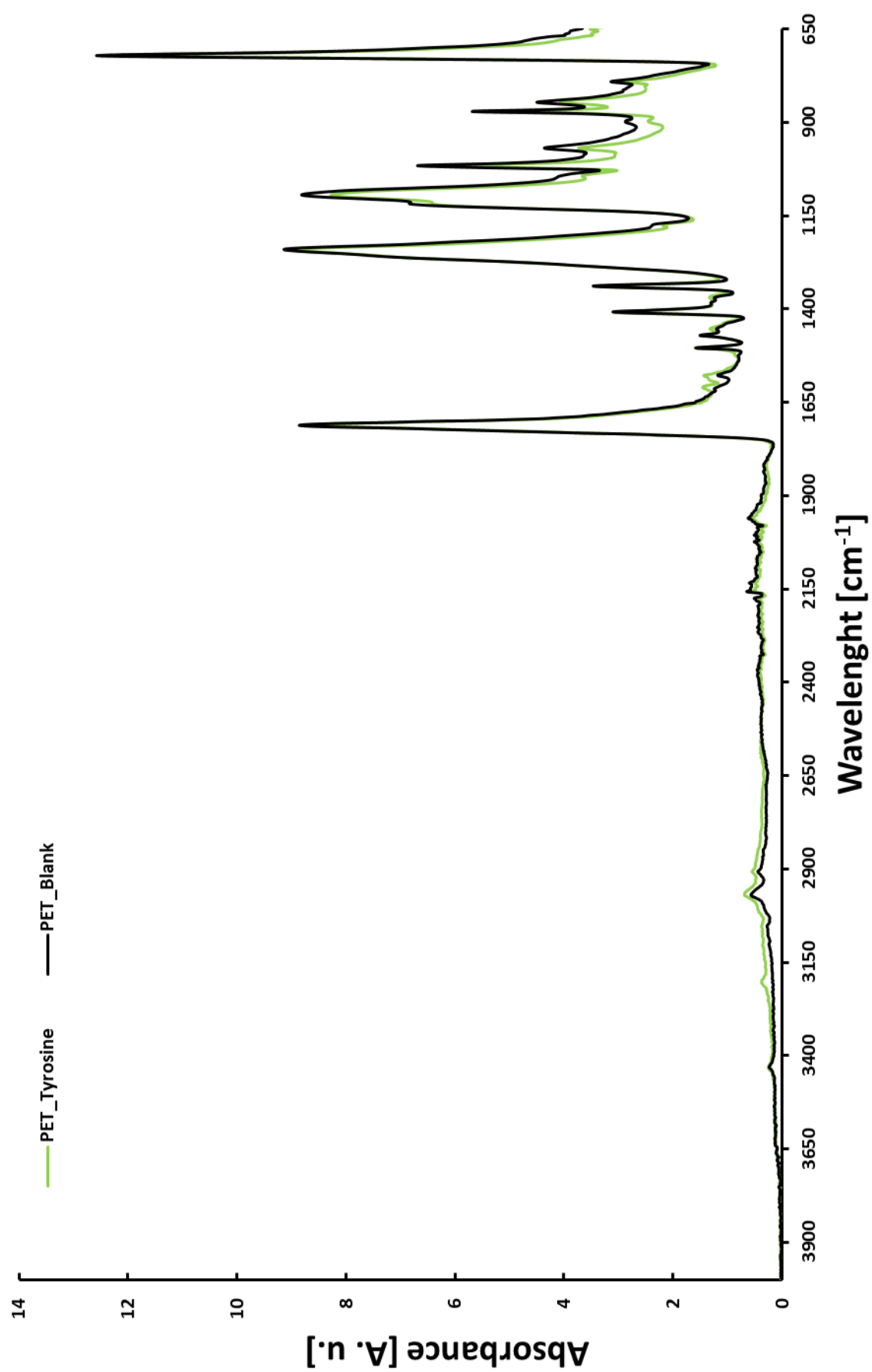
By increasing the surface reactivity *via* enzymatic hydrolysis and using Tyrosine as crosslinking agent between polymer surface and biomolecules, DNA has shown to be a promising flame-retardant compound which should be further investigated to successfully replace the commercial ones.

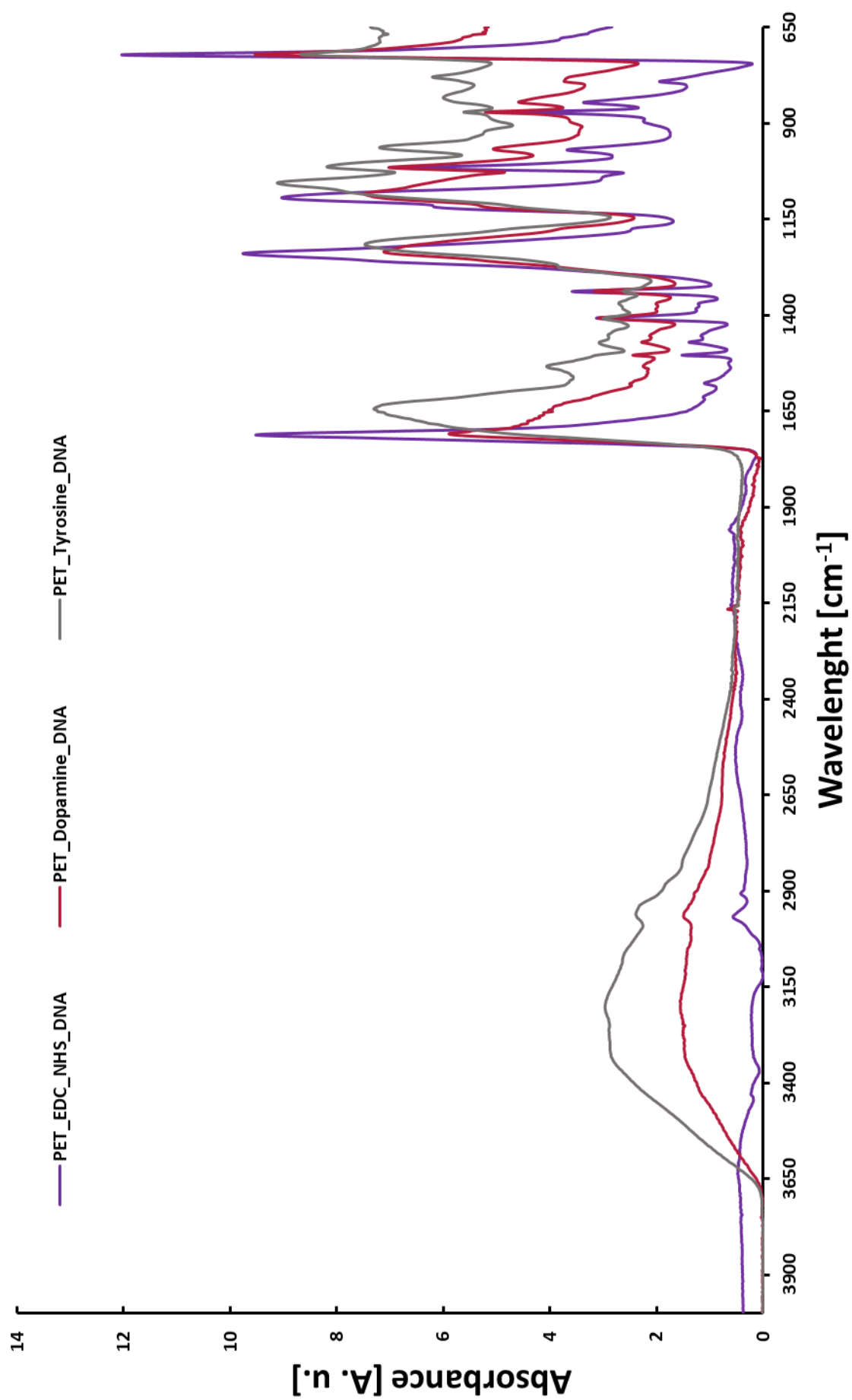
5. Appendix

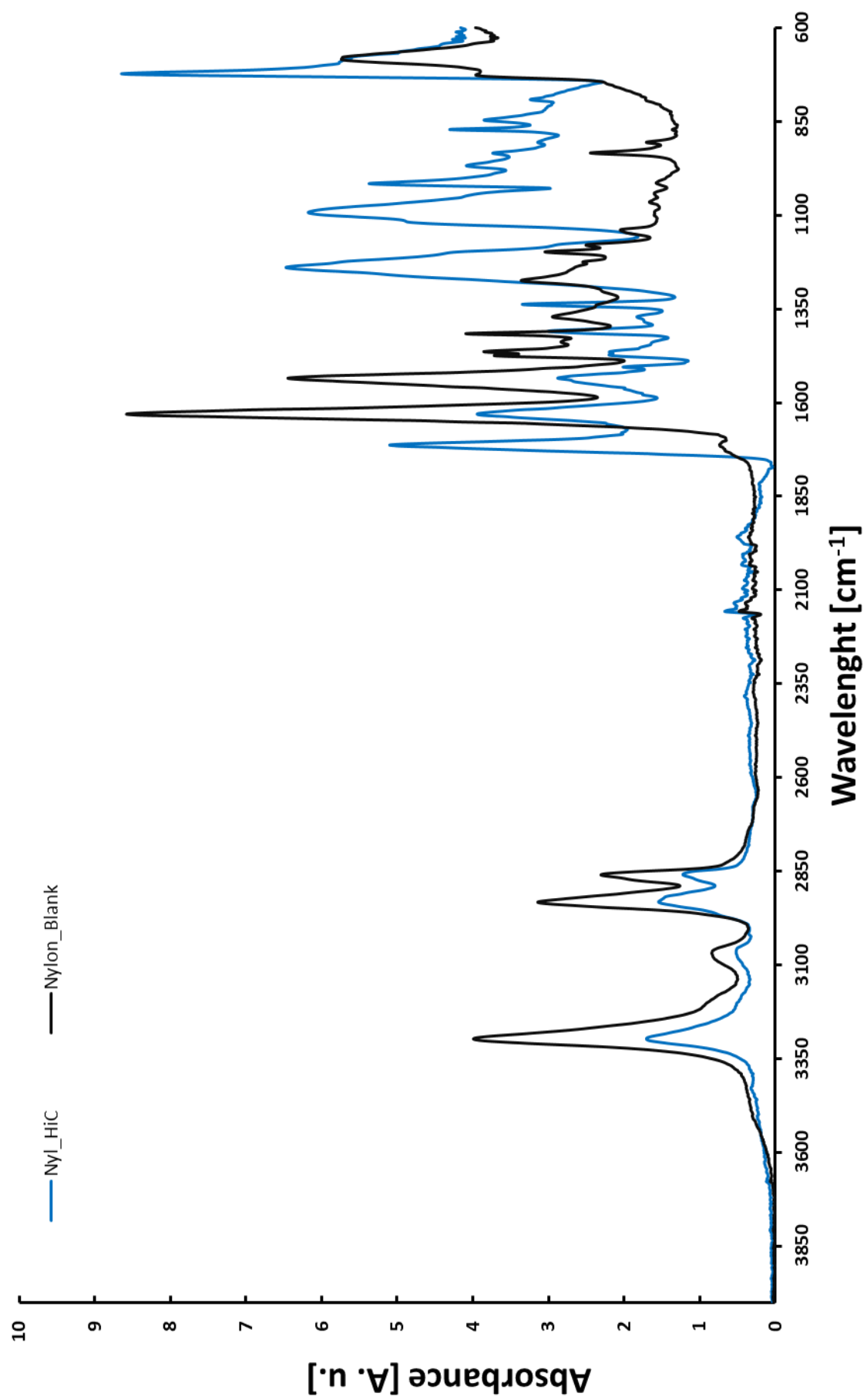
5.1. FT-IR Spectra

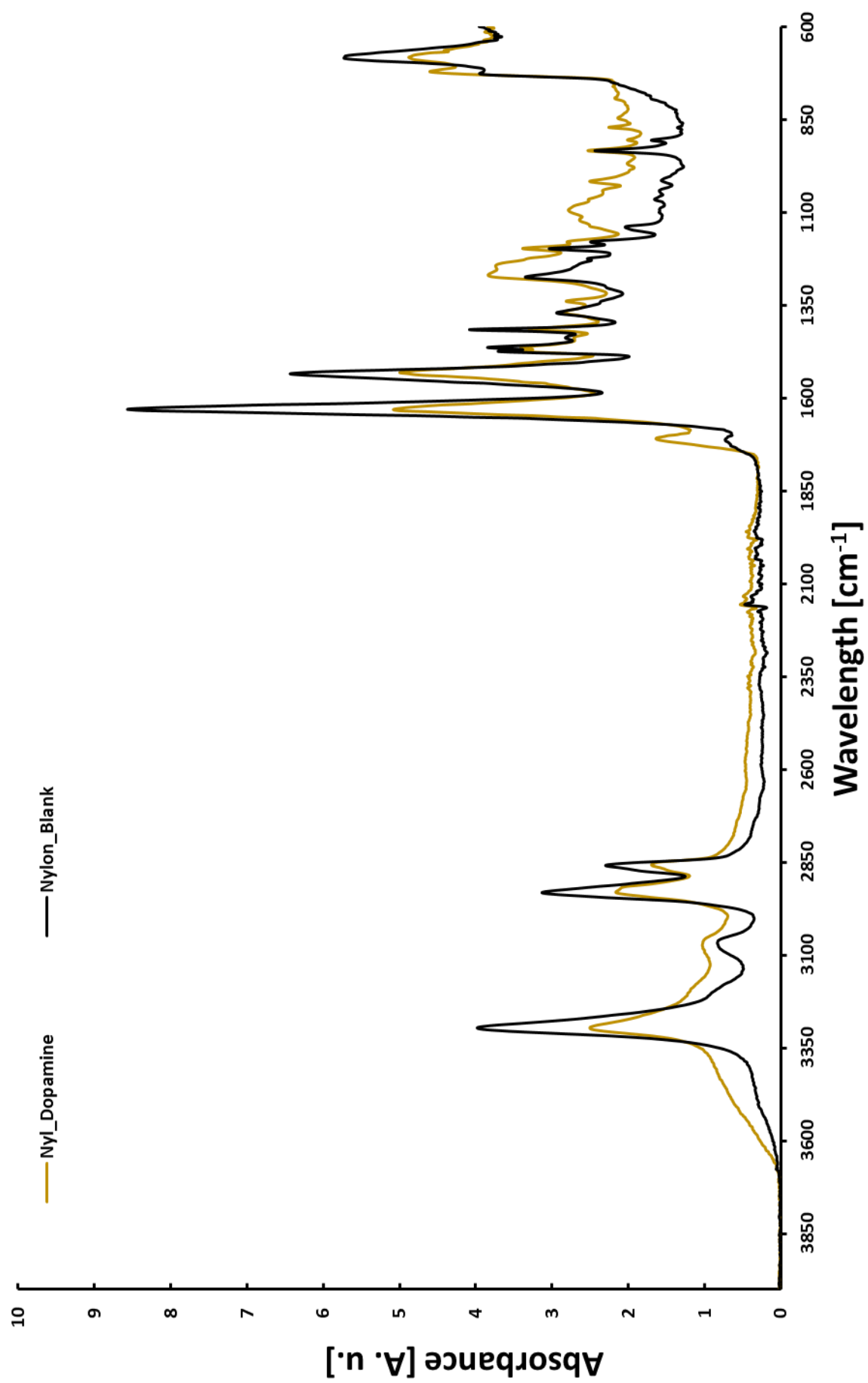


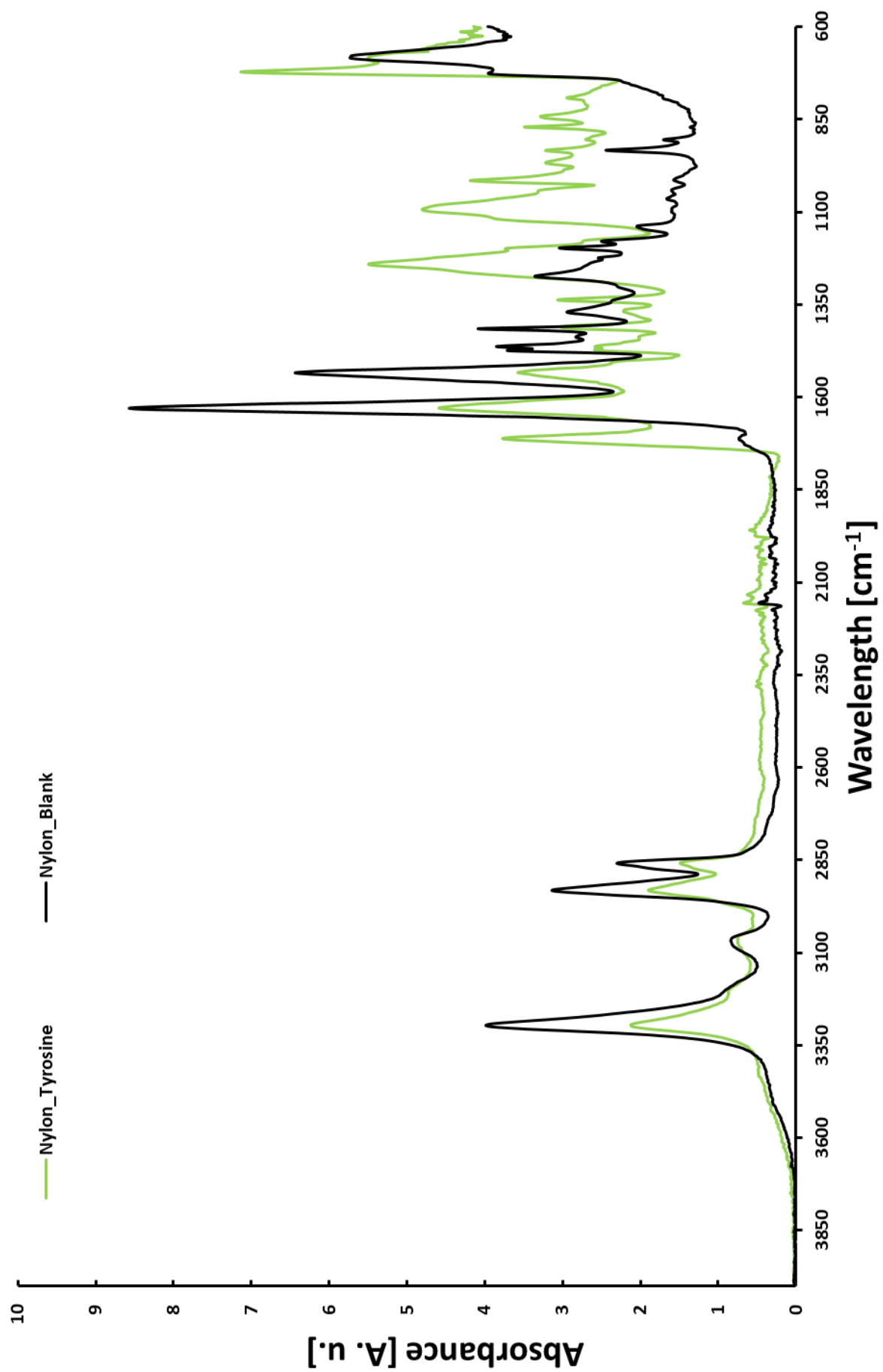


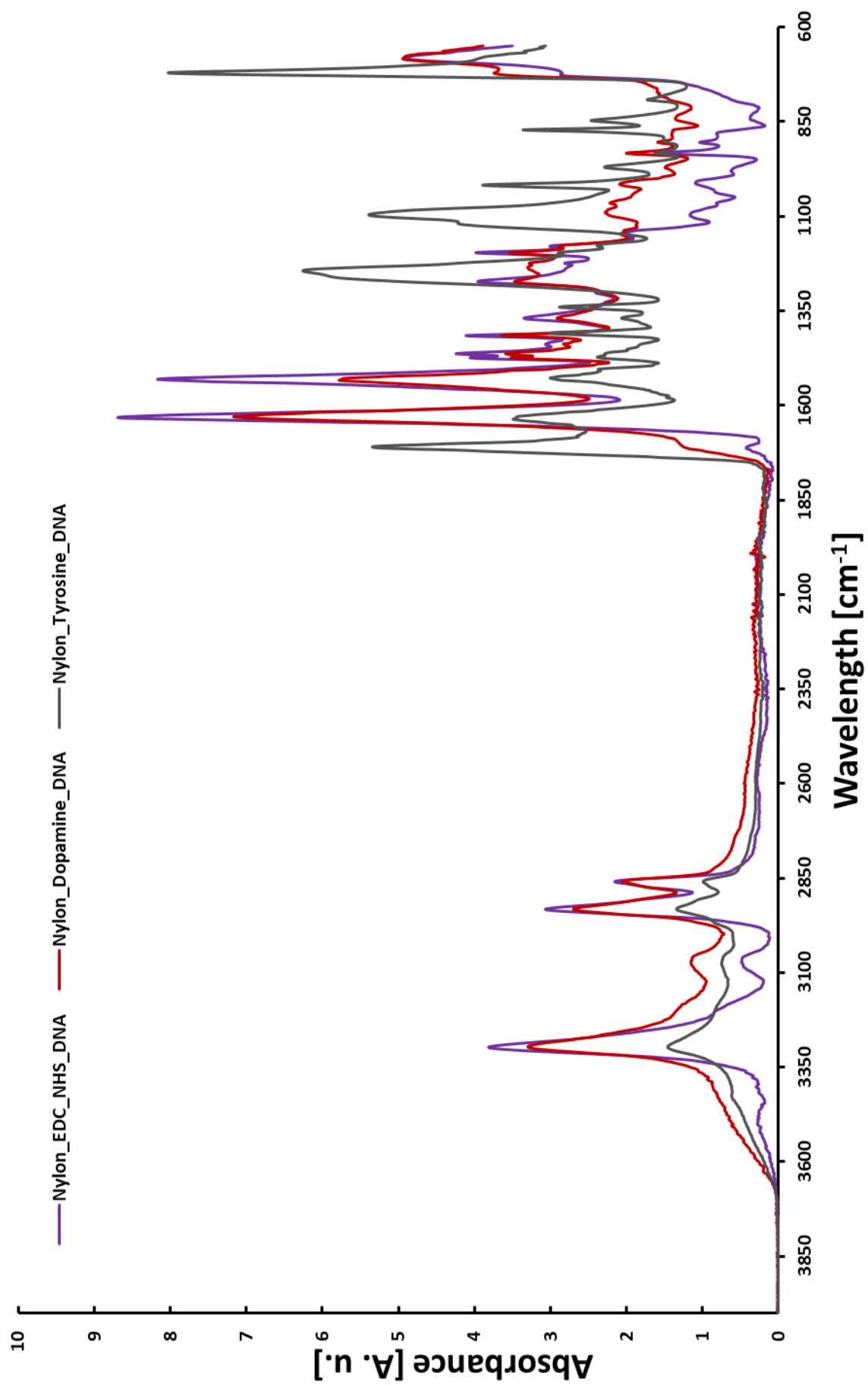






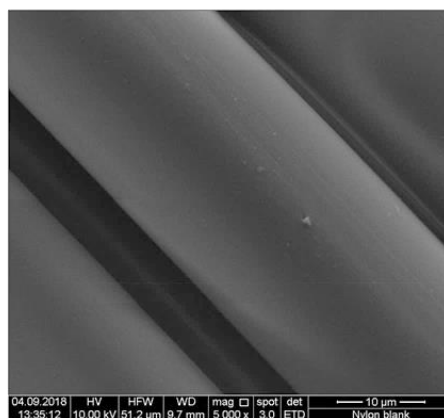
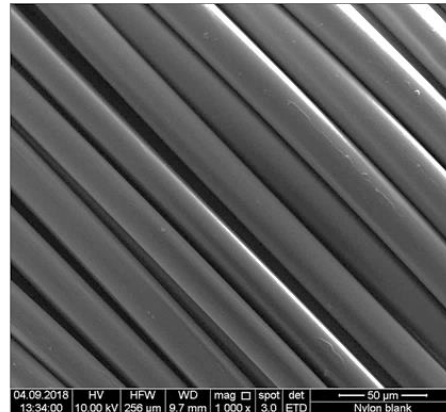
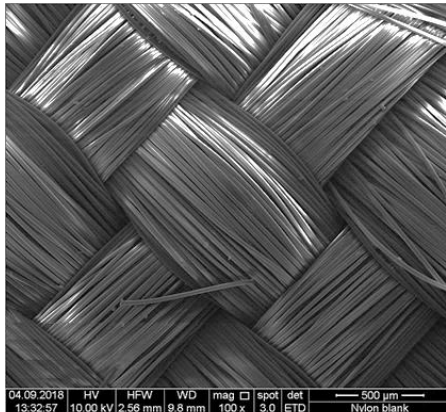




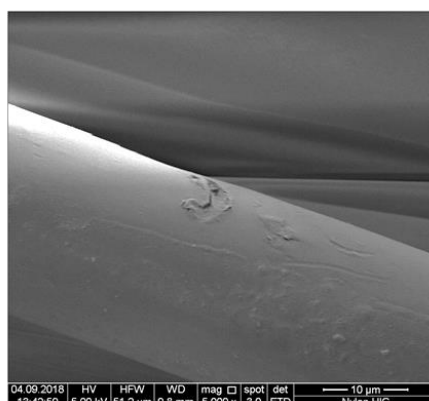
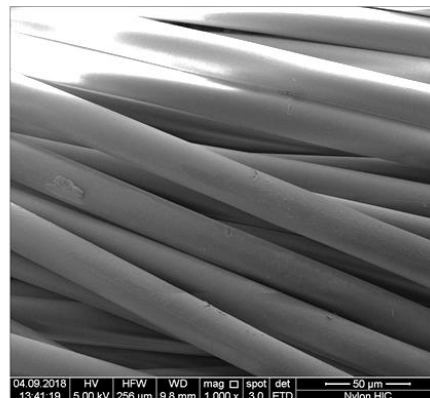
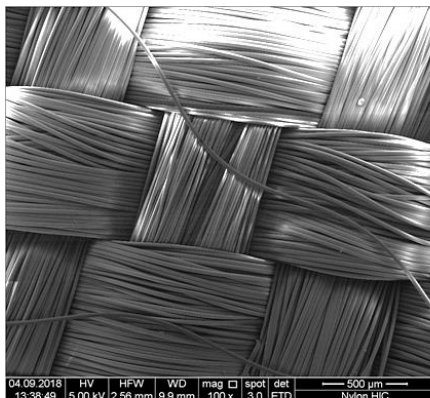


5.2. ESEM

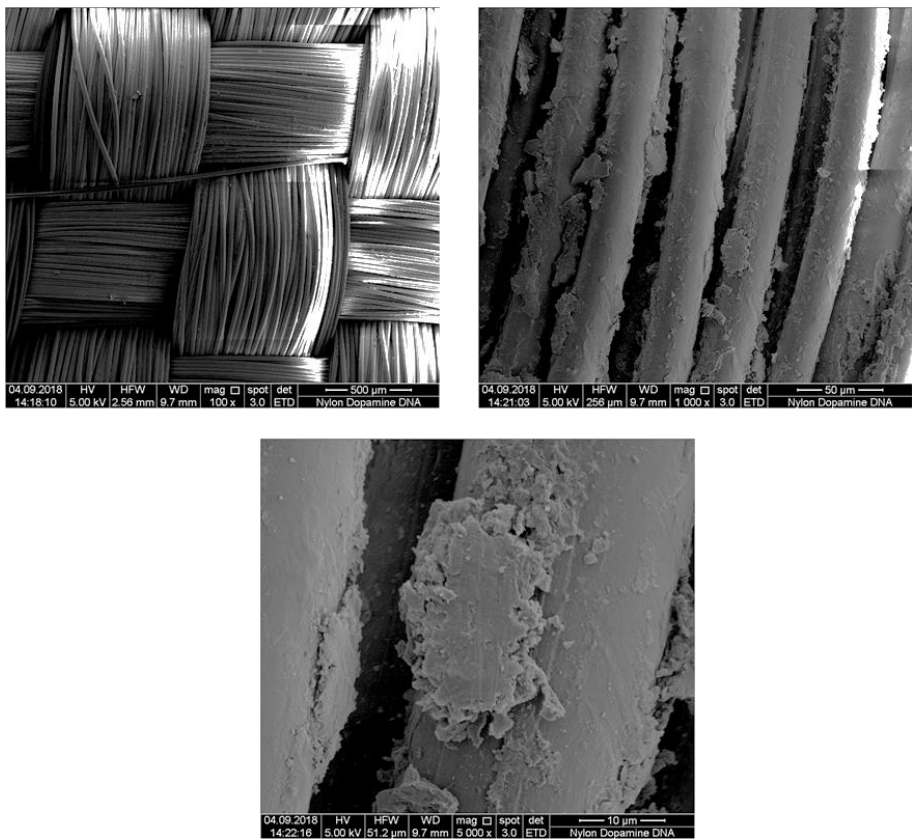
Nylon Blank



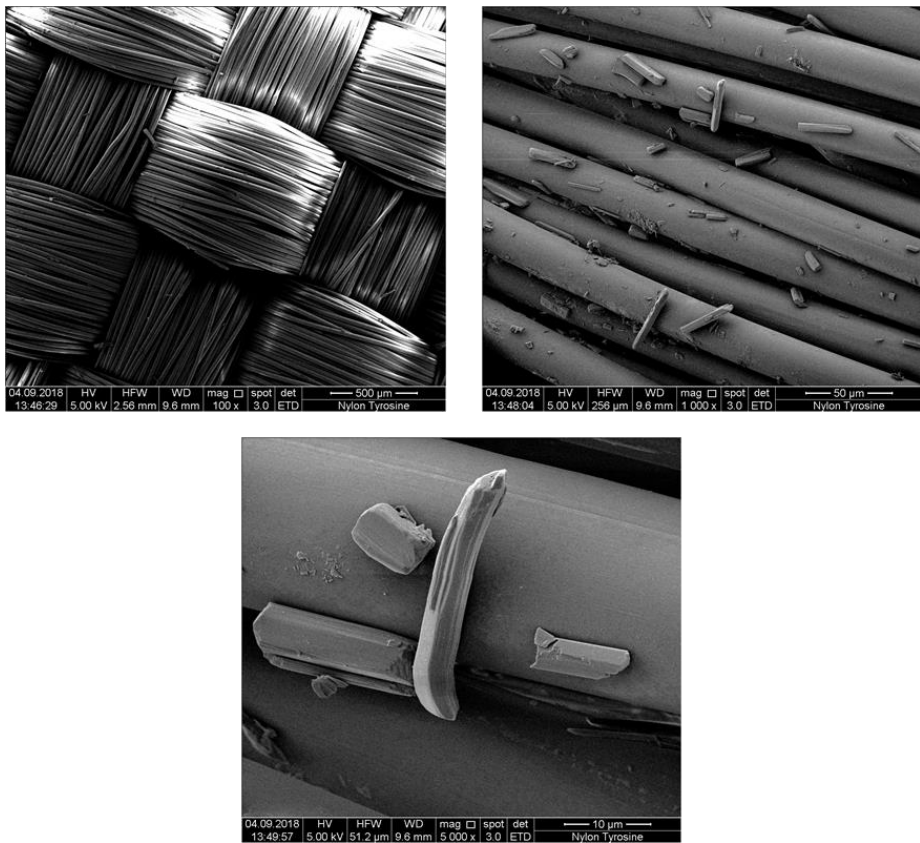
Nylon HiC



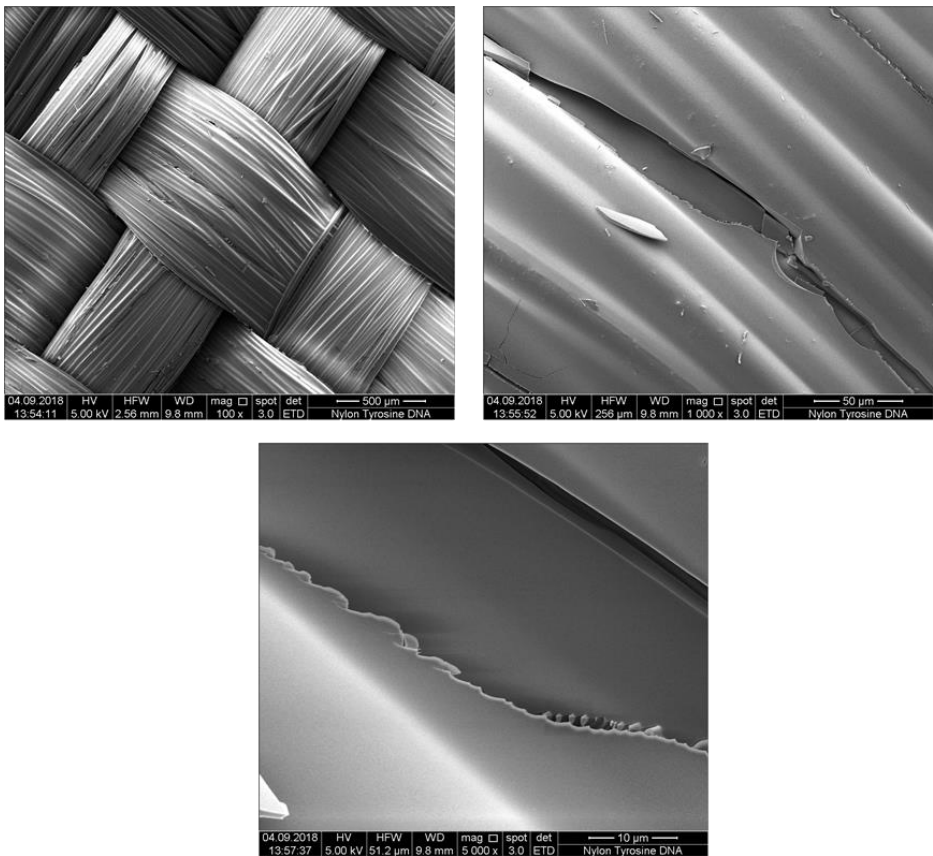
Nylon/Dopamine/DNA



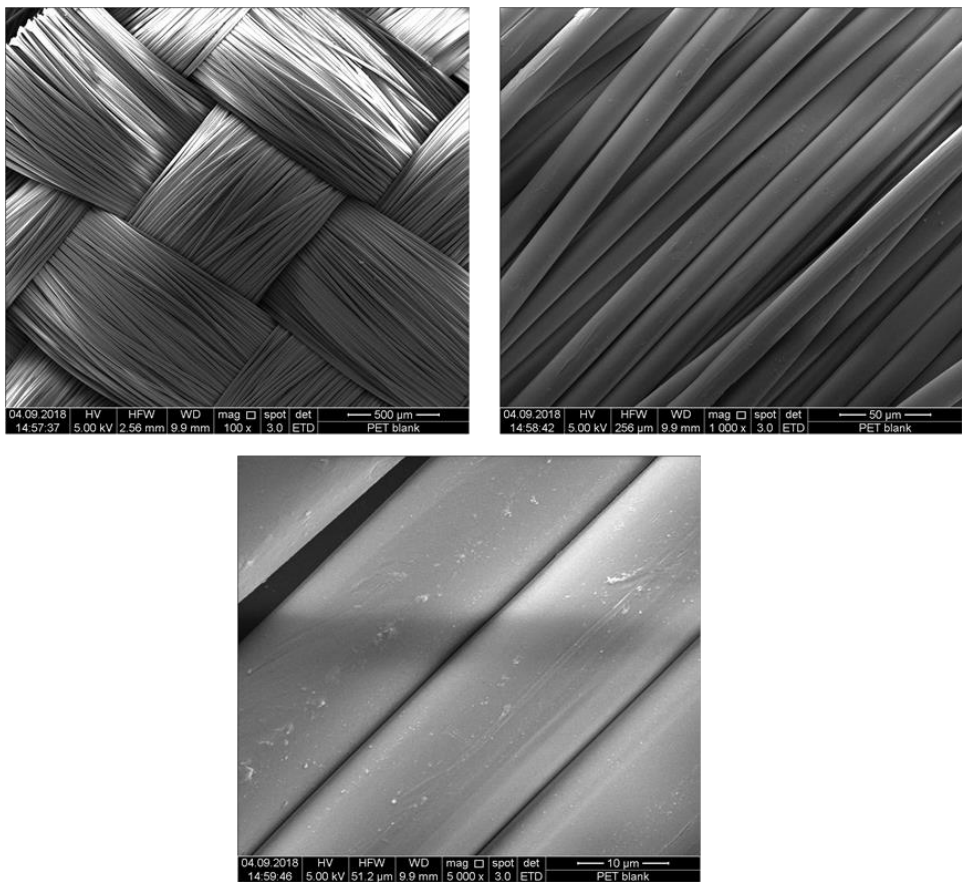
Nylon/Tyrosine



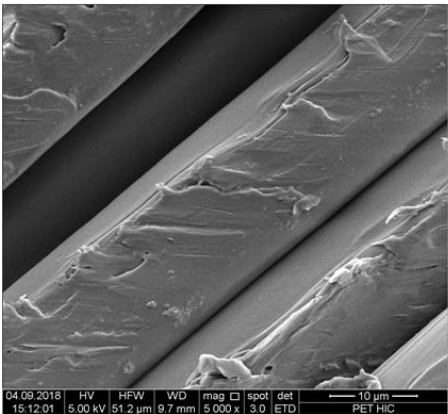
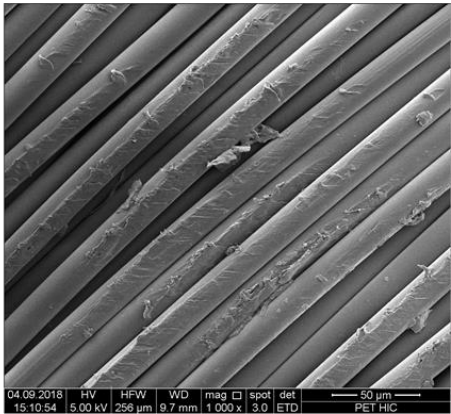
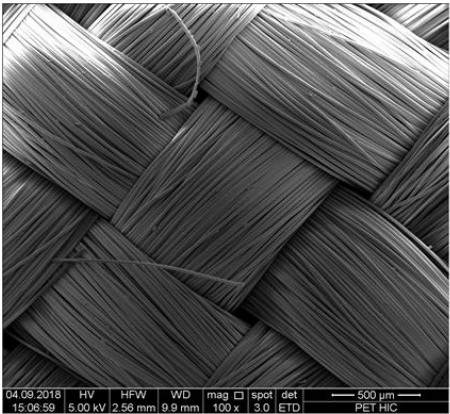
Nylon/Tyrosine/DNA



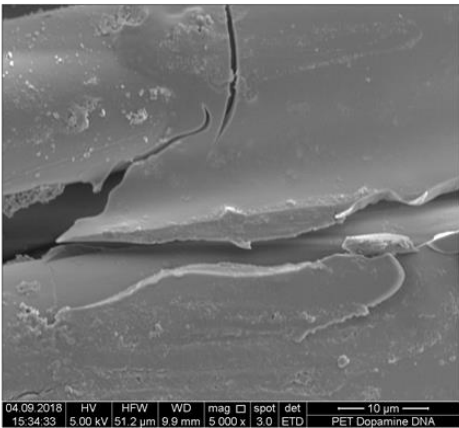
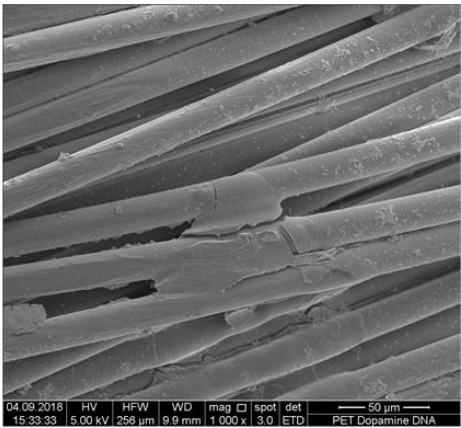
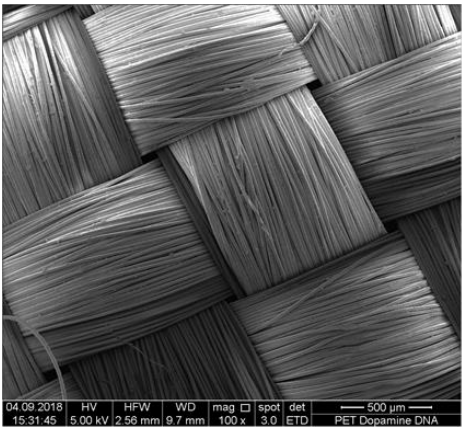
PET Blank



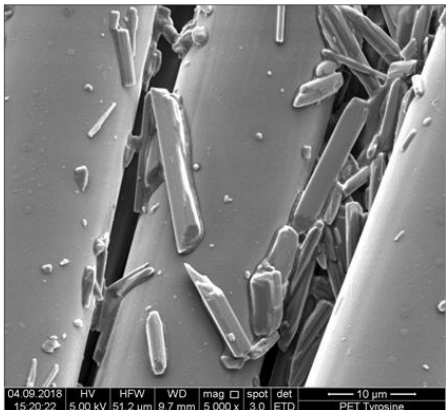
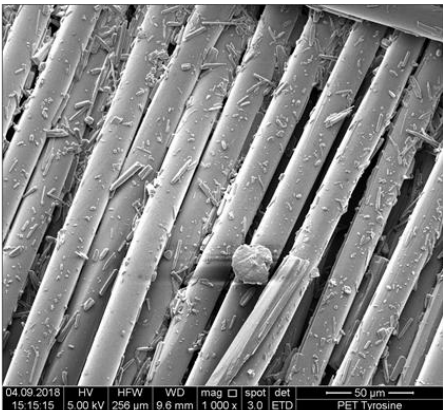
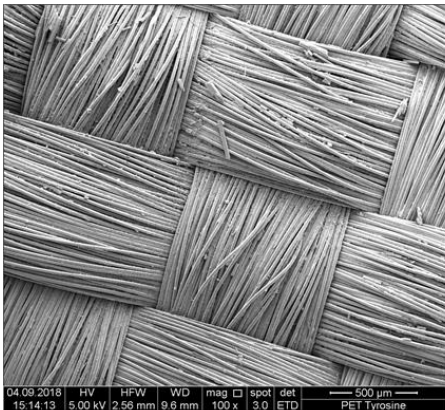
PET HiC



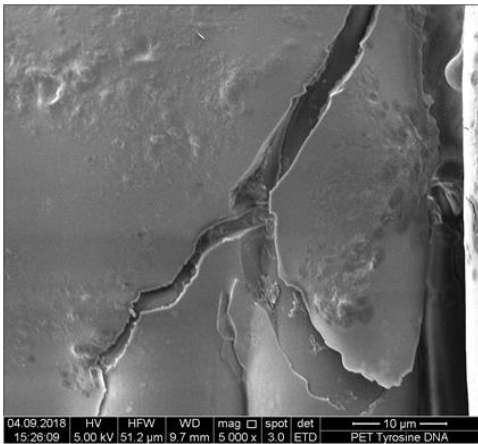
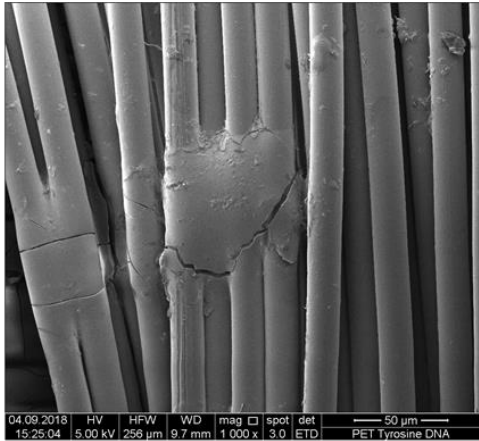
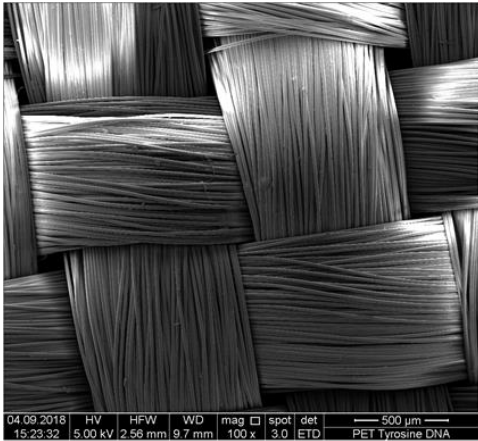
PET/Dopamine/DNA



PET/Tyrosine



PET/Tyrosine/DNA



6. References

1. Guha, S. B. & Shah, S. R. Enzymatic Scouring of Cotton Fabric. *J. Text. Assoc.* **61**, 215–218 (2001).
2. Government of India. Global Trade Analysis of Synthetic Fibre Global Trade Analysis of Synthetic Fibre. (2014).
3. Serini, V. Polycarbonates. *Ullmann's Encycl. Ind. Chem.* **29**, 603–611 (2000).
4. Limited, W. P. *Advances in Textile Biotechnology | 978-1-84569-625-2 | Elsevier.*
5. Center of Fire statistics. World Fire Statistics. Bulletin N°22. *Int. Assoc. Fire Rescue Serv.* 56 (2017).
6. Brandschutz 12 Info. 1–4 (2014).
7. Citation, O., Casale, A., Access, O. & Article, P. Politecnico di Torino Biomacromolecules : A sustainable approach for the design of fire retardants for textiles. (2017). doi:10.6092/polito/porto/2673802
8. Efra, R. A., Steukers, V. & Drohmann, D. Flame retardants : European Union risk assessments Flame retardants are recognized as providing lifesaving benefits European risk assessments . On behalf of the European Flame. 26–29 (2006).
9. Watanabe, I. & Sakai, S. I. Environmental release and behavior of brominated flame retardants. *Environ. Int.* **29**, 665–682 (2003).
10. Darnerud, P. O. Toxic effects of brominated flame retardants in man and in wildlife. *Environ. Int.* **29**, 841–853 (2003).
11. Betts, K. S. Rapidly rising PBDE levels in North America. *Environ. Sci. Technol.* **36**, 50A–52A (2002).
12. Alongi, J. *et al.* Caseins and hydrophobins as novel green flame retardants for cotton fabrics. *Polym. Degrad. Stab.* **99**, 111–117 (2014).
13. Wösten, H. A. B. & Scholtmeijer, K. Applications of hydrophobins: current state and perspectives. *Appl. Microbiol. Biotechnol.* **99**, 1587–1597 (2015).
14. Grote, J. G. *et al.* DNA-based materials for electro-optic applications: current status. **5934**, 593406 (2005).
15. Ferreira, I. M. P. L. V. O., Pinho, O., Vieira, E. & Tavela, J. G. Brewer's *Saccharomyces* yeast biomass: characteristics and potential applications. *Trends Food Sci. Technol.* **21**, 77–84 (2010).
16. Yang, Z. H., Xiao, Y., Zeng, G. M., Xu, Z. Y. & Liu, Y. S. Comparison of methods for total community DNA extraction and purification from compost. *Appl. Microbiol. Biotechnol.* **74**, 918–925 (2007).
17. Alongi, J. *et al.* DNA: a novel, green, natural flame retardant and suppressant for cotton. *J. Mater. Chem. A* **1**, 4779 (2013).
18. Biundo, A., Ribitsch, D. & Guebitz, G. M. Surface engineering of polyester-degrading enzymes to improve efficiency and tune specificity. 3551–3559 (2018).
19. Chen, S., Su, L., Chen, J. & Wu, J. Cutinase: Characteristics, preparation, and application. *Biotechnol. Adv.* **31**, 1754–1767 (2013).
20. Kold, D. *et al.* Thermodynamic and structural investigation of the specific SDS binding of humicola insolens cutinase. *Protein Sci.* **23**, 1023–1035 (2014).

21. Beck, H., Dobritzsch, D. & Pis, J. *Saccharomyces kluyveri* as a model organism to study pyrimidine degradation. 1209–1213 (2018). doi:10.1111/j.1567-1364.2008.00442.x
22. Lohkamp, B., Andersen, B., Pis, J. & Dobritzsch, D. The Crystal Structures of Dihydropyrimidinases Reaffirm the Close Relationship between Cyclic Amidohydrolases and Explain Their Substrate Specificity *. **281**, 13762–13776 (2006).
23. Haernvall, K. *et al.* Hydrolysis of Ionic Phthalic Acid Based Polyesters by Wastewater Microorganisms and Their Enzymes. (2017). doi:10.1021/acs.est.7b00062
24. Vecchiato, S. *et al.* Enzymatic Functionalization of HMLS-Polyethylene Terephthalate Fabrics Improves the Adhesion to Rubber. (2017). doi:10.1021/acssuschemeng.7b00475
25. Pellis, A. *et al.* The Closure of the Cycle : Enzymatic Synthesis and Functionalization of Bio-Based Polyesters. *Trends Biotechnol.* **34**, 316–328 (2016).
26. O'Driscoll, K. F. [12] Techniques of Enzyme Entrapment in Gels. *Methods Enzymol.* **44**, 169–183 (1976).
27. Thallinger, B. Functionalization of catheters with antimicrobial enzymes. (2015).
28. Lee, H., Rho, J. & Messersmith, P. B. Facile conjugation of biomolecules onto surfaces via mussel adhesive protein inspired coatings. *Adv. Mater.* **21**, 431–434 (2009).
29. Fixe, F., Dufva, M., Telleman, P. & Christensen, C. B. V. One-step immobilization of aminated and thiolated DNA onto poly(methylmethacrylate) (PMMA) substrates. *Lab Chip* **4**, 191 (2004).
30. Bradford, M. M. A rapid and sensitive method for the quantitation of microgram quantities of protein utilizing the principle of protein-dye binding. *Anal. Biochem.* **72**, 248–254 (1976).
31. Biundo, A. *et al.* Characterization of a poly (butylene adipate- co -terephthalate) -hydrolyzing lipase from *Pelosinus fermentans*. 1753–1764 (2016). doi:10.1007/s00253-015-7031-1
32. Sepharose, C. Purification and properties of 5,6-dihydropyrimidine amidohydrolase from calf liver. **435**, 431–435 (1989).
33. Song, J. E. & Kim, H. R. Improvement in nylon fabrics' reactivity via enzymatic functionalization. *J. Text. Inst.* **108**, 155–164 (2017).
34. Noel, S., Liberelle, B., Robitaille, L. & De Crescenzo, G. Quantification of primary amine groups available for subsequent biofunctionalization of polymer surfaces. *Bioconjug. Chem.* **22**, 1690–1699 (2011).
35. Cole, K. C. & Guevremont, J. Characterization of Surface Orientation in Poly (ethylene terephthalate) by Front-Surface Reflection Infrared Spectroscopy. *Appl. Spectrosc.* 1513–1521 (1994).
36. Donelli, I. *et al.* Enzymatic surface modification and functionalization of PET: A water contact angle, FTIR, and fluorescence spectroscopy study. *Biotechnol. Bioeng.* **103**, 845–856 (2009).
37. Socrates, G. *Infrared and Raman characteristic group frequencies. Infrared and Raman characteristic group frequencies* (2004). doi:10.1002/jrs.1238

38. Luo, B., Wang, X., Wang, Y. & Li, L. Fabrication, characterization, properties and theoretical analysis of ceramic/PVDF composite flexible films with high dielectric constant and low dielectric loss. *J. Mater. Chem. A* **2**, 510–519 (2014).
39. Wang, Y. *et al.* A Novel Technological Process of Extracting L-Tyrosine with Low Fluorine Content from Defatted Antarctic Krill (*Euphausia superba*) By-product by Enzymatic Hydrolysis. *Food Bioprocess Technol.* **9**, 621–627 (2016).